1980

A solar-heated grain dryer for the tropics

Virgilio G. Gayanilo
Iowa State University

GAYANILO, VIRGILIO G.

A SOLAR-HEATED GRAIN DRYER FOR THE TROPICS

Iowa State University PH.D. 1980

A solar-heated grain dryer

for the tropics

by

Virgilio G. Gayanilo

A Dissertation Submitted to the

Graduate Faculty in Partial Fulfillment of the

Requirements for the Degree of

DOCTOR OF PHILOSOPHY

Major: Agricultural Engineering

Approved:

Signature was redacted for privacy.

In Charge of Major Work

Signature was redacted for privacy.

For the Major Department

Signature was redacted for privacy.

For the Graduate College

Members of the Committee:

Signature was redacted for privacy.

Signature was redacted for privacy.

Signature was redacted for privacy.

Signature was redacted for privacy.

Signature was redacted for privacy.

Signature was redacted for privacy.

Iowa State University
Ames, Iowa

1980

TABLE OF CONTENTS

INTRODUCTION

Renewed interest in the use of solar energy as an alternative energy source has been attributed to the increasing cost of conventional energy sources such as coal, gas and fuel oil, and the realization that these fossil-derived energy sources are limited in supply and will eventually become exhausted. Until recently, very little research has been done on the utilization of solar energy for mechanical drying of grain crops.

In the humid tropical regions, where most developing countries are located, grain crops such as rice and corn are usually harvested and left in the field to sun-dry before they are husked or threshed for storage. This method requires as long as several days, depending on weather conditions. Aside from being cumbersome and inefficient, only a small fraction of the crop can be dried at a time and this is usually done under constant threat of rain.

Recent improvements in grain production technology and management have increased the volume of grain produced in developing countries. However, it has also created a secondary problem of grain spoilage and germination, a result of poor and inadequate drying and storage facilities. Introduction of low-cost portable mechanical grain dryers designed to solve these problems gained wide acceptance among tropical farmers at the village level, however, the increasing cost of the fuel oil used in the heating process has discouraged their use.

Countries in the tropical belt between ± 20 degrees latitude receive the highest average annual insolation rate. Hence, there is greater potential for the use of solar energy as an alternative heat source for mechanical grain drying in the tropics. A well-designed solar-heated grain drying system could economically reduce the dependence of tropical farmers on heating fuels such as kerosene and LP gas. In rural areas of most tropical countries, electricity is not usually available. Consequently, internal combustion engines must be used for fan power. Utilization of waste heat from fan engines of mechanical grain dryers can provide further supplemental heating.

Applications of sophisticated western technology have, in the past, proved to be inappropriate for developing countries due to the conditions that are unique in the region. A solar-heated grain drying system for the tropics was therefore developed along the concept of an intermediate technology wherein the system is low in cost, small in scale, simple in construction and makes use of materials available locally in the region.

OBJECTIVES

The research project was undertaken to investigate the use of solar energy for drying of grain crops in the tropical region, particularly rice and corn. Specifically, the objectives of the research study were:

1. To analyze previously-developed solar collector designs which can be applied to grain drying systems in the tropics.
2. To develop design criteria for tropical conditions on grain drying systems using solar energy.
3. To design and construct a simple low-cost grain drying system which uses solar heat energy supplemented by engine waste heat.
4. To test and evaluate the performance of the grain drying system and,
5. To do an economic analysis of the grain drying system.

This study was also intended to provide basic information as well as experience in the design, construction and testing of a low-cost solar grain drying system and, furthermore, serve as a basis for future research on improving or designing simple solar drying systems for other tropical crops.

LITERATURE REVIEW

Solar Radiation Intensity

To be able to utilize solar energy for engineering application, it is necessary to know the availability of the supply. Adequate knowledge of solar radiation intensity and its frequency of occurrence at a particular locality will be helpful in the proper design of a solar heat collector for grain drying.

Solar constant

The actual amount of thermal radiation received from the sun, defined as the solar constant measured at a mean distance from the earth's surface, has been extensively evaluated in several research works. Value of the solar constant varies with each investigation. From 1913 to 1953, the most widely used and accepted value proposed by C. G. Abbott, as cited in Yellot (1977), was 1357 W/m^2 with a variation of ± 1.80 percent. This was later revised by Johnson (1954) to 1393 W/m^2 after analyzing different solar constant values taken from later measurements.

Recent measurements with high altitude aircraft, balloons and spacecraft have permitted direct measurements of solar radiation intensity outside the earth's atmosphere. These measurements were reviewed and summarized by Thekaekara and Drummond (1971) giving rise to a new standard value of 1353 W/m^2 with a maximum probable error of ± 1.50 percent.

Solar radiation at the earth's surface

As solar radiation passes through the earth's atmosphere, depletion of direct radiation occurs by scattering and absorption due to air molecules, dust, water vapor and ozone. Transmission of direct solar radiation varies at different portions of the solar spectrum as a result of selective properties of various atmospheric elements.

At the outer limits of the earth's atmosphere, spectral distribution of direct solar radiation was given by ASHRAE (1977) as follows:

Spectral region	Wavelength range (microns)	Percent of total energy
ultraviolet	0.29 to 0.40	9.0
visible	0.40 to 0.70	38.0
infrared	0.70 to 3.50	53.0

Some of the shortwave radiation is scattered by air molecules and dust and reaches the earth's surface in the form of diffuse radiation while most of it is absorbed by ozone in the upper atmosphere. The total solar energy reaching the earth's surface is the sum of direct and diffuse components - the value of which varies widely as to moisture and dust content of the atmosphere.

The general relationship is given by

$$I_t = I_D + I_d \tag{1}$$

where

I_t = total incident solar radiation at the earth's surface, W/m^2

I_D = direct incident solar radiation, W/m^2

I_d = diffuse solar radiation, W/m^2

Earlier attempts on predicting the intensity of solar radiation as it passes through the earth's atmosphere and into the earth's surface were made by Kimball (1927) and later by Moon (1940), Klein (1948) and Fritz (1955).

Becker and Boyd (1957) did an extensive study of solar radiation intensity as affected by season, latitude, altitude, degree of cloudiness and orientation of receiving surface for different localities in the U.S. A similar study was also done by Buelow (1967) wherein he developed equations predicting the quantity of solar energy falling on a surface on earth when latitude, time of year, slope and orientation of surface are known. His results were tabulated for a latitude range of 0 to 60 degrees north and for six surface orientations and configurations.

The most comprehensive approach was derived from results of research by Threlkeld and Jordan (1958) at the University of Minnesota. The results were later adapted by Farber and Morrison (1977) in developing a computer program for predicting clear-day design values of solar radiation for various locations and surface orientations on the twenty-first day of each month.

Direct solar radiation From the work of Threlkeld and Jordan, the direct normal radiation at the earth's surface on a clear day, I_{DN}, is represented by

$$I_{DN} = \frac{A}{\exp\ (B/\sin\beta)} \quad W/m^2 \tag{2}$$

where

A = apparent solar radiation at air mass = 0, W/m^2

B = atmospheric extinction coefficient, dimensionless

β = solar altitude angle, degrees

Values of A and B vary during the year and are given in Appendix A. Solar altitude angle, β, may be obtained from the relationship

$$\sin\beta = \cos L \cos \delta \cos \omega + \sin L \sin \delta \quad (3)$$

where

L = latitude angle of location, degrees

δ = declination angle at the date in question, degrees

ω = absolute value of solar hour angle measured from solar noon, degrees

The latitude angle, L, of a locality may be easily obtained from a World Atlas. Solar declination, δ, may be derived from an approximate equation of Cooper (1969) adapted by Duffie and Beckman (1974) and given by

$$\delta = 23.45 \sin \left(360 \frac{284 + n}{365}\right) \quad (4)$$

where n is the day of the year. Hour angle, ω, is obtained from the relationship

$$\omega = 15 \times (\text{number of hours from solar noon}) \quad (5)$$

The direct incident solar radiation, I_D, that falls on any surface on earth is therefore expressed as

$$I_D = I_{DN} \times \cos \theta \quad W/m^2 \quad (6)$$

where θ is the angle of solar incidence on the surface, in degrees, and obtained from the relationship

$$\cos \theta = \cos \beta \cos \gamma \sin \Sigma + \sin \beta \cos \Sigma \tag{7}$$

where

Σ = surface tilt angle from the horizontal, degrees

γ = surface-solar azimuth, degrees

For south-facing surfaces, surface-solar azimuth, γ, is equal to the solar azimuth, ϕ, obtained from the relationship

$$\sin \phi = \frac{\cos \delta \sin \omega}{\cos \beta} \tag{8}$$

Diffuse solar radiation The diffuse radiation component, I_d, varies widely from 15 percent on clear days to 100 percent on completely overcast days. Because of wide variations in day-to-day atmospheric conditions, intensity of diffuse solar radiation is difficult to predict. For clear sky conditions, Threlkeld and Jordan gave a simplified general relationship for the diffuse solar radiation falling on the surface expressed approximately by

$$I_d = C\, I_{DN}\, F_{ss} \quad W/m^2 \tag{9}$$

where

C = diffuse radiation factor, dimensionless

F_{ss} = angle factor, dimensionless

The constant C can be obtained from Appendix A and angle factor, F_{ss}, from the relationship

$$F_{ss} = \frac{1 + \cos \Sigma}{2} \tag{10}$$

Except for snow-covered ground, effect of reflected solar radiation from ground and surrounding structures on the receiving surface may be considered negligible.

Solar Heat Collectors

General description

A simple solar heat collector consists basically of an absorbing surface, usually painted black, which absorbs solar energy and transmits it, in the form of heat energy, to a working fluid. Provision is made to transport the collected energy by circulating water through tubes in thermal contact with the collecting surface or by circulating air through an air space between the collecting surface and a backplate.

Hottel and Woertz (1942) classified solar heat collectors according to the type of insulation, degree of concentration of solar radiation, and nature of orientation.

Upward heat loss from the collector can be decreased by use of one or more transparent coverplates above and parallel to the absorbing surface. Coverplate materials used are glass, plexiglass and clear plastic which are capable of transmitting short-wave solar radiation but opaque to long-wave radiation from the collecting surface. In some cases, a bare plate collector (no cover) is used. Backward heat loss from the collector is also reduced by using some form of insulation on the underside such as glass wool, mineral wool, wood or dead-air space.

Solar collectors may be designed with or without solar radiation concentration. Flat-plate type collectors which are commonly used in thermal processes, have a concentration of unity, that is, the area absorbing solar radiation is the same as the area intercepting solar radiation. The amount of solar radiation absorbed by flat-plate solar collectors can be increased by increasing the absorptance of the collecting surface with the use of selective surfaces. Among those of interest are the use of selective paint coatings and proper configurations such as corrugations and V-shaped grooves on the collecting surface.

Solar radiation intensity may be increased appreciably by focusing-type collectors utilizing optical systems that concentrate a given amount of solar radiation on a smaller collector area. These types of collectors, however, are used only on high-temperature and specialized applications such as steam generation.

Orientation of solar collector may be such that it can be (1) stationary and horizontal, (2) stationary but tilted toward the sun on an east-west axis, (3) mounted on an east-west axis to follow the sun's seasonal motion, (4) mounted on the north-south axis to follow the diurnal motion of the sun, or (5) mounted on both equatorial and transverse axes to fully-track the sun and maintain the collector normal to the sun's rays at all times.

Solar collectors may also be described as being passive or active solar collection systems, and as being free standing or attached as an integral part of a building roof or wall structure.

Flat-plate solar collectors

Hottel and Woertz (1942) described the flat-plate solar collector as the simplest and basic type. According to Pelletier (1959), it is the most frequently proposed method of collecting thermal energy at low to medium temperatures.

Howe (1955) stated that low-temperature applications of solar energy such as solar heating for agriculture involves temperatures of 65° C or less and are almost entirely served by flat-plate type collectors. For small temperature rises of 2.8 to 8.3° C, Sobel and Buelow (1963) stated that the collector can be of simple design and hence, low in cost.

Conventional flat-plate collectors for air heating are shown schematically in Figure 1. In bare-plate collectors, air is drawn between the absorber plate and backplate which may be insulated to reduce heat loss. On covered plate collectors, air may be drawn on one or both sides of the absorber plate.

Solar collector performance

In view of potential applications to solar grain drying and for reasons mentioned earlier, analysis of solar collector performance is confined to simple air-heating flat-plate collectors with fixed orientation. Many of the items, however, will be equally applicable to other types of solar collectors. An understanding of the factors affecting performance of solar collectors will be useful in problems involving solar collector design and testing.

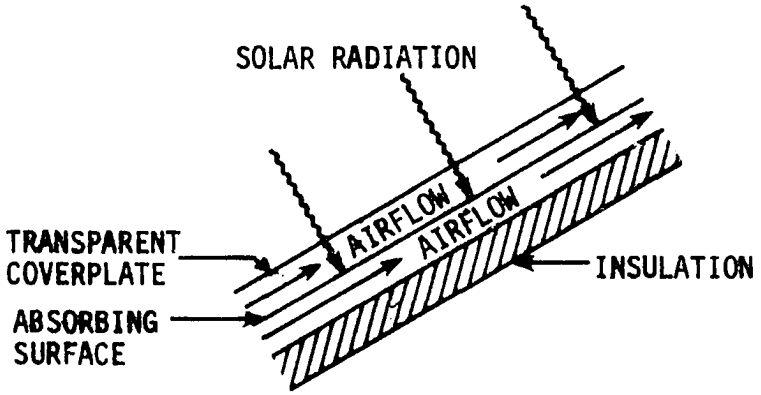

COVERED PLATE SOLAR COLLECTOR

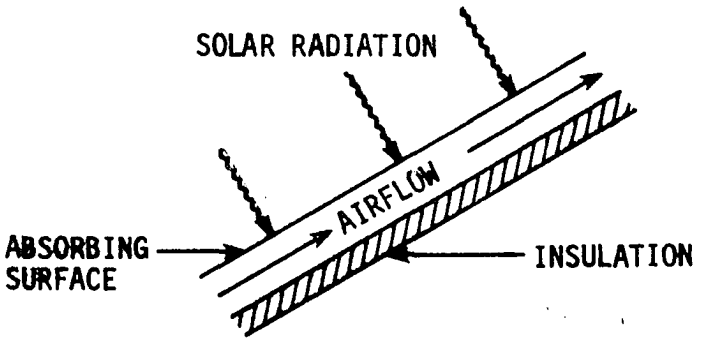

BARE PLATE SOLAR COLLECTOR

Figure 1. Schematic diagrams of conventional flat-plate solar collectors for air heating

The pioneering work of Hottel and Woertz (1942) on flat-plate solar collector performance has led other researchers in developing empirical equations describing performance of various types of solar collecting devices. The methods of calculations presented here are essentially based on derivations by Hottel and Woertz (1942), Hottel and Whillier (1955), Tabor (1955), Bliss (1959) and Whillier (1953, 1977). Common objectives were evaluation of useful energy gain and collection efficiency.

Basic energy balance To evaluate collector performance, one determines the amount of solar energy incident on the collector surface, the fraction of incident energy absorbed by the collector absorber plate and the amount of useful energy transferred to a working fluid. Under steady-state conditions, energy balance on the collector may be written as

$$q_u = q_a - q_l \tag{11}$$

where

q_u = rate of useful energy collection per unit area of collector surface, W/m^2

q_a = rate of absorption of solar energy by the collector plate per unit area, W/m^2

q_l = rate of energy losses from the collector to the surroundings by radiation, convection and conduction, W/m^2

In the work of Klein et al. (1974), assumption of steady-state conditions was found to be adequate for time intervals of 15 to 60

minutes. Most calculations assuming steady-state are hence done on an hourly basis.

Energy absorbed in the collector q_a The rate at which solar energy is absorbed in the collector is mainly dependent on (1) the insolation rate, (2) the absorptivity of the collecting surface to solar radiation, and (3) the transmissivity of the collector cover-plate. For bare plate collectors with no cover, the third factor may be ignored.

In evaluating the rate of solar energy absorption, Whillier (1977) pointed out that not all incident solar radiation comes directly from the sun. Diffuse sky radiation accounts for about 10 percent of the total incident radiation in dry climates and may go as high as 40 percent in the humid tropics. In general, the average angle of incidence of diffuse sky radiation differs from that of a direct beam solar radiation, hence, direct and diffuse components of solar radiation have to be treated separately.

Based on the research work of Hottel and Woertz (1942), Hottel and Whillier (1955) expressed the energy absorption rate on a covered flat-plate collector in the form

$$q_a = [(H-H_d)\ R_D\ (\tau_e\alpha)_D + H_d R_d\ (\tau_e\alpha)_d]\ (1-D)(1-S) \qquad (12)$$

where

H = total insolation rate on a horizontal surface, W/m^2

H_d = diffuse sky radiation falling on a horizontal surface, W/m^2

R_D, R_d = orientation factors to convert horizontal incidence to incidence on tilted collector, for direct and diffuse components, respectively

$(\tau_e\alpha)_D$, $(\tau_e\alpha)_d$ = effective transmittance-absorptance products of the cover-absorber plate combination, for direct and diffuse components, respectively

S = shading factor to allow for shading of absorber plate by cover supports

D = dirt factor to allow for reduction in transmittance due to dirt deposits on the cover

Neglecting the effects of shading and dirt factors, Duffie and Beckman (1974) reduced the equation to

$$q_a = HR_D(\tau\alpha)_D + HR_d(\tau\alpha)_d \tag{13}$$

where subscripts D and d refer to the direct and diffuse components, respectively. Evaluation of the transmittance-absorptance product, $\tau\alpha$, was also described by Duffie and Beckman.

Extensive studies by Liu and Jordan (1960) on the interrelationships of direct, diffuse and total solar radiation on a horizontal surface have made it possible to estimate the direct and diffuse components with good accuracy once the total solar radiation is known.

The orientation factor, R_D, to convert direct horizontal incidence to incidence on the tilted collector may be found from the relationship

$$R_D = \frac{\cos\theta}{\sin\beta} \tag{14}$$

where angles β and θ are determined from equations (3) and (7), respectively, for a given time and location. The diffuse orientation factor, R_d, is the same as the angle factor, F_{ss}, obtained in equation (10).

For bare plate collectors, equation (13) is further reduced to

$$q_a = HR_D\alpha_D + HR_d\alpha_d \tag{15}$$

wherein the transmittance factor, τ, is eliminated in the absence of a coverplate, and α is the absorptance of the bare collector plate.

For design purposes, clear-day values for direct and diffuse components of solar radiation falling on a tilted surface may be calculated from equations (6) and (9), respectively, wherein

$$I_D = HR_D \tag{16}$$

$$I_d = HR_d \tag{17}$$

and from equation (1)

$$I_t = I_D + I_d = HR_D + HR_d \tag{18}$$

Thermal losses from the collector q_l Thermal losses from solar heat collectors occur as long as the collector plate temperature is greater than its surroundings. In simple flat-plate collectors, Whillier (1977) categorized thermal losses into (1) upward heat loss from the top of the collector, (2) downward or bottom heat loss through the rear insulation, and (3) sideways heat loss through the edge insulation.

Thermal losses in the collector involve the three modes of heat transfer: conduction, convection and radiation. Duffie and Beckman (1974) conveniently described the heat transfer mechanism in flat-plate

solar collectors by a thermal resistance network as shown in Figure 2 wherein T_a is the ambient air temperature, U_l, the overall collector heat loss coefficient and T_{pm}, the mean collector plate temperature.

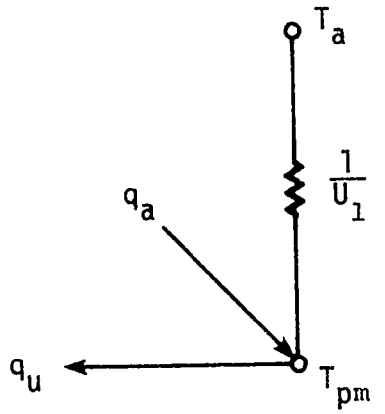

Figure 2. Equivalent thermal resistance network for a flat-plate solar collector

The collector heat loss coefficient, U_l, embodies all the losses in the collector and is equivalent to

$$U_l = U_t + U_b + U_{edge} \left(\frac{A_p}{A_c}\right) \tag{19}$$

where

U_t = top or upward heat loss coefficient, $W/m^2 \cdot °C$

U_b = bottom or back heat loss coefficient, $W/m^2 \cdot °C$

U_{edge} = edge heat loss coefficient, $W/m^2 \cdot °C$

A_p = perimeter area of collector, m^2

A_c = area of collector absorber plate, m^2

The thermal loss from flat-plate collectors can thus be expressed by

$$q_l = U_l \ (T_{pm} - T_a) \tag{20}$$

where

T_{pm} = mean collector plate temperature, °C

T_a = ambient air temperature, °C

U_l = overall collector heat loss coefficient, $W/m^2 \cdot °C$

q_l = heat loss from the collector, W/m^2

Methods of calculating U_l have been described by Duffie and Beckman (1974) and Whillier (1977) for most collector designs. Under certain circumstances, the overall heat loss coefficient will have to be slightly modified to account for geometry of specific collector designs.

Useful energy from solar collector, q_u From previous equations, the rate of useful energy collection per unit area of collector surface may be rewritten as

$$q_u = [HR_D(\tau\alpha)_D + HR_d(\tau\alpha)_d]-U_l \ (T_{pm} - T_a) \tag{21}$$

The relationship implies that the rate of useful heat gain is a function of several factors and through careful design of the heat-removal system, optimum combination of these factors may be obtained for a desired application.

Whillier (1977) cited that one factor difficult to evaluate is the mean absorber plate temperature, T_{pm}, the value of which is not usually known. Hottel and Whillier (1955) earlier noted that the absorber plate

temperature depends primarily on the temperature of incoming fluid stream used to remove useful energy from the collector and, to a lesser extent, upon the geometric details of the collector-plate and fluid flow circuits, the fluid flow-rate and the intensity of solar radiation.

In expressing the useful heat gain in terms of known collector dimensions, fluid flow characteristics and local fluid temperature, Hottel and Woertz (1942) earlier proposed the use of a heat-removal factor, F_R.

A convenient expression for the useful heat gain of slightly different form is given by

$$q_u = F_R [q_a - U_l (T_{fi} - T_a)] \tag{22}$$

where

F_R = heat-removal factor, dimensionless

T_{fi} = transport fluid temperature at the collector inlet, °C

The above expression, however, is restricted by the assumption that fluid temperature at collector inlet, T_{fi}, is greater than the ambient air temperature, T_a.

Derivations of F_R were first presented by Whillier (1953) and later by Bliss (1959). The methods used by each one were similar and end results were in close agreement. F_R is basically a function of the transport fluid flow-rate and is given by

$$F_R = (Gc_p/U_l) [1 - \exp (- F'U_l/Gc_p)] \tag{23}$$

where

G = mass flow rate of transport fluid per unit of collector area, $kg/h \cdot m^2$

c_p = specific heat of transport fluid, kJ/kg·°C

U_l = heat-loss coefficient of collector, kJ/h·m^2·°C

F' = collector efficiency factor determined wholly by the collector design, dimensionless

The above expression is generally applicable to any type of collector. Whillier (1953) noted that the value of F_R is essentially independent of solar intensity and the operating temperature of the collector, other than the latter's influence on the heat-transfer coefficients.

Derivation of the collector efficiency factor, F', was originally presented by Whillier (1953) and subsequently discussed in detail by Bliss (1959). Equations for evaluating F' are given by Duffie and Beckman (1974) and Whillier (1977) for several common flat-plate collector designs.

In actual tests, the rate of useful heat gain may be directly evaluated from the basic heat equation:

$$Q_u = m_a c_p (T_{fo} - T_{fi}) \tag{24}$$

where

Q_u = net rate of useful energy gain, kJ/h

m_a = mass flow-rate of transport fluid, kg/h

c_p = specific heat of transport fluid, kJ/kg·°C

T_{fo} = transport fluid temperature at collector outlet, °C

T_{fi} = transport fluid temperature at collector inlet, °C

A measure of collector performance is the collector efficiency, η_{coll}, defined by Duffie and Beckman (1974) as the ratio of useful heat gain over any time period to the incident solar radiation over the same time period:

$$\eta_{coll} = \frac{\int q_u dt}{\int I_{coll} dt} \times 100 \qquad (25)$$

where

η_{coll} = collector efficiency, percent

I_{coll} = total insolation rate incident on a unit area of collector surface, W/m^2

q_u = rate of useful heat collection per unit area of collector surface, W/m^2

dt = differential time element

Solar Grain Drying

Early studies

One of the earlier research studies on the potential use of solar energy for grain drying was reported by Buelow and Boyd (1957). Their work was based on previous studies by Hottel and Woertz (1942), Carnes (1932), Hottel and Whillier (1955) and Buelow (1956). Design of the solar collector for air heating was a covered flat-plate type which consisted of a metal absorber plate with 1.27-cm air spaces between a standard window glass cover above the absorber plate and insulation below. Collector efficiency of 70 percent was reported for an air

temperature rise of 2.8° C and airflow rate of 0.023 m^3/s per square meter of collector area.

From information gathered by Buelow and Boyd (1957), Buelow (1958) conducted solar grain drying tests employing two types of solar collectors: single-glass covered and 'no-glass cover', mounted as an integral part of a farm building roofing oriented to the south. Test results showed average temperature rises of 5.6 and 2.5° C and collector efficiencies of 84 and 45.6 percent for the glass-covered and the 'no-glass' or bare plate collector, respectively. With a non-heated control system as reference, it was also reported that the glass-covered and 'no-glass' solar collectors increased the drying rates by factors of 3.1 and 2.8, respectively.

In a similar study, Lipper and Davis (1960) reported on the use of a clear plastic-covered solar collector with a black-painted corrugated sheet metal absorber for corn drying tests. It was found that corn dried better and faster with the solar dryer using 50 percent less electricity than a conventional system.

Research studies during the first half of the 1960s were conducted primarily to investigate some of the factors influencing the design and performance of solar air-heating collectors for grain drying.

At West Virginia University, Longhouse (1961) conducted experimental tests on plastic-covered solar heat collectors of different absorber plate configurations: curved, flat and corrugated, all made of aluminum and painted flat black. No significant differences in efficiencies were found among the three types. Average collector efficiencies reported

were 52.3, 50.4 and 50.1 percent for the curved, flat and corrugated collectors, respectively. It was, however, noted that collector efficiencies of 50 percent and above were attained when insolation rates exceeded 18.2 MJ/m^2 · day and decreased to just over 30 percent during an overcast day when insolation rate was 7.95 MJ/m^2 · day.

Remmers (1962) reported a collector efficiency of approximately 50 percent on a test conducted at the University of California, Davis. The solar collector used was a 3.41-m^2 glass-covered type, 4.8 m long consisting of a 26 gage corrugated metal absorber with corrugations running parallel to the airflow. At an air velocity of 2.07 m/s, a temperature rise of 2.8° C through the collector was observed. Remmers also found that conduction heat loss from the collector was relatively small in comparison to that lost by convection and radiation. It was further noted that polyethylene plastic cover material which was originally used in the experiment had a tendency to stretch or melt when the collector became hot.

At Michigan State University, Sobel and Buelow (1963) built and tested an experimental bare-plate solar collector which was similar to a roof section of a building. It was noted that the simple form can be easily incorporated into the construction of a conventional building roof, thus reducing the initial cost of the collector. The only additional feature necessary was having some type of material at the underside to form an air duct. Parameters investigated included effects of various roof-surface conditions and configurations, air passage depths and airflow characteristics on collector efficiency.

Sobel and Buelow found that the most desirable roof surfaces for solar heating were corrugated surfaces with corrugations at right angles to the airflow and with either a new-painted, weathered or weathered-painted surface condition. It was also reported that 7.62- and 10.16-cm nominal air passage depths had a low enough pressure drop to be of practical value, and that no significant difference in collector efficiency was found between the two depths. Although 2.54- and 5.08-cm air passage depths were found to have higher efficiencies, the pressure drops were considered impractical for most applications. Collector efficiency of 42 percent was reported for weathered galvanized steel roof surfaces with corrugations at right angles to airflow, 10.16-cm air passage depth and airflow rate of 0.051 m^3/s per square meter of collector surface.

In England, Bailey and Williamson (1965) experimented on direct use of solar energy for grain drying with particular application to tropical crops such as rice. The apparatus used was basically a free-convection solar grain drying system consisting of a damp-resistant hardboard painted matt-black on which material to be dried was spread thinly at a depth of 2.13 to 5.08 cm. A transparent roof of clear cellulose acetate plastic was placed over the material as protection from rain. Results showed no difference between plastic-covered direct solar drying and drying grains spread on a plastic bed laid on the ground. It was noted that drying was considerably improved when airflow was

controlled and directed downwards through the material laid on perforated metal flooring. Controlled airflow rate used was 0.0051 m^3/s per square meter of grain surface area.

Solar collectors used for grain drying

Research studies on solar grain drying were temporarily interrupted due to the predominance of high-temperature, high-capacity grain drying systems which use the more reliable fossil fuel. Interest on solar grain drying was restored in response to the 1973 fuel crisis.

Recent efforts have been directed toward the use of simple and inexpensive solar collectors. Numerous research studies, mostly in the midwestern states of the U.S., have indicated feasibility of low-temperature solar and solar-assisted grain drying systems.

Foster and Peart (1976) assessed the state of the art of solar grain drying and described several solar heat collectors used in grain drying tests. Heid (1978) also reviewed and analyzed the performance and economic feasibility of various solar grain drying systems used or in progress.

Solar heat collectors used in low-temperature grain drying may be categorized into four general types: (1) bin wall or wrap-around solar collectors, (2) integrated building roof-wall solar collectors, (3) free-standing flat plate solar collectors, and (4) air-supported inflatable plastic collectors. Other types of solar collector designs are also described.

Wrap-around solar collectors Peterson (1973) reported on drying of shelled corn from 24 to 14 percent moisture content in 4.5 days using

a solar collector built into the drying and storage bin with no other heat source except that obtained from the electric motor of the dryer fan. The collector was a suspended bare-plate type wrapped around the southern two-thirds wall of a typical round bin. Heid (1978) described the collector as having a 10.16-cm air space and average airflow rate of 0.0895 m^3/s per square meter of collector area. Airflow rate to grain volume ratio was 0.124 m^3/s per cubic meter. Peterson and Hellickson (1976) later tested several types of solar collector designs mounted on the bin wall and found that black-painted bare sheet corrugated collectors can be just as efficient as plastic-covered collectors and can be installed at a lower cost. They further reported that a solar supplemented bin drying system used 26 percent less energy per percentage point of moisture removed compared with conventional low-temperature drying systems.

A similar approach was used by Morrison and Shove (1975) at the University of Illinois in drying shelled corn from 24 to 16.5 percent moisture content. Test results indicated collection efficiencies of 12 percent for the unpainted collector and 30 percent when collector surface was painted black. Temperature rise through the collector was reported to be 2.2° C at an airflow rate of 0.99 m^3/s.

Stone and Currelly (1979) reported a recent study on a wrap-around solar heat collector used in low-temperature grain drying at Ontario, Canada. The solar collector consisted of a black-painted flat galvanized metal absorber covering the southern half of a grain bin wall, and a fiberglass coverplate forming a 15-cm air space between them. The

southern half of the bin roof was also utilized as a solar collector. No collector performance tests were reported. However, it was found that total annual costs per unit of grain dried was lower than two other low-temperature units tested.

Integrated building roof-wall solar collectors Bauman et al. (1975) described a successful grain drying installation and management scheme wherein solar heat was collected from the corrugated galvanized metal roof of a metal storage building to which rather simple modifications were made. The approach was similar to that proposed earlier by Sobel and Buelow (1963). The 22.9-m by 18.3-m unpainted roof served as the bare-plate solar absorber. One-third of the roof area was fitted with a false ceiling from which a 20.3-cm deep air channel was formed. The installation was intended to provide supplemental solar heat to a nearby low-temperature grain drying bin.

Initial tests in 1974 and 1975 indicated collection efficiencies of 10 and 20 percent, respectively, at an airflow rate of 0.051 m^3/s per square meter of the ducted roof collector area. Results of a five-year series of drying tests at Markesan, Wisconsin were summarized by Bauman and Finner (1979). They noted that with improvements in the management of the natural/solar drying system, energy and cost savings of approximately 50 percent can be realized.

Hall (1978) reported on a solar collector with clear fiberglass cover built into the roof of a farm machinery shed located near Quincy, Illinois. The system was designed to provide low-cost energy for grain drying and supplemental heat for a shop area of the building. The

464-m^2 roof collector consisted of a 1.27-cm asphalt impregnated fiber board solar absorber and a fiberglass roof with an air channel formed in-between. Air is pulled through the collector under negative pressure by dryer fans of two grain bins ducted to the building. Airflow rate measured was 0.33 m^3/s or an equivalent of 0.000712 m^3/s per square meter of collector area. Pressure drop through the collector was 112.1 Pa.

Test results for a 13-day period indicated an average collector efficiency of 25.0 percent at an average 10-h day temperature rise of 5.9° C. It was observed that asphalt impregnated fiber board used as the absorbing surface lost its strength at high temperatures and showed extreme sagging.

In Southeast Virginia, Lambert and Vaughan (1978) designed and tested an integrated shed solar collector for batch drying peanuts and grains. The roof collector consisted of translucent corrugated fiberglass panels. In addition, a flat-plate absorber consisting of matte-finish, perforated black polyester sheet with 50 percent of the material punched out, was installed between the rafter and purlins. Below the rafter, black-painted plywood sheets were installed. The matrix material was added to improve the collection efficiency.

Collection efficiency determined from a homogeneous section of the roof collector was reported to vary from 22 to 86 percent at an airflow rate of 0.217 m^3/s through the section. It was reasoned that higher efficiencies were probably due to heat gains from thermal storage in the building materials and from variations in data collection due to cloud cover on non-instantaneous recordings. The solar drying facility

was found to be economically feasible for multiple crop use with a pay-back period of about 5 years and a collector cost of $\$16.15/m^2$ of surface area.

Air-inflated plastic collectors Research studies involving use of air-inflated plastic collectors for grain drying were reported by several investigators.

Meyer et al. (1975) used a 3.7-m by 25.6-m plastic air-supported solar collector available commercially, for drying soybean seed and shelled corn. The collector was described as having three layers of 0.25-mm thick vinyl ultra-violet stabilized plastic with the top clear, middle layer tinted (primary absorber) and the one nearest the ground opaque. The ground-anchored collector was supported by air at a static pressure of 37.4 Pa delivered by a 0.373-kW centrifugal fan.

Collection efficiency variations were observed at different times of the year with the lowest in January at 25 percent and the highest in April at 49 percent. Preliminary results on a series of drying tests indicated that the solar collector may be feasible for drying soybeans, however, it was suggested that a backup heating system should be provided to insure against spoilage in the event of prolonged unfavorable weather conditions.

Williams et al. (1976) conducted a full scale demonstration of solar grain drying at Purdue University using an inflatable black tunnel plastic collector purchased from a private manufacturer. The unit was air-inflated by a 0.373-kW fan delivering 1.13 m^3/s of air. Overall collector efficiencies of 21, 26 and 27.2 percent were obtained for 8-h day operations

during 1974, 1975 and 1976 tests, respectively. Collector operation was nearly trouble free except that the inflatable collector has a limited useful life of 6 years with 2-month exposures each year.

McLendon and Allison (1978) also reported on shelled corn drying tests at the University of Georgia using an air-inflated plastic collector similar to that used earlier by Meyer et al. (1975). They found that there was a 50 percent reduction in heat requirement compared with a conventionally heated system although drying time was 2 to 4 times longer with the solar drying system. They also noted that the probability of successfully using a total solar drying system was remote due to the extended drying period.

Chau et al. (1978) designed and constructed an experimental air-inflated plastic solar collector at the University of Florida for use in grain drying under conditions of high ambient air temperatures and humidity. Collection efficiency of the 3.7-m by 29.3-m collector was determined for a range of airflow rates. Expressed in equation form it is:

$$\eta = (-1.395 \times 10^{3})X^{2} + 43.31X \qquad (26)$$

where

η = collection efficiency, percent

X = airflow rate through the collector, $m^3/s \cdot m^2$ of collector surface area

Results of tests showed that the collector was capable of raising the air temperature by an average of 22.2° C during the day. It was also observed that aflatoxin production in the grain was minimal when drying time was less than 6 days.

Free-standing flat-plate solar collectors At Iowa State University, Kranzler et al. (1975) investigated the economic feasibility of a solar-heat supplemented low-temperature grain drying system using a plastic covered flat-plate solar collector. The unit consisted of a clear polyethylene plastic cover, a suspended black polyethylene absorbing surface and a plywood bottom. Air was drawn through the top and bottom of the absorber plate at the rate of 0.991 m^3/s. Average daytime collection efficiency reported was 40 percent with a maximum air temperature rise of 5.6° C. From results of drying tests, it was found that solar energy can supply 18 percent of the energy requirement in low-temperature shelled corn drying with a savings of 24 percent in energy costs over a conventional system.

Roa and Macedo (1976) also utilized a suspended flat-plate solar collector in successfully drying 'carioca' beans in Brazil. The 0.8-m by 10-m collector consisted of a black-painted galvanized iron sheet absorber plate with polyethylene plastic film covers above and below it. An average collector efficiency of 45 percent was reported at an airflow rate of 0.0163 m^3/s per square meter of collector area and an average air temperature rise of 16.5° C.

Heid (1978) described a portable flat-plate collector used in corn drying experiments at the U.S. Grain Marketing Research Center in Manhattan, Kansas. The 148.6-m^2 collector was built in two sections with one section having a corrugated sheet metal roofing absorber and the other section with deep V-shaped design absorber plate. The collector has a translucent polyvinyl coverplate and a styrofoam-insulated plywood

base. Air is drawn through a 7.62-cm channel at the rate of 0.0034 m^3/s per square meter of collector surface area. No collection efficiency was reported; however, results of a corn drying test from one bin showed moisture content reduction from 22 to 11.7 percent in 12 days at an estimated total drying cost of $\$5.08/m^3$ of grain dried.

Heid (1978) noted that later generation flat-plate collectors have corrugated fiberglass covers with a projected life of 20 years.

Other types of solar heat collectors Heid (1978) described several other types of solar collector designs used in grain drying experiments. One of them is a stationary intensifier solar system which utilized a solar reflector that intensified solar radiation at a concentration ratio of 4:1 on a vertical corrugated steel collector surface.

Another type was a portable multi-use glass-covered solar collector connected to a rock heat-storage bin. The system was designed to provide heat for nighttime drying.

Foster and Peart (1976) described a fiberglass covered solar collector-rock heat storage unit containing 29.0 metric tons of fist-size screened limestone rocks which served as the heat collecting and storage medium. The collector-storage unit also supplied most of the heat during nighttime drying.

Favorable results on corn drying experiments have been reported on the use of the intensifier system and solar collector-rock heat storage units, however, capital investment costs were too high.

Exell and Kornsakoo (1978) developed a low-cost solar rice dryer at the Asian Institute of Technology in Thailand. The system functions

by natural air convection wherein air is drawn over a solar collecting surface made of burnt rice husks spread on the ground. Air is heated to temperatures of 40 to 45° C and enters a batch drying compartment containing rice grains stacked 15 cm deep.

It was reported that drying of 1/2 ton of rice can be completed in one sunny day or in two or three days of cloudy weather.

Comparisons of solar collector designs and performance

Performance of pilot-scale solar collectors of various designs for use in grain drying was reported by Kline (1977). Both air-supported and rigid-frame collectors were included. Collector absorbing surfaces used were of flat and curved designs, both covered and bare, and either single-air channeled or with suspended absorber plates. Materials used included plastic film, rigid plastic, glass, metal and wood. Collector configurations vary but all were 9.1 m long with an effective collection area of 8.4 m^2. Airflow rates in each collector were identical for comparative tests. The pilot-scale collection efficiencies were summarized for noon hours and for full day operations.

Results of the tests showed that lowest efficiencies were obtained with bare plate collectors. Highest efficiencies were observed for suspended plate collectors with insulated backplates. Kline noted that performance of low efficiency collectors was enhanced by using planar reflectors made of either plywood or chipboard and covered with aluminum foil. Overall collector efficiencies for full day operations ranged from 11 to 57 percent. It was also reported that collection efficiency increased with an increase in airflow rates.

Wrubleski et al. (1979) reported on the assessment of three types of solar collectors for use in grain drying and livestock building heating. The three full-scale solar collector models were: (1) wrap-around solar collector, (2) integrated roof-wall collector, and (3) A-frame collector with rock heat-storage.

Choice of the three collector configurations was based on the summary report of Heid (1978) on performance and economic feasibility of solar grain drying systems. The researchers believed that many problems show themselves when full scale models are used and that results would be more credible to farmers.

Test results showed that the integrated roof-wall collector on a square bin was the most practical and most efficient design. The A-frame collector-storage combination system was found to be impractical due to excessive costs. The wrap-around collector on the round bin was found to work well enough to dry grain but was found to be a difficult system to construct.

Simulation of solar grain drying

Drying simulation models that were developed for predicting performance of grain dryers and grain drying systems in the past have recently been employed to predict drying results for solar and solar-supplemented grain drying systems.

Pierce and Thompson (1976) used a computer simulation model by Thompson (1972) in comparing possible advantages of solar energy in grain drying over other low-temperature grain drying modes. Simulation results

indicated that proper airflow rate was the most important factor required to successfully complete drying for a given set of conditions. Solar energy was found to be more effective in reducing airflow requirements in warmer, more humid areas and that it reduces the drying time and increases the probability that drying will be completed at a specific period of time. Pierce and Thompson also cited the problem of excessive overdrying which occurred with the addition of supplemental heat in full-bin drying.

Troeger and Butler (1977) reported on simulation of solar peanut drying using TRNSYS, a transient simulation program developed by the Solar Energy Lab at the University of Wisconsin. Modification and additions were made on the TRNSYS program to include simulation of hourly ambient air temperature and solar radiation from daily data and a program for simulating deep-bed drying of peanuts. Results of comparisons with actual experimental data showed that simulated results gave reasonable estimates of the real data.

Foster and Peart (1976) cited other simulation work in progress at various locations, most of which were mainly directed toward verification of simulation models with available data and development of improved models for solar collector performance for grain drying.

Morey et al. (1978) reported on the status of grain drying simulation in general and indicated that further work is needed in developing models which would accurately predict grain quality in both low-temperature and heated-air drying.

Engine Waste Heat Utilization

Soemangat et al. (1973) reported on rice drying using waste heat from the engine driving the fan of a low-temperature flat-bed mechanical dryer. Tests were conducted to simulate rice drying under tropical conditions of 29.4° C and 80 percent relative humidity.

Results of tests on fan-engine performance showed that decreasing the airflow rate increased the air temperature rise through the engine. However, the energy added to the air was reduced.

Drying tests using engine heat as the only heat source showed that the highest drying rate attained with no reduction in grain quality was 107.7 kg/h at a drying air temperature of 32.2° C, an airflow rate of 0.051 m^3/s per square meter of bed area, and a grain depth of 0.305 m. It was also found that when auxiliary heat was added to increase the drying air temperature to 35 and 43.3° C, drying rate increased to 128 and 189 kg/h, respectively.

Soemangat et al. noted that the percentages of total heat contributed by engine waste heat and auxiliary heat to raise the temperature of the drying air to 35 and 43.3° C were:

Drying air temperature (°C)	Engine waste heat (percent)	Auxiliary heat (percent)
35	66.7	33.3
43.3	33.6	66.4

No reduction in grain quality was detected on the dried grain with the above drying air temperatures.

Baryeh (1972) earlier reported on the design of a corn dryer for tropical conditions wherein the exhaust heat of the fan engine was directly utilized to raise the temperature of the drying air. No tests were, however, done on the quality of the dried product.

Results of drying tests showed that corn was dried from 19.9 percent to 14 percent moisture content, wet basis, in 30 hours of drying time. Average air temperature rise through the 2.98-kW engine with the casing insulated was 7.6° C. Engine speed was 1600 r/min.

DESIGN AND CONSTRUCTION

Design Considerations

Based on the review of literature, it was shown that solar air heating can be technically and economically feasible for use in low-temperature grain drying systems. Most investigations, however, were concentrated on drying systems which involved temperature rises of a few degrees and drying over extended periods of several weeks or months while the grain is in storage.

In the tropics, ambient air temperature and relative humidity are so much higher that grains are readily susceptible to spoilage unless steps are taken to quickly reduce the grain moisture content to a safe level. Selection of grain drying systems for developing countries in the tropics must also be based on economic factors; thus, it is of primary importance that equipment have low costs and be simple for ease of local production and operation.

Situation in the tropics

To effectively design a solar grain drying system for the tropics, it is worthwhile to consider certain factors inherent in the region. A comprehensive report presented at the Symposia of the Association of Japanese Agricultural Scientific Societies (1975) fully described the rice production and processing situation in tropical Asia. Baryeh (1972) and Soemangat et al. (1973) also provided some insights on the conditions in the tropics. A summary report from the University of the Philippines

Weather Station (1977) furnished updated information on normal values of typical weather conditions in the tropics, specifically in the Philippines. A list of typical conditions and trends that exist in the tropics are as follows:

1. Ambient air temperature - 29.4° C.
2. Relative humidity - 80 percent.
3. Average wind speed and direction - 1.44 m/s NE.
4. Mean annual percent possible sunshine - 50 percent.
5. The daily insolation rate is highest in April at 22.97 $MJ/m^2 \cdot day$ and lowest in January at 10.25 $MJ/m^2 \cdot day$.
6. Major crops grown are rice and corn, with rice as the dominant and staple crop.
7. Average grain yields are 2640 kg/ha for rice and 2735 kg/ha for corn.
8. There are two harvest seasons: wet season harvest is from September to December, and dry season harvest is from May to June. Wet season crops are generally heavier and are mostly rice.
9. Grain moisture content at harvest range from 20 to 25 percent, wet basis.
10. Farm sizes range from 1 to 10 hectares.
11. Trend is in the adoption of short-duration rice varieties of 90 to 120 days.
12. Majority of tropical farmers still dry their grain by spreading it on the ground under the sun.

13. Electricity is not available to most smaller towns and farms.
14. Mechanical grain dryers are available in government demonstration farms and in some farm cooperatives. These dryers are powered by gasoline engines which are also used in driving power tillers and threshers.
15. Most rural houses and farm storage buildings are constructed with corrugated galvanized steel roofing materials.
16. Locally available materials also include plywood, lumber and hardware.
17. There is an abundance of cheap manual labor in the rural sector.
18. Technical assistance to the farmers is available through government agricultural extension workers.
19. Farmers are encouraged to avail themselves of government financial assistance through the rural banks.
20. Government programs are directed towards the consolidation of small farm hectarage into compact farm cooperatives having sizes of 30 to 50 hectares.

Solar heat collector

Choice of the type of solar heat collector would depend largely on the availability of solar heat absorbing materials, material and construction costs, and simplicity of the design. The logical choice would be a bare metal plate solar collector which doubles as roof of a farm house, machinery shed or storage building.

As mentioned earlier, common roofing materials used in the tropics are corrugated galvanized steel sheets. An existing building roof can be installed with a false ceiling to form an air channel which can be ducted to a grain drying unit with a minimum of construction cost. New farm buildings may also be designed with an integrated roof collector having a slope and orientation that would be optimum during the drying months. Use of weathered or flat-black painted corrugated roof would further increase the efficiency of the collector.

Use of a transparent cover on the roof collector such as clear plastic, fiberglass or window glass to increase collection efficiency and heat gain has been considered; however, higher capital investment costs and other related costs such as maintenance and replacement costs may prove to be an economic burden for a tropical farmer with limited financial resources.

Design and construction details of a bare plate roof collector have been described earlier by Buelow (1958), Sobel and Buelow (1963) and Bauman et al. (1975).

Grain drying unit

The design of a solar heat collector for grain drying is basically dependent on the capacity of the grain drying unit. Unlike in the U.S. and other highly productive countries in the West, the type and capacity of grain drying systems in the tropics are constrained by several factors: (1) the slow rate at which the crop is harvested or threshed, (2) the

necessity of drying the grain within 24 hours to prevent germination and mold growth and (3) financial limitations.

Economic factors dictate that design of a grain drying system for tropical conditions must be simple and inexpensive and yet perform its intended use. The concept of intermediate technology would be appropriate in this situation.

Boyd (1976) described two low-cost portable mechanical grain dryers that are commercially available and are being used by tropical farmers at the village level. A flat-bed batch type dryer designed by the International Rice Research Institute in the Philippines is simple and easy to manufacture and operate. The kerosene-fired dryer can dry a ton of rice in 4 to 6 hours of operation. Waste heat from the fan engine is also utilized in the drying process.

A similar type was also developed at the Institute of Agricultural Engineering and Technology of the University of the Philippines. The dryer consisted of a plywood grain drying bin, a kerosene burner for air heating and a gasoline engine-powered fan. The dryer was designed to dry 1760 kg of rice in 6 to 8 hours of operation.

Both dryers, however, suffer from high operating costs since the cost of kerosene fuel has risen rapidly. It is thought that retrofitting the existing units with solar heat collectors and making use of the waste engine heat would maintain the drying capacity of the units without necessarily sacrificing the simplicity and ease of operation of the drying systems.

Theoretical Design Calculations

A method of calculation is presented to predict the performance of a bare plate solar heat collector operating under tropical conditions. Calculation of solar collector area necessary to provide solar heat energy for a typical grain drying system in the tropics is also presented. Basic information used in the calculations are derived from 'design considerations' and are presented in Table I.

Collector dimensions

The basic design of a bare plate solar heat collector installed as an integral part of a roof structure is shown schematically in Figure 3. The longitudinal section along the direction of airflow is shown in Figure 3a. Figure 3b illustrates the roof construction with purlins between the corrugated roofing absorber plate and plywood back-plate. The air channel depth is specified at 6.35 cm based on recommendations of Sobel and Buelow (1963).

The depth and effective width of collector air channel determine the air velocity on the collector for a given airflow rate. Kreith (1973) stated that high air velocities increase the turbulence of fluid flow and effectively contribute to higher rates of heat transfer. For optimum design of a heat exchanger, Kreith recommends fluid velocities corresponding to Reynolds numbers not exceeding 5×10^4. Turbulent flow exists at Reynolds number greater than 1×10^4.

Table I. Basic information used in the design of a solar-heated grain drying system

Factor	Specification
Location and Latitude	Philippines, Latitude 14° N
Date	September 21
Collector type	Bare-plate
Collector absorber plate	Corrugated galvanized steel roofing sheet, painted flat-black
Backplate insulation	Plywood, 12.7-mm thick
Ambient air temperature, °C	29.4
Relative humidity, %	80
Wind speed, m/s	1.44
Grain to be dried	Rice
Grain initial m.c., %, w.b.	22.5
Grain final m.c., %, w.b.	14.0
Grain drying unit:	
type	Flat-bed, batch type
bed dimensions	1.83 m by 3.66 m
capacity, kg.	1760
power source	3.73-kW gasoline engine
fan capacity, m^3/s	1.42
Drying period, h per day	8 (8:00 a.m. to 4:00 p.m. solar time)

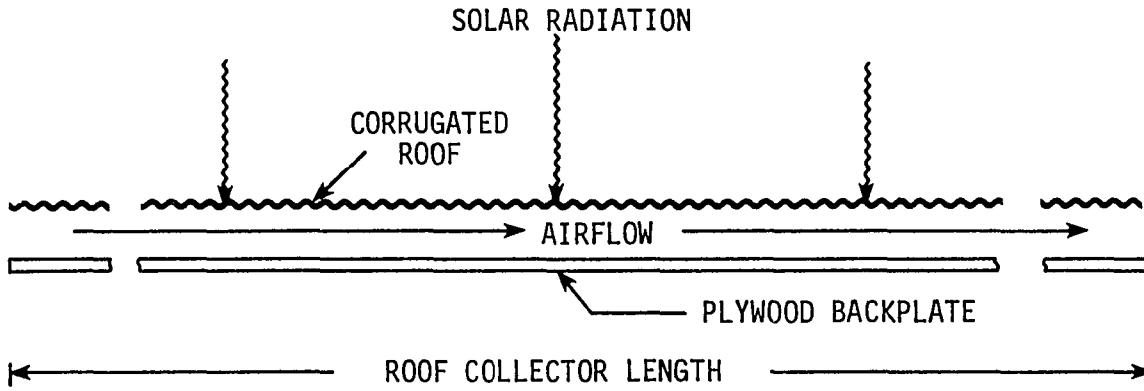

(a) LONGITUDINAL SECTION OF ROOF COLLECTOR CHANNEL

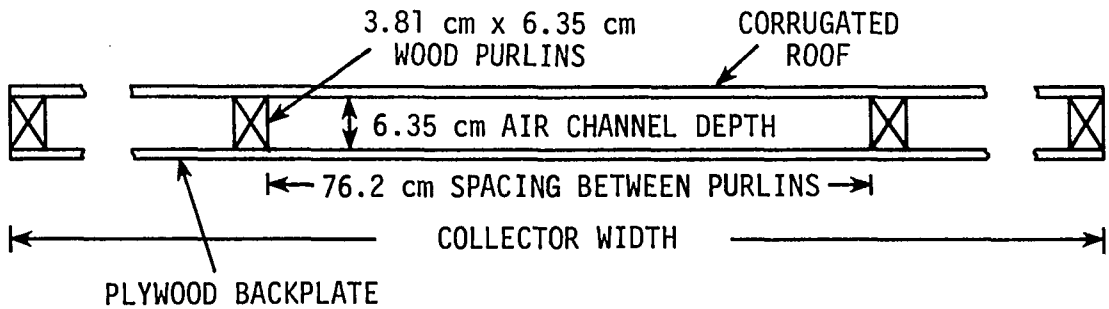

(b) CROSS-SECTION OF ROOF COLLECTOR CHANNEL

Figure 3. Schematic diagrams of bare-plate solar roof collector

The effective air channel width may be obtained from known dimensions of typical corrugated roofing materials. Commercially available materials have a size of 2.4 m by 0.91 m with corrugations along the length.

Considering a roof section consisting of two corrugated metal roofing sheets with 1.52-cm overlap on the shorter side, resting on 3.81-cm by 6.35-cm purlins 76.2 cm apart, as shown in Figure 3b, the roof collector would have an effective air channel width of 4.46 m. At an airflow rate of 1.42 m^3/s (from Table I), the air velocity, V, through the collector is

$$V = \frac{1.42}{(0.0635)(4.46)} = 5 \text{ m/s}$$

The characteristic length is the hydraulic radius, D_H, which for flat plates is twice the channel depth. Assuming a collector mean air temperature of 35° C, air density, ρ_a, is 1.1397 kg/m^3 and air viscosity, μ_a, is 19.123 x 10^{-6} Pa·s. The Reynolds number is

$$Re_{D_H} = \frac{\rho_a V D_H}{\mu_a} = \frac{(1.1397)\ (5)\ (2 \times 0.0635)}{19.123 \times 10^{-6}} = 3.78 \times 10^4$$

Hence, airflow in the collector channel is turbulent.

Reynolds number can be further increased by increasing the air velocity. This can be done by either decreasing collector width or depth, or, by increasing the airflow through the collector. For a fixed airflow rate and air channel depth, Reynolds number can only be increased by reducing the effective width of the collector. In reducing the collector width to half of the original dimension, air velocity and Reynolds number will be doubled. However, twice as much

collector length would be required and higher air pressure drops would occur.

Optimum collector tilt angle

For September 21 and at latitude 14° north (from Table I), the optimum collector tilt angle, Σ, determined at solar noon and with a south-facing collector is

$$\Sigma = 90 - \beta$$

where

Σ = optimum tilt of collector, degrees

β = solar altitude angle at solar noon, degrees

Figure 4 illustrates the geometric relationship of solar altitude and collector tilt angles at solar noon.

The hour angle, ω, at solar noon is zero. From Appendix A, solar declination on September 21 is zero degree, hence, solar altitude angle, β, from equation (3) is

$$\beta = \sin^{-1} (\cos 14 \cos 0 \cos 0 + \sin 14 \sin 0) = 76°$$

and the optimum collector tilt angle, Σ, is

$$\Sigma = 90 - 76 = 14°$$

Solar heat energy absorbed by collector

Solar heat energy absorbed by the collector is a function of solar absorptance of the absorber plate and insolation rate incident on collector surface. Kreider and Kreith (1977) noted that solar absorptance to direct radiation, α_D, varies with the angle of incidence, θ.

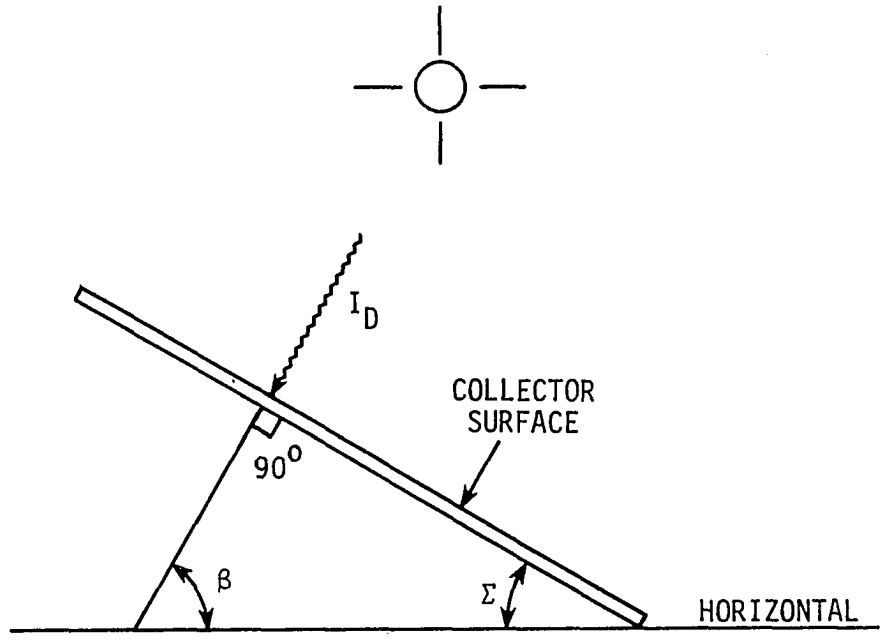

Figure 4. Geometric relationship of solar altitude and collector tilt angles at solar noon

Table II shows the angular variation of solar absorptance of a typical non-selective black-painted surface. Kreider and Kreith adapted the data in Table II from the work of Löf and Tybout (1972). Solar absorptance to diffuse sky radiation, α_d, can be obtained by taking the specular absorptance of the absorber plate at an incidence angle, θ, of 60 degrees.

Calculation of half-day insolation rates on the tilted collector are presented in Table III. Data in the table are clear day values on September 21 at latitude 14° north. Collector tilt angle is 14° from the horizontal and facing south. A sample calculation at 8:00 a.m. solar time is presented in Appendix B. From Table III, the mean daily total

Table II. Angular variation of solar absorptance of lamp-black paint[a]

Incidence angle, θ (degrees)	Absorptance, α_D (dimensionless)
0 - 30	0.96
30 - 40	0.95
40 - 50	0.93
50 - 60	0.91
60 - 70	0.88
70 - 80	0.81
80 - 90	0.66

[a]Source: Löf and Tybout (1972).

Table III. Half-day calculated values of incident solar radiation rates and related data on September 21

Solar time	I_{DN} (W/m^2)	$I_{D,coll}$ (W/m^2)	$I_{d,coll}$ (W/m^2)	I_{coll} (W/m^2)
8	798.8	399.4	72.4	471.8
9	889.0	628.6	80.6	709.2
10	932.1	807.2	84.5	891.7
11	952.6	920.2	86.4	1006.6
12	958.8	958.8	86.9	1045.7

incident insolation rate $\bar{I}_{coll}$ calculated from 8:00 a.m. to 4:00 p.m. solar time is 800.48 W/m^2. Insolation rates from 1:00 p.m. to 4:00 p.m. solar time were assumed symmetrical to the first half of the day.

From equations (15), (16) and (17), the rate at which solar energy is absorbed in the collector, q_a, may be written as

$$q_a = \alpha_D I_{Dcoll} + \alpha_d I_{dcoll} \quad W/m^2$$

where

I_{Dcoll} = HR_D. Direct solar radiation incident on collector surface, W/m^2

I_{dcoll} = HR_d. Diffuse sky radiation falling on the tilted collector, W/m^2

α_D, α_d = solar absorptance to direct and diffuse radiation, respectively, dimensionless

Tabulated results of calculations for the rate of solar heat energy absorbed in the collector based on information provided in Tables II and III, are presented in Table IV. The mean daily rate of solar energy absorption, $\bar{q}_a$, calculated from 8:00 a.m. to 4:00 p.m. solar time is 753.96 W/m^2.

Thermal loss coefficient

Duffie and Beckman (1974) noted that the collector thermal loss coefficient, U_l, is a function of absorber plate temperature. To determine U_l, an iterative approach is necessary since the absorber plate temperature is not usually known and varies along the collector

Table IV. Half-day calculated values of solar energy absorption rate in the collector and related data on September 21

Solar time	Incidence angle, θ (degrees)	α_D (dimensionless)	α_d (dimensionless)	$(\alpha I)_{Dcoll}$ (W/m^2)	$(\alpha I)_{dcoll}$ (W/m^2)	q_a (W/m^2)
8	60	0.91	0.91	363.5	65.9	429.4
9	45	0.93	0.91	584.6	73.3	657.9
10	30	0.95	0.91	766.9	76.9	843.8
11	15	0.96	0.91	883.4	78.6	962.0
12	0	0.96	0.91	920.4	79.1	999.5

length and during the day. A mean collector plate temperature, T_{pm}, may, however, be approximated.

A heat balance on the collector absorber plate is employed to derive an approximate value of the mean plate temperature based on certain assumptions. Hottel and Whillier (1955) noted earlier that the absorber plate temperature depends primarily on the temperature of the incoming fluid stream and to a lesser extent on other factors. A mean collector fluid temperature, T_{fm}, of 35° C assumed earlier will be used for an initial approximation of the mean absorber plate temperature.

Figure 5 shows the heat transfer factors affecting the heat balance on the collector absorber plate where:

T_{fm} = mean air fluid stream temperature, 35° C

$T_b = T_{fm}$. Backplate inner surface temperature, °C.

T_a = ambient air temperature, 29.4° C

$T_s = T_a$ · Sky temperature, °C

T_{pm} = mean absorber plate temperature, °C

$\bar{q}_a$ = rate of solar energy absorption in the collector, 753.96 W/m^2

h_w = convective heat transfer coefficient between the collector plate and the surroundings, $W/m^2 \cdot °C$

h = convective heat transfer coefficient in the collector channel, $W/m^2 \cdot °C$

$h_{r,p-s}$ = radiative heat transfer coefficient between the plate and the sky, $W/m^2 \cdot °C$

$h_{r,p-b}$ = radiative heat transfer coefficient between the collector plate and backplate, $W/m^2 \cdot °C$

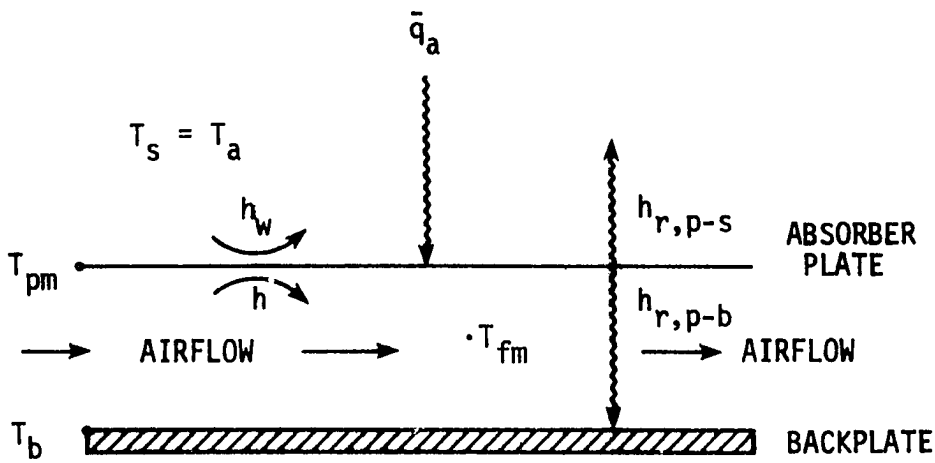

Figure 5. Heat transfer factors affecting heat balance on bare plate solar absorber

The assumption that ambient air temperature, T_a, can be used instead of sky temperature, T_s, was utilized by Hottel and Woertz (1942) and recommended by Tabor (1955). Duffie and Beckman (1974) and others also used the same assumption in their analyses.

The backplate inner surface temperature, T_b, was assumed equal to the air fluid stream temperature, T_{fm}. An experimental investigation by Tan and Charters (1970) on asymmetrical heating of a rectangular duct showed a very small difference between the bulk air temperature and the unheated inner wall of the duct. They further suggested that for flat plate solar heat collectors, the convective heat transfer coefficient, h, should be obtained from the relationship

$$Nu = 0.018 \quad Re^{0.8} Pr^{0.4}$$

where

$Nu = \frac{h D_H}{\kappa_a}$ · Nusselt number, dimensionless

Re = Reynolds number, dimensionless

Pr = Prandtl number, dimensionless

κ_a = air thermal conductivity, W/m·°C

For an assumed collector mean air temperature, T_a, equal to 35° C, air thermal conductivity, κ_a, is 0.02665 W/m·°C and Prandtl number, Pr, is 0.72. From previous calculations, hydraulic radius, D_H, is twice the air channel depth or 0.127 m and Reynolds number, Re, for a two-length roof section is 3.78×10^4, hence,

$$Nu = \frac{h D_H}{\kappa_a} = 0.018 \ (3.78 \times 10^4)^{0.8} \ (0.72)^{0.4} = 72.477$$

and

$$h = (72.477)\frac{\kappa_a}{D_H} = (72.477)\frac{0.02665}{0.127} = 15.21 \quad W/m^2 \cdot °C$$

The convective heat transfer coefficient, h_w, between the exposed absorber plate and the surroundings was related to the wind speed by McAdams and presented by Duffie and Beckman (1974) as

$$h_w = 5.7 + 3.8V_w$$

where V_w is the wind speed in meters per second. For the given wind speed of 1.44 m/s (from Table I),

$$h_w = 5.7 + 3.8(1.44) = 11.172 \ W/m^2 \cdot °C$$

Assuming steady-state conditions and no heat storage, heat balance on the collector absorber plate is

$$\bar{q}_a = q_{co} + q_{ro} + q_{ci} + q_{ri}$$

where

$\bar{q}_a$ = mean rate of solar energy absorption by collector absorber plate, 753.96 W/m^2

$q_{co} = h_w (T_{pm} - T_a)$. Heat loss due to convective air currents on top of bare plate collector, W/m^2

$q_{ro} = \varepsilon_p \sigma (T_{pm}^4 - T_a^4)$. Heat loss due to radiation from exposed absorber plate, W/m^2

$q_{ci} = h(T_{pm} - T_{fm})$. Convective heat transfer from collector plate to fluid stream, W/m^2

$$q_{ri} = \frac{\sigma(T_{pm}^4 - T_b^4)}{\frac{1}{\varepsilon_p} + \frac{1}{\varepsilon_b} - 1}$$. Radiative heat transfer between collector plate and backplate, W/m^2

ε_p = emittance of absorber plate, dimensionless

ε_b = emittance of backplate, dimensionless

$\sigma = 5.6697 \times 10^{-8}$ $W/m^2 \cdot °K^4$. Stefan-Boltzman constant

From Aldrich et al. (1972), emissivity of black-painted steel, ε_p, is 0.5462. From Kreith (1973), emissivity of wood, ε_b, is approximately 0.93.

Substituting corresponding values to the heat balance equation

$$753.96 = 11.172\ (T_{pm} - 302.55) + 0.5462\ (5.6697 \times 10^{-8})$$

$$(T_{pm}^4 - 302.55^4) + 15.21\ (T_{pm} - 308.15)$$

$$+ \frac{5.6697 \times 10^{-8}\ (T_{pm}^4 - 308.15^4)}{\frac{1}{0.5462} + \frac{1}{0.93} - 1}$$

where all temperature values are in degree Kelvin, absolute.

Rearranging terms and simplifying

$$9.3487 \times 10^3 = 6.0713 \times 10^{-8}\ T_{pm}^4 + 26.382\ T_{pm}$$

By trial and error, the mean collector plate temperature, T_{pm}, is 328° K or 55° C.

Assuming that solar collector area would be large compared with collector perimeter area, edge losses may be neglected, hence, equation (19) is reduced to

$$U_l = U_t + U_b$$

The top heat loss coefficient, U_t, for bare plate collectors is found by adding the convective and radiative heat loss coefficients at the top of the collector:

$$U_t = h_w + h_{r,p-s}$$

where h_w was found to be 11.172 $W/m^2 \cdot °C$

From Duffie and Beckman (1974)

$$h_{r,p-s} = \varepsilon_p \sigma (T_{pm}^2 + T_a^2)(T_{pm} + T_a)$$

and substituting corresponding values,

$$h_{r,p-s} = (0.5462)(5.6697 \times 10^{-8})(328^2 + 302.55^2)(328 + 302.55)$$

$$= 3.89 \ W/m^2 \cdot °C$$

Top heat loss coefficient is thus

$$U_t = 11.172 + 3.89 = 15.062 \ W/m^2 \cdot °C$$

Heat from the collector plate is also lost by convection and radiation to the backplate. The convective heat transfer coefficient, h, was found earlier to be 15.21 $W/m^2 \cdot °C$. From Duffie and Beckman (1974), radiative heat transfer coefficient, $h_{r,p-b}$, is

$$h_{r,p-b} = \frac{\sigma (T_{pm}^2 + T_b^2)(T_{pm} + T_b)}{\frac{1}{\varepsilon_p} + \frac{1}{\varepsilon_b} - 1}$$

$$= \frac{5.6697 \times 10^{-8}(328^2 + 308.15^2)(328 + 308.15)}{\frac{1}{0.5462} + \frac{1}{0.93} - 1}$$

$$= 3.833 \ W/m^2 \cdot °C$$

Finally, backward heat loss from the collector occurs through the plywood backplate and into the atmosphere. Neglecting radiative heat losses from the backplate to the surroundings, bottom heat loss coefficient, U_b, is found from a relationship given by Duffie and Beckman (1974):

$$U_b = \frac{1}{\frac{1}{h + h_{r,p-b}} + R_b + \frac{1}{h_w}}$$

where h, $h_{r,p-b}$ and h_w were defined earlier and R_b is the thermal resistance of the plywood backplate. A thermal resistance, R_b, of 0.284-$m^2 \cdot °C/W$ for the 1.27-cm thick plywood backplate is given in the MWPS Structure and Environment Handbook (Midwest Plan Service, 1977).

Substituting corresponding values, U_b is found to be equal to

$$U_b = \frac{1}{\frac{1}{15.21 + 3.833} + 0.284 + \frac{1}{11.172}} = 2.347 \text{ W/m}^2 \cdot °C$$

The total heat loss coefficient, U_l, is thus

$$U_l = U_t + U_b = 15.062 + 2.347 = 17.41 \text{ W/m}^2 \cdot °C$$

and the mean rate of heat loss per unit area of collector, $\bar{q}_l$, from equation (20) is

$$\bar{q}_l = U_l (T_{pm} - T_a) = 17.41 (55 - 29.4) = 445.7 \text{ W/m}^2$$

Collector performance

Using the data from previous calculations, the mean rate of useful heat collection per unit area of collector surface, $\bar{q}_u$, is found from equation (11):

$$\bar{q}_u = \bar{q}_a - \bar{q}_l = 753.96 - 445.7 = 308.26 \text{ W/m}^2$$

The theoretical average collection efficiency, η_{coll}, of the bare plate solar heat collector tilted at 14° north and operating from 8:00 a.m. to 4:00 p.m. solar time is therefore

$$\eta_{coll} = \frac{\bar{q}_u}{\bar{I}_{coll}} \times 100 = \frac{308.26}{800.48} \times 100 = 38.5\%$$

Verification of the assumptions used in the calculations would involve a collector of known surface area. However, by using the same methods of calculation and assuming a range of collector mean air temperatures, variations in the performance characteristics of the collector may be described.

Table V illustrates the effect of varying the assumed mean air temperature, T_{fm}, on collector mean plate temperature, T_{pm}, thermal loss coefficient, U_l, rate of useful heat collection, q_u, and collector efficiency, η_{coll}, assuming all other factors constant.

The calculated results of Table V clearly show that regardless of the assumed collector mean air temperature, the collector mean plate temperature, T_{pm}, and collector thermal loss coefficient, U_l, do not significantly vary. The useful heat gain, q_u, is observed to be sensitive to changes in the collector mean air temperature. However, collection efficiency did not vary as much.

It is further noted that the theoretical collection efficiencies in Table V are quite high for a bare plate solar heat collector. Typical

Table V. Effect of variation in assumed collector mean air temperature on collector performance characteristics

T_{fm} (°C)	T_{pm} (°C)	U_l ($W/m^2 \cdot °C$)	q_u (W/m^2)	η_{coll} (%)
31	53	17.37	344.03	42.98
33	54	17.39	326.17	40.75
35	55	17.41	308.26	38.51
37	56	17.43	290.32	36.27

collection efficiencies for bare plate collectors reported in previous studies ranged from 10 to 20 percent (Bauman et al. 1975), 4 to 37 percent (Kline, 1977) and up to 42 percent (Sobel and Buelow, 1963).

The higher collection efficiency may be attributed to the following factors: (1) high airflow rate used in the design, (2) high insolation rate in the lower latitude tropics, and (3) high ambient air temperatures and low wind speeds which accounted for the low thermal heat loss from the collector.

Solar collector area

The area of a solar heat collector for grain drying depends primarily on the drying heat load, Q_{load}, of the system. The heat load is determined by the amount of grain to be dried, its initial and final moisture contents, and the time required to complete the drying operation.

The collector heat load, Q_{coll}, and hence the collector area, may be reduced by addition of waste heat from the dryer fan engine.

Heat energy required for drying From information in Table I, a grain load of 1760 kg of rice at 22.5 percent moisture content, wet basis, is to be dried down to 14 percent in 8 hours of operation.

The initial amount of moisture in the grain, W_i, is

$$W_i = (0.225)(1760) = 396 \text{ kg}$$

and the dry matter weight, W_{dm}, is

$$W_{dm} = 1760 - 396 = 1364 \text{ kg}$$

The final amount of moisture in the grain, W_f, at 14 percent moisture content, is found from the relationship

$$0.14 = \frac{W_f}{W_f + W_{dm}}$$

hence

$$W_f = \frac{0.14\ (1364)}{0.86} = 222.05 \text{ kg}$$

The amount of moisture to be removed, W_r, is therefore

$$W_r = W_i - W_f = 396 - 222.05 = 173.95 \text{ kg}$$

Assuming a heat of vaporization of rice equal to 2.553 MJ/kg of water removed, heat energy required for drying, Q_{load}, is

$$Q_{load} = (173.95)(2.553) = 451.797 \text{ MJ}$$

Actual rice drying data reported by the Institute of Agricultural Engineering and Technology, University of the Philippines (Anonymous, 1976) showed that for similar grain drying conditions, heat energy supplied by a

kerosene fuel burner ranged from 421.99 MJ to 562.66 MJ in 6 to 8 hours of drying (based on kerosene fuel consumption rate of 1.5 to 2 l/h and kerosene heating value of 35.166 MJ/l).

Waste heat available from fan engine Utilizing the waste heat from engine of the dryer fan not only reduces the heat load on the solar collector but it also represents a steady source of heat energy during periods of cloudiness. Soemangat et al. (1973) reported engine waste heat recovery of 30 to 50 percent on a fan engine of a flat-bed mechanical grain dryer designed for tropical conditions.

For gasoline engines, about 25 percent of the energy input goes into mechanical energy, hence, for a 3.73-kW engine (from Table I),

$$\text{Fuel energy input} = \frac{3.73}{0.25} = 14.92 \text{ kW}$$

At a conservative waste heat recovery of 30 percent, as found in Soemangat et al. (1973), heat energy available from the engine, q_{en}, is

$$q_{en} = (0.30)(14.92) = 4.476 \text{ kW}$$

The total waste heat energy in 8 hours of operation, Q_{en}, is thus

$$Q_{en} = (4.476)(8) = 35.808 \text{ kWh or } 128.91 \text{ MJ}$$

The heat load of the solar collector, Q_{coll}, is the difference between the drying heat load, Q_{load}, and the available engine waste heat, Q_{en}:

$$Q_{coll} = Q_{load} - Q_{en} = 451.797 - 128.91 = 322.887 \text{ MJ}$$

The solar heat collector should therefore be designed to provide about seventy percent of the total heat requirement of the drying system.

From previous calculations, the mean total insolation rate incident on a surface tilted at 14° from the horizontal and facing south on September 21 and at latitude 14° north is 800.48 W/m^2. Taking a conservative collector efficiency of 30 percent, the useful heat gain in the collector, q_u, is

$$q_u = (0.30)(800.48) = 240.14 \text{ W/m}^2$$

For 8 hours of operation, the total collector heat gain, q_{ut}, is

$$q_{ut} = (240.14)(8) = 1.912 \text{ kWh/m}^2 \text{ or } 6.916 \text{ MJ/m}^2$$

Therefore, the total area of a bare plate solar heat collector, A_c, that would satisfy the heat requirements of the grain drying system operating on a clear day with a collection efficiency of 30 percent under tropical condition is

$$A_c = \frac{Q_{coll}}{q_{ut}} = \frac{322.887}{6.916} = 46.7 \text{ m}^2$$

Methods and Materials of Construction

Experimental set-up

An experimental solar-heated grain drying system approximately one-half the size specified in the design, was constructed at Iowa State University Woodruff farm near Ames, Iowa to obtain actual test data. An overall view of the experimental set-up is shown in Figure 6. A rear view of the set-up is shown in Figure 7. Although the system was intended for drying of tropical crops, particularly rice, at tropical insolation

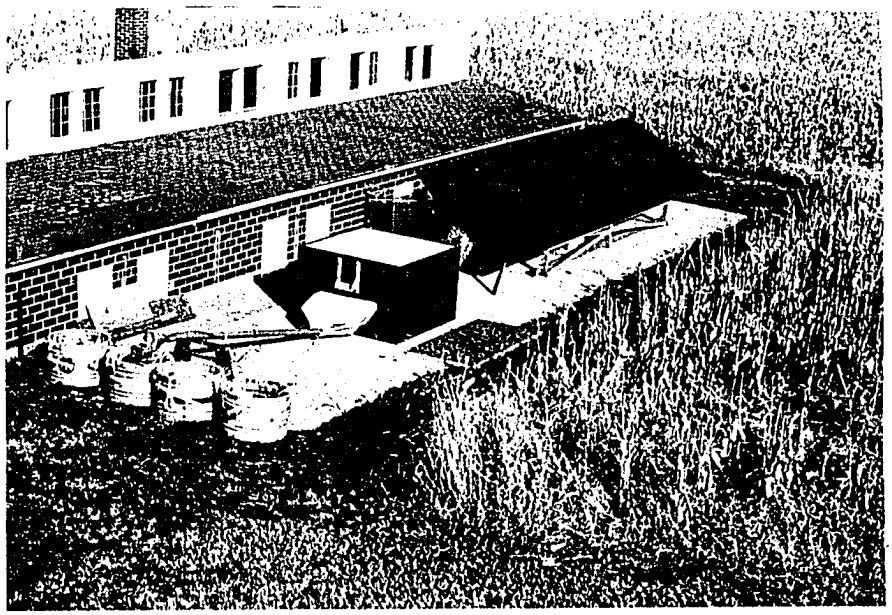

Figure 6. Overall view of experimental solar grain drying set-up

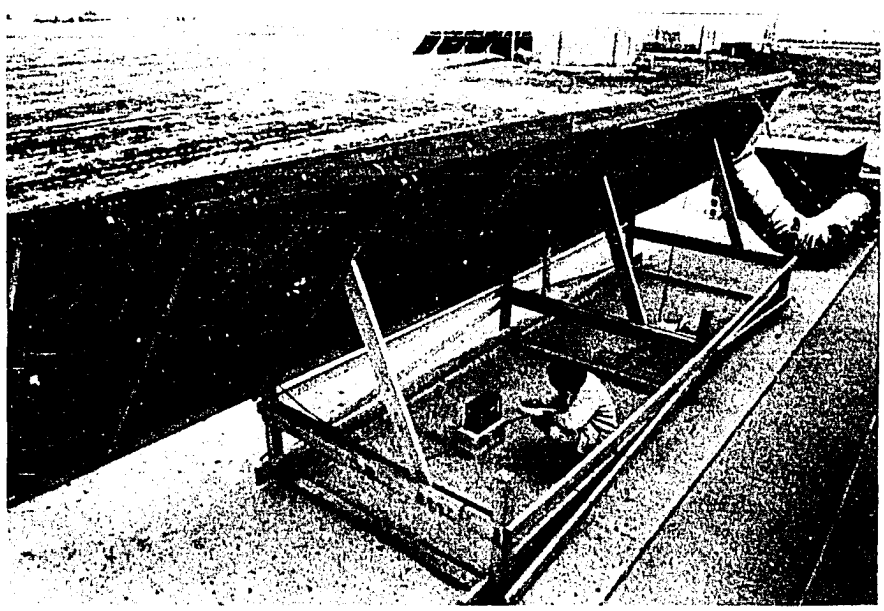

Figure 7. A rear view of the experimental set-up

rates and ambient conditions, tests with corn under Iowa summer conditions would at least provide an indication of solar heat utilization and drying rates to be expected. In constructing the system, use of standard materials that are also available in the tropics was also considered necessary.

The experimental system consisted of a 2.44-m by 9.75-m bare-plate solar collector, a 1.53-m^3 batch capacity plywood drying bin, and a 58.42-cm diameter dryer fan powered by a 170.9-cc Briggs and Stratton[1] internal combustion engine. The bare-plate collector consisted of corrugated steel roofing (ga.29) painted flat-black which acted as the solar absorber, 1.27-cm thick chipboard backplate and a 6.35-cm air channel in-between. Sections of the solar grain drying system are shown schematically in Figure 8.

Choice of the bare-plate solar collector was based primarily on simplicity of construction and low costs. The experimental solar collector was designed basically as a solar roof collector which can be installed on a farm house, machine shed or storage building with minor modifications and at minimum construction costs. Common roofing materials used in tropical countries are corrugated steel sheets.

---

[1]Reference to a company or product name is for specific information only and does not imply approval or recommendation of the product by Iowa State University or USDA to the exclusion of others that may be suitable.

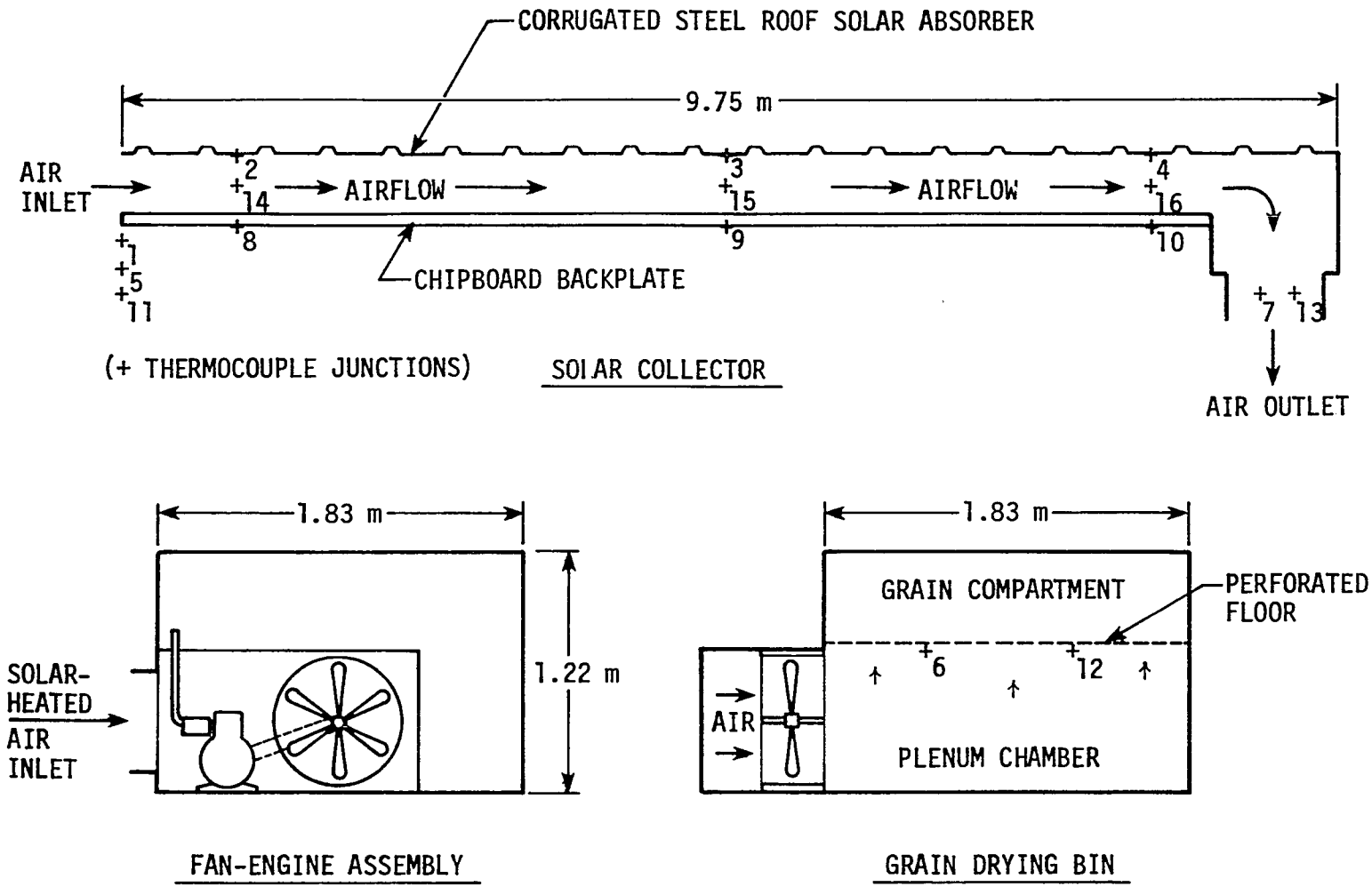

Figure 8. Sections of solar grain drying system showing solar collector, fan-engine assembly, grain drying bin and thermocouple positions

The grain drying bin and fan-engine assembly were patterned after an existing design of a portable flat-bed batch type mechanical grain dryer introduced by the Institute of Agricultural Engineering and Technology of the University of the Philippines (Anonymous, 1976).

The drying bin in the experimental set-up is one-half the size of the original design. The dryer fan used was originally a truck radiator fan bought from a junkyard dealer. Truck radiator fans have been used by the Institute of Agricultural Engineering and Technology of the University of the Philippines in their design for the reasons that they are cheap, easily procured from automotive suppliers or in junkyards, and can be easily assembled in a small shop. It was also found that it can deliver as much as 1.4 m^3/s of air at a static pressure of 0.249 kPa.

Construction details

Solar heat collector Figure 9 shows the framework and supports of the solar collector. For testing purposes, the collector was designed to tilt at different angles with respect to the horizontal along an east-west axis. The 2.44-m by 9.75-m collector frame was constructed from 5.1-cm by 10.2-cm lumber and mounted on 10.2-cm by 10.2-cm and 5.1-cm by 15.2-cm wooden supports.

Figure 10 shows the 1.22-m by 2.44-m chipboards 1.27 cm thick nailed on top of the collector frame after it was laid down horizontally. The 2.44-m chipboard length fit perfectly with the width of the collector frame. An opening was provided at one end of the collector for installation of an air exhaust duct.

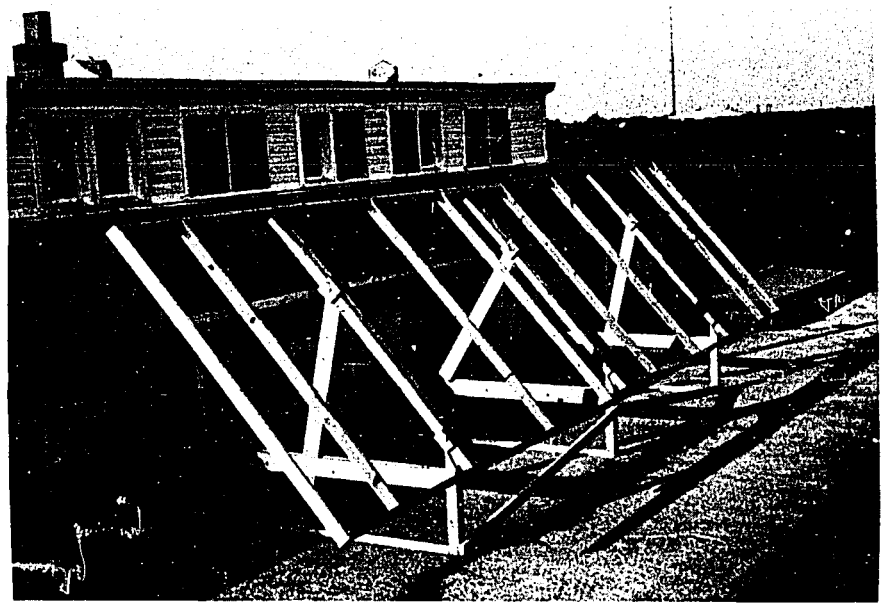

Figure 9. Framework and supports of solar collector

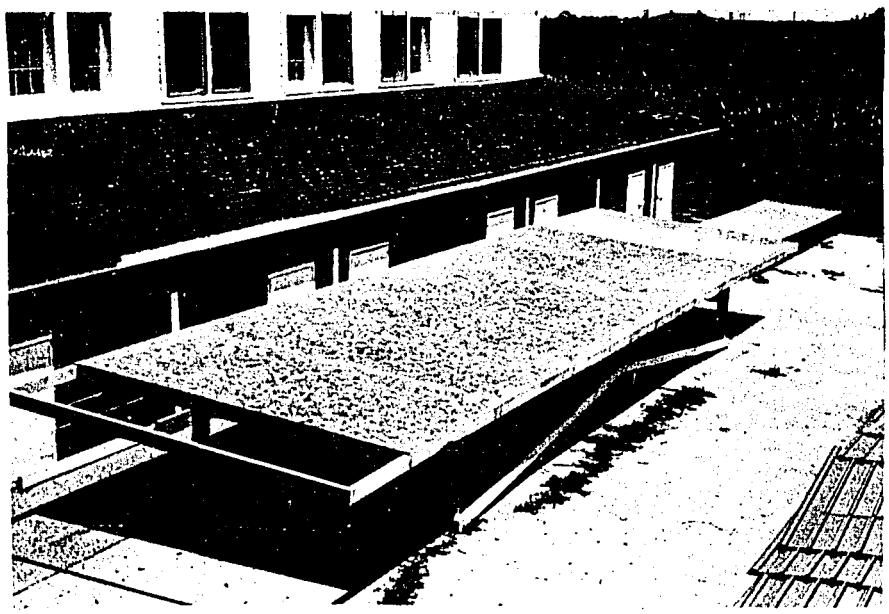

Figure 10. Chipboard backplate installed on top of collector frame

The next phase in the construction was the installation of 3.81-cm by 6.35-cm wood purlins on top of the chipboard along the collector length as shown in Figure 11. Purlins were spaced 80.01 cm on centers and fastened to the chipboard and collector frame by corner brackets and wood screws. Figure 12 shows the air collection duct with a 50.8-cm diameter exhaust opening. Latex caulking compound was liberally applied in sealing all joints along the collector channel to minimize air leakage.

Figure 13 shows the bare-plate solar collector with black-painted corrugated steel roof sheets installed. Corrugation end openings were filled with wood chips and caulked.

Grain drying bin Figure 14 shows a view of the drying bin with a load of corn. Also shown is the flexible insulated ducting which connects the collector outlet to an inlet on the fan-engine assembly housing attached to the bin. The bin was constructed using 1.91-cm thick exterior plywood and dimension lumber. It has a bed area of 3.34 m^2 which consisted of perforated metal sheets 45.7 cm from the top of the bin. The bottom of the perforated bed formed the air plenum chamber enclosed by 0.635-cm thick plywood flooring. All joints were caulked with latex compound.

Fan-engine assembly Figure 15 shows a view of the fan-engine assembly attached to the drying bin. A 170.9-cm^3 gasoline engine is shown connected to the dryer fan pulley with a V-belt. Air coming from

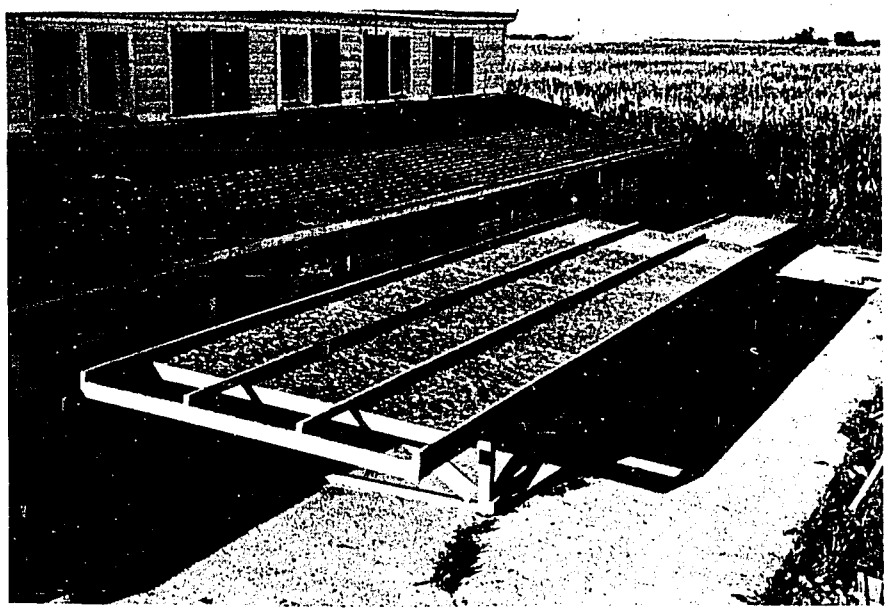

Figure 11. Installation of purlins on top of chipboard along collector length

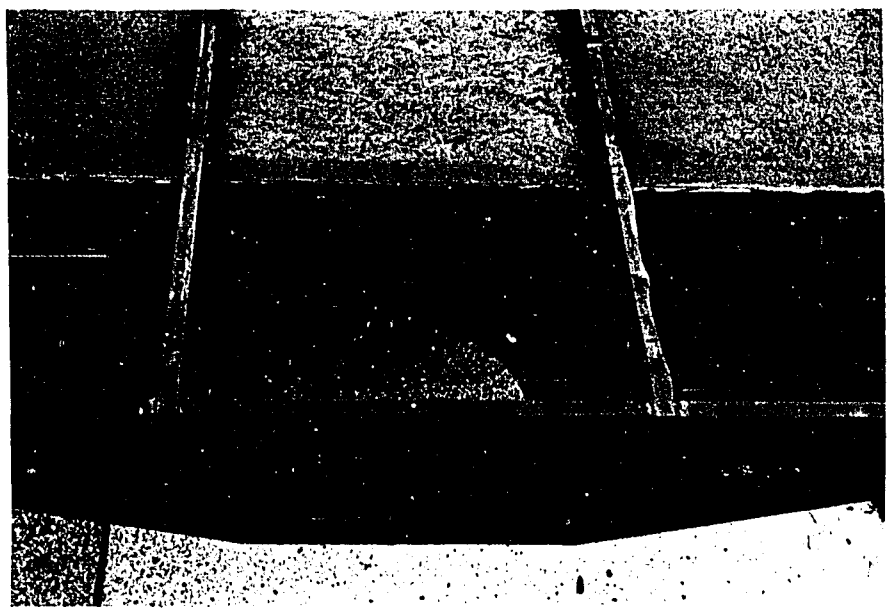

Figure 12. Air collection duct and exhaust opening

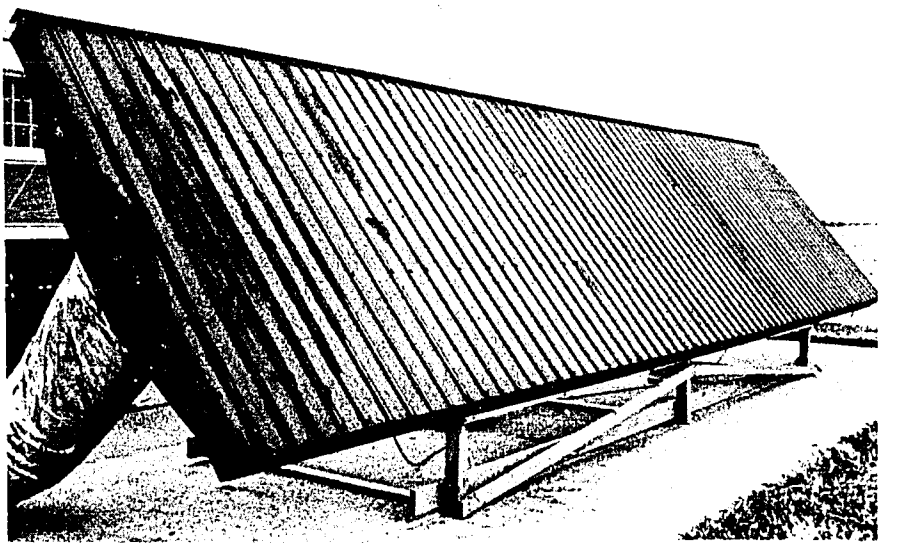

Figure 13. Black-painted corrugated steel roofing sheets installed

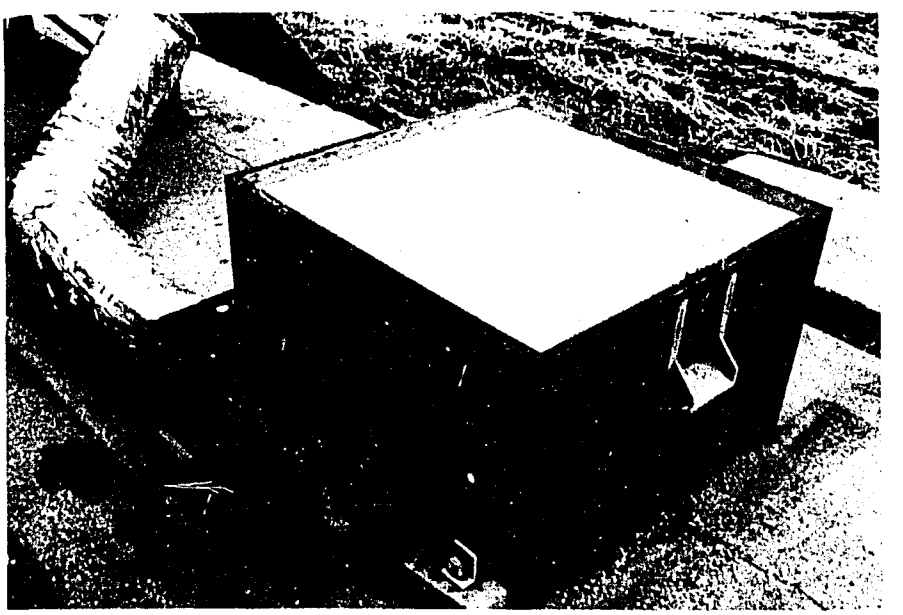

Figure 14. Drying bin with a load of corn

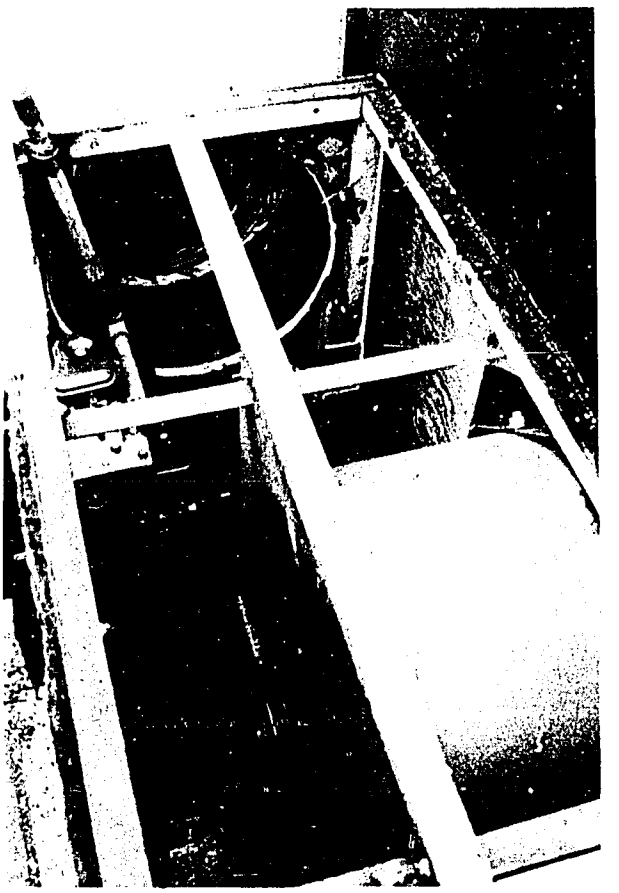

Figure 15. Fan-engine assembly housing

the collector through the flexible ducting passes over the engine before entering into the plenum chamber. Gas exhaust from the engine is piped out of the fan-engine housing.

The fan assembly shown in Figure 16 consisted of a 58.42-cm diameter truck radiator fan mounted on a 2.54-cm diameter steel shaft and two flange bearings. The flange bearings are rigidly attached to the angular iron bar frame by 1.59-cm diameter steel rods.

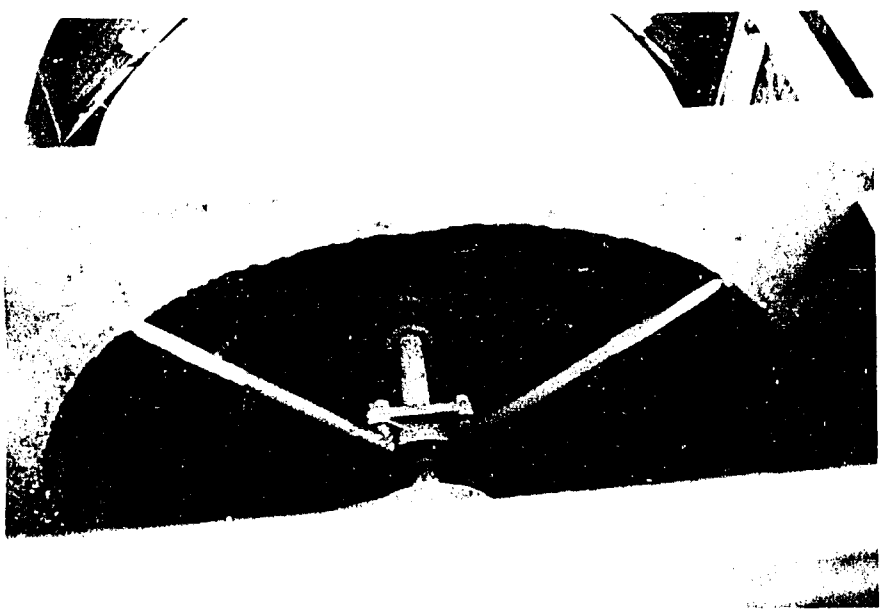

Figure 16. Fan assembly

TESTING AND EVALUATION

In the summer of 1979, tests were conducted on the performance of the experimental solar heat collector and the available waste heat from the fan engine of the grain drying unit. Actual grain drying tests were done in the fall season when wet corn from the field was available.

Instrumentation

Prior to the operation of the experimental solar grain drying system, several instruments were installed for measuring and recording test data.

A 16-point Brown recording potentiometer (Figure 17) was used to measure temperature at various locations in the collector and grain drying unit. Thermocouple positions are shown in Figure 8. Temperatures were recorded every 30 seconds and the cycle completed every 8 minutes. The numbered thermocouples were identified as follows:

Thermocouple number	Location
1, 5, 11	Collector inlet
2, 3, 4	Underside of collector absorber plate
6, 12	Plenum chamber
7, 13	Collector outlet
8, 9, 10	Outer surface of collector backplate
14, 15, 16	Collector channel

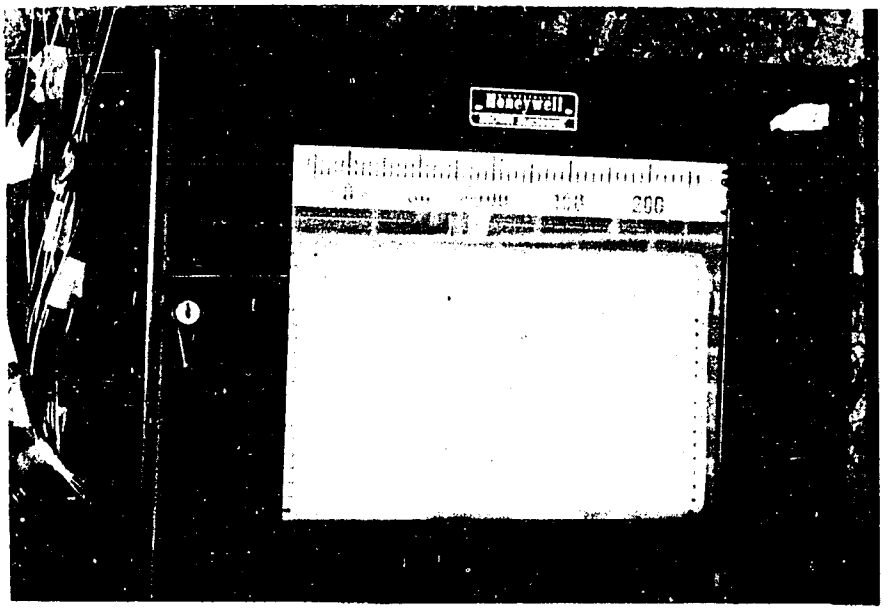

Figure 17. Brown recording potentiometer

An Eppley black and white (no. 645-48) pyranometer (Figure 18) mounted on an instrument trailer approximately 50 m from the experimental set-up, was used in measuring the insolation rate. The pyranometer was mounted at a horizontal position to measure total horizontal insolation rates. An Esterline Angus integrator-recorder (Figure 19) housed in the trailer recorded the millivolt output of the pyranometer. Each millivolt was equivalent to 85.34 W/m^2. Printed output of the recorder gave instantaneous and 30-minute integrated values of solar radiation.

Ambient air conditions were recorded continuously by a hygrothermograph placed under the collector (Figure 20). Wind speed and direction were also monitored in the trailer by a Dwyer wind speed indicator and a wind vane, respectively.

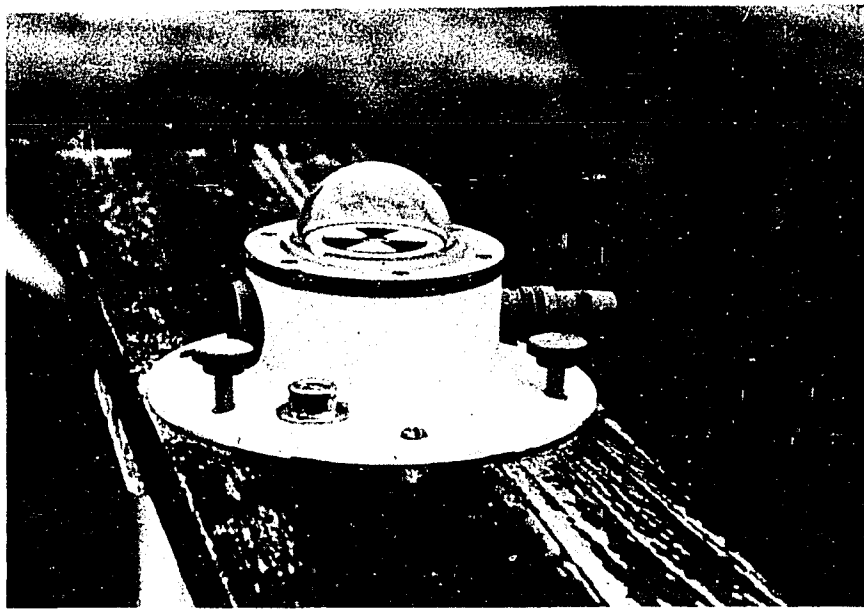

Figure 18. Eppley black and white pyranometer

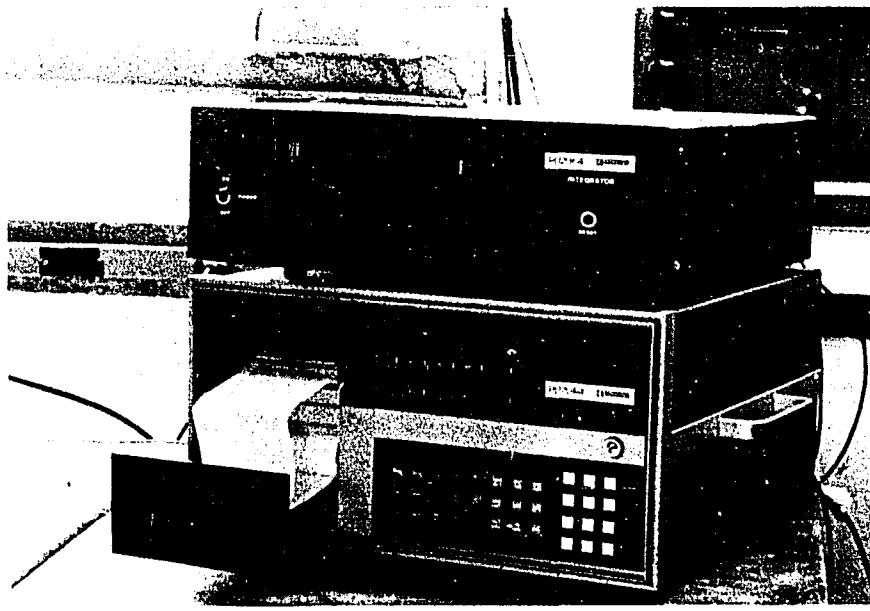

Figure 19. Esterline Angus integrator-recorder

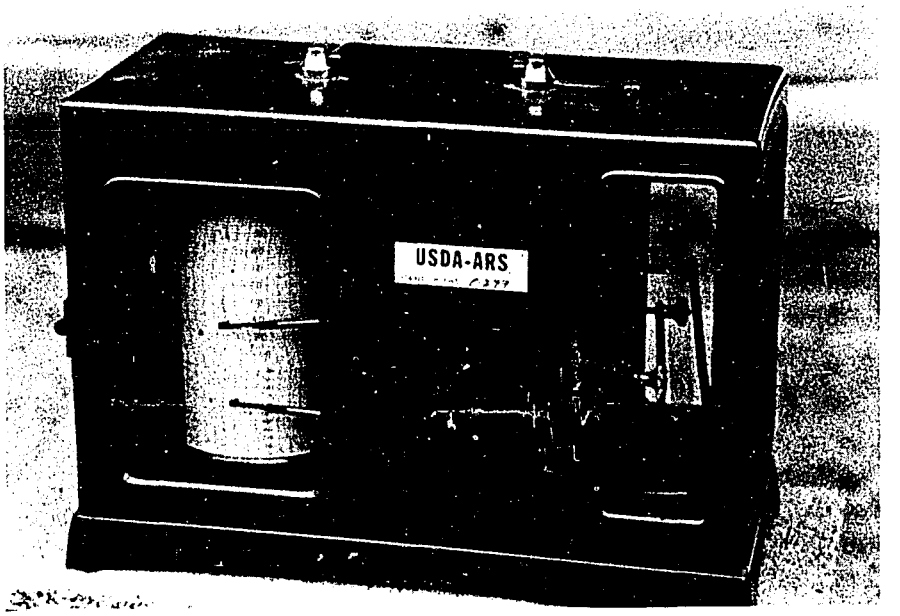

Figure 20. Hygrothermograph

Pressure drop through the collector was measured by 3.45-kPa magnehelic pressure gage at a distance of 7.32 m between two points along the collector channel. A 6.9-kPa magnehelic pressure gage was used in measuring the air static pressure at the plenum chamber.

A wet and dry-bulb thermometer combination and a dial thermometer were also installed to enable instantaneous observation of the drying air condition at the plenum chamber.

Test Procedures

Collector performance

Basic data required to determine useful collector heat gain and collector efficiency included the air mass flow rate, m_a, the air

temperature rise through the collector, ΔT_1, and the total insolation rate incident on the collector, I_{coll}. Different airflow rates were used in the tests to determine their effect on air temperature rise through the collector, rate of useful heat gain and collector efficiency. All tests on collector performance were run for 8 hours starting at 8:30 a.m. and ending at 4:30 p.m. solar time.

Other pertinent data recorded were: date of test, location and elevation, collector tilt angle and ambient conditions. Ambient conditions were described by air temperature and relative humidity, wind speed and direction, and prevailing sky conditions.

Location, elevation and test dates The experimental set-up was located at the ISU Woodruff Farm about 8 km southwest of Iowa State University campus in Ames, Iowa, latitude 42° north and elevation 306 m above sea level. Collector performance tests were conducted during clear and partly cloudy days from June 29 to July 19, 1979.

Optimum collector tilt angle Prior to the test runs, an optimum collector tilt angle for the test dates in question was determined using the method discussed in 'theoretical calculations'. The range of optimum tilt angles from June 29 to July 19, 1979 were calculated as follows:

Date	Optimum collector tilt angle, degrees
June 29	18.8
July 4	19.1
July 11	19.9
July 18	21.0
July 19	21.2

The collector tilt angle for the entire test period was, hence, fixed at 20 degrees from the horizontal with a maximum variation of ± 1.2 degrees from optimum collector tilt angles of extreme test dates. The collector was adjusted and checked for correct angle by a carpenter's level and protractor. Collector was tilted toward the south along an east-west axis.

Airflow-pressure drop calibration test For ease of measurement, airflow through the collector was calibrated in terms of the pressure drop. This was done by first running the fan engine and adjusting a cover on top of the drying bin until a desired pressure drop reading on the collector was obtained. Air velocities at different points across the collector channel cross-section were measured using a hot-wire anemometer (Figure 21).

Figure 22 shows the schematic diagrams of collector channel cross-section and locations of velocity measurements. The sum of the products of velocity readings, V_i, and corresponding cross-sectional areas, A_i, was the overall collector airflow rate at the given pressure drop. The same procedure was repeated in obtaining overall collector airflow rates

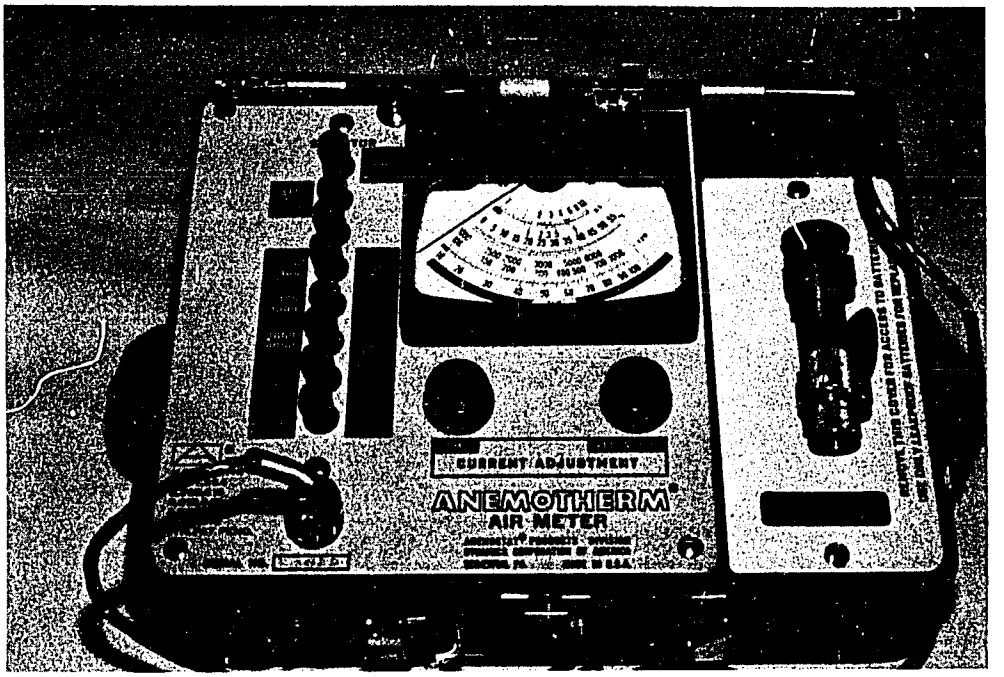

Figure 21. Hot-wire anemometer

for other pressure drop values. Figure 23 shows the calibration chart for airflow through the collector as a function of air pressure drop.

Mass flow rate With airflow rate determined from pressure drop readings on the collector, mass flow rate was obtained from the relationship

$$m_a = \frac{3600\ Q}{\nu} \quad \text{kg/h}$$

where

m_a = air mass flow rate, kg/h

Q = airflow rate, m^3/s

ν = air specific volume, m^3/kg

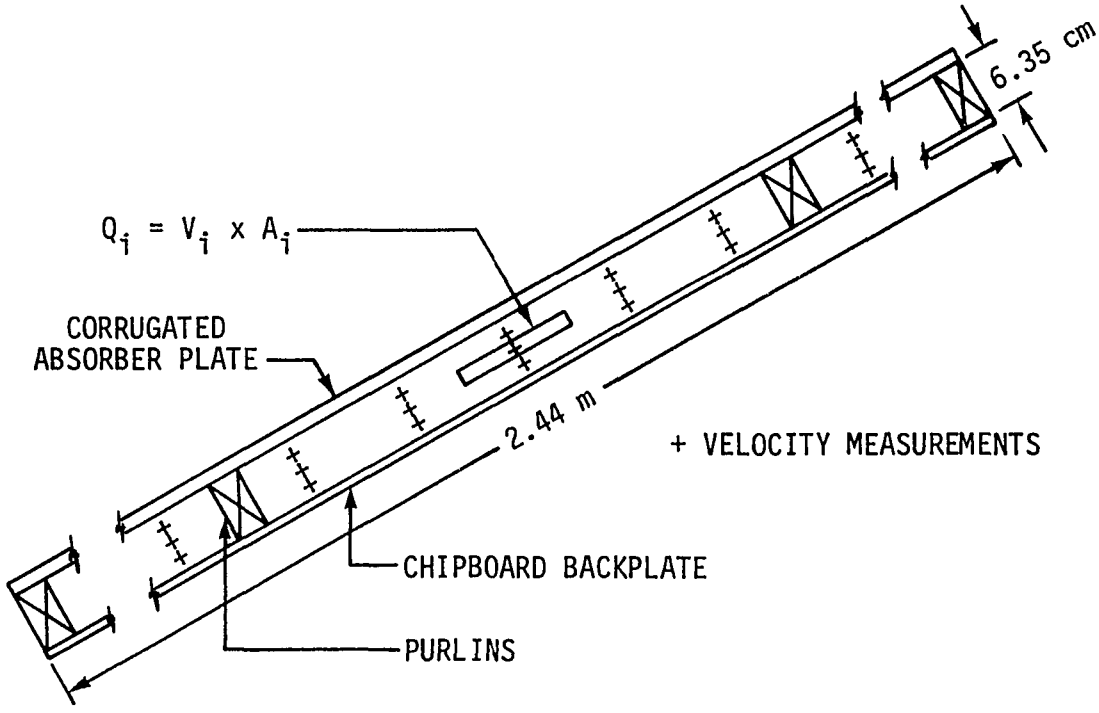

COLLECTOR CHANNEL CROSS-SECTION

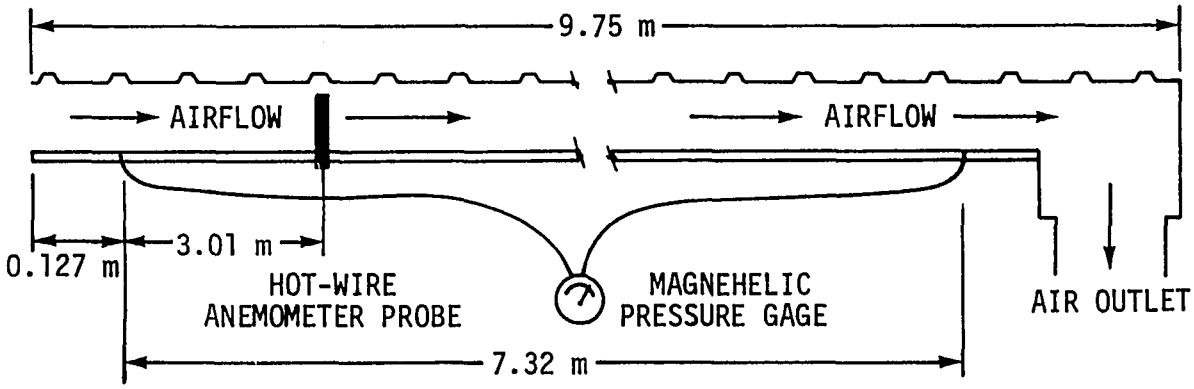

LONGITUDINAL SECTION OF COLLECTOR

Figure 22. Sections of collector showing velocity and pressure drop measurement positions

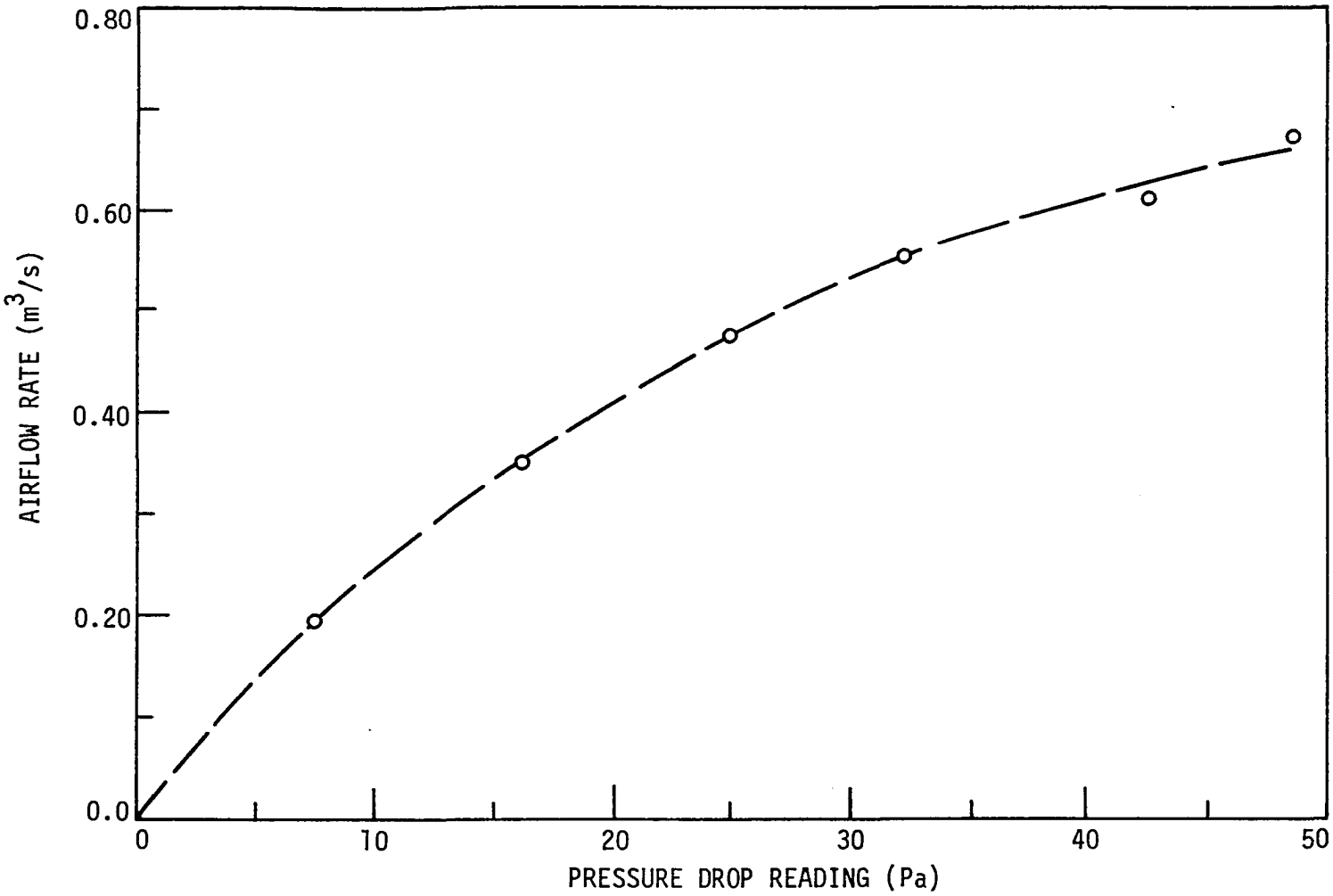

Figure 23. Airflow-pressure drop calibration chart

The specific volume, ν, was calculated from psychrometric relationship

$$\nu = \frac{R_a T}{P - P_w} \quad m^3/kg$$

where

R_a = gas constant for air, 287.045 5/kg·°K

T = absolute temperature of air, °K

P = standard atmospheric pressure at given elevation, kPa

P_w = water vapor pressure at given air temperature, kPa

From ASHRAE (1977), standard atmospheric pressure, P, at elevation 306 m above sea level is 97.73 kPa. The water vapor pressure, P_w, was determined from the product of the air relative humidity and saturated vapor pressure, P_{ws}, at the given temperature. P_{ws} was obtained from steam tables.

Temperature rise through collector Air temperature rise through the collector, ΔT_1, was obtained from the difference between collector outlet air temperature and collector inlet air temperature data recorded by the Brown recording potentiometer:

$$\Delta T_1 = T_{fo} - T_{fi}$$

where

ΔT_1 = air temperature rise through the collector, °C

T_{fo} = collector outlet air temperature, °C

T_{fi} = collector inlet air temperature, °C

All temperature values used in the calculations were averages of temperature readings at intervals of 30 minutes.

Insolation rates The total incident solar radiation rates on the tilted collector, I_{coll}, were derived from 30-minute integrated values of total horizontal insolation, H, obtained from the pyranometer. Conversion to total incident insolation required separate treatments of direct and diffuse components, hence,

$$I_{coll} = I_{Dcoll} + I_{dcoll}$$

where

I_{Dcoll} = direct solar radiation incident on collector, W/m^2

I_{dcoll} = diffuse sky radiation falling on tilted collector, W/m^2

Diffuse component Diffuse sky radiation falling on the tilted collector, I_{dcoll}, was related to diffuse horizontal solar radiation, H_d, by

$$I_{dcoll} = R_d \times H_d$$

where R_d was the angle factor. At collector tilt angle, Σ, equal to 20 degrees, angle factor, R_d, was found from equation (10):

$$F_{ss} = R_d = \frac{1 + \cos 20}{2} = 0.96895$$

Diffuse horizontal solar radiation, H_d, was derived from the known total horizontal insolation, H, using the method proposed by Liu and Jordan (1960). Liu and Jordan found that there was a definite relationship between the ratios H_d/H and H/H_o as shown in Figure 24. H_o is

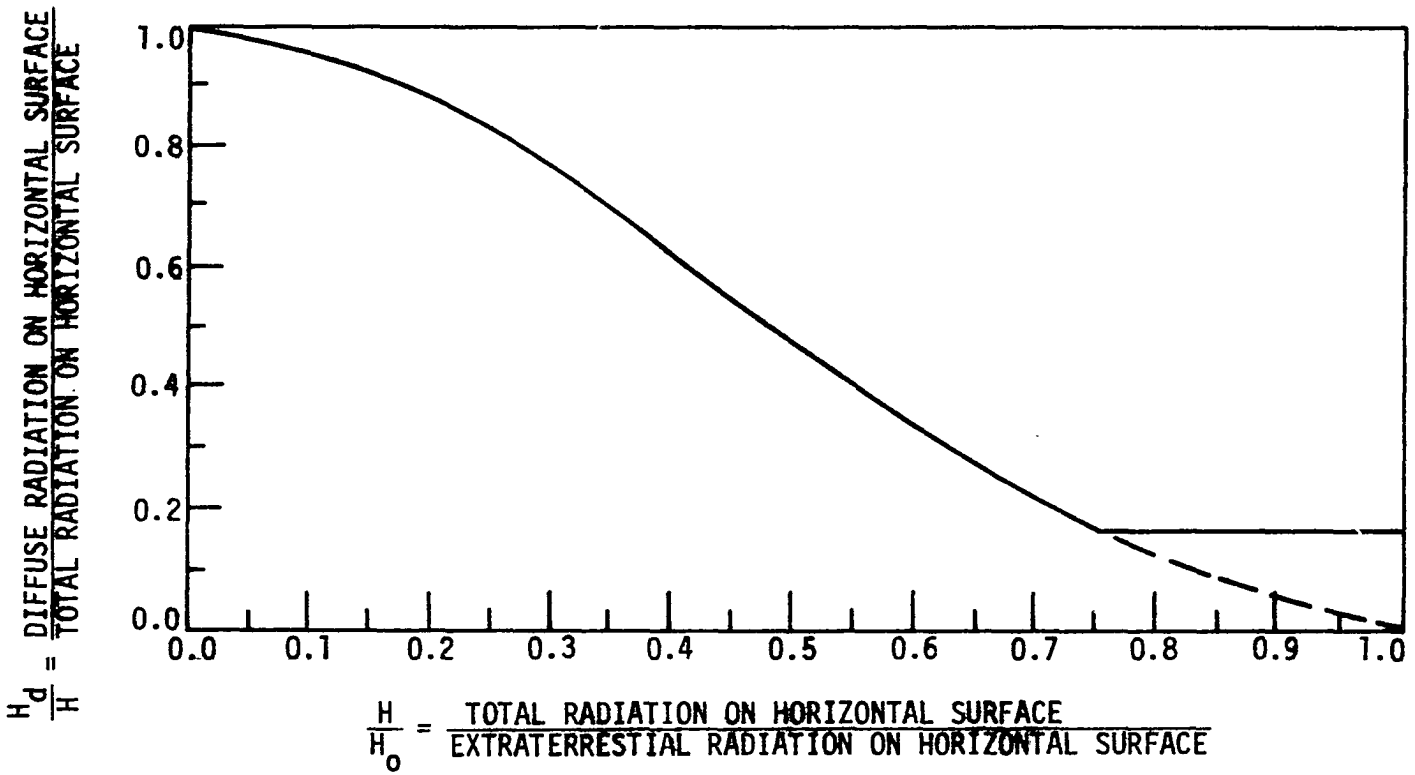

Figure 24. The ratio of diffuse radiation, H_d, to total radiation on a horizontal surface, H, as a function of the cloudiness index, H/H_o. Adapted from Liu and Jordan (1960)

the extraterrestial insolation on a horizontal surface for a specific time of day and was calculated from

$$H_o = \sin\beta \times I_{oN} \quad W/m^2$$

where β is the solar altitude angle, in degrees, and I_{oN} is the extraterrestial solar radiation on a normal surface in watts per square meter.

I_{oN} was related to the solar constant, I_{sc} by

$$I_{oN} = r\, I_{sc}$$

where r is a ratio which is dependent on solar declination. The solar constant, I_{sc}, used by Liu and Jordan was 1393 W/m^2. Values of r and I_{oN} for the test dates are shown in Appendix C.

Direct component With diffuse horizontal solar radiation, H_d, determined previously, the direct horizontal component, H_D, was obtained by taking the difference between the total horizontal insolation and the diffuse horizontal component:

$$H_D = H - H_d \quad W/m^2$$

The direct solar radiation incident on the collector, I_{Dcoll}, was then related to the direct horizontal insolation component by an expression given in equation (16) rewritten as

$$I_{Dcoll} = R_D\, H_D$$

where R_D was the orientation factor obtained from equation (14):

$$R_D = \frac{\cos\theta}{\sin\beta}$$

Solar angles and related factors used in conversion from horizontal to incident insolation on the tilted collector were determined at mid-points of each 30-minute interval. For example, the solar altitude, β, used in converting direct horizontal insolation, H_D, to direct incident insolation on the tilted collector, I_{Dcoll}, at a 30-minute interval from 8:30 a.m. to 9:00 a.m. solar time, was determined at 8:45 a.m. solar time.

Temperature distribution in the collector To have an insight into the temperature distribution along the collector channel, a test was conducted with the thermocouples arranged as shown schematically in Figure 25. Temperatures were measured along the collector channel at distances of 1.6 m, 5.3 m and 8.9 m from the collector inlet. Absorber plate temperatures were measured by thermocouples 2, 3 and 4. Thermocouples 5 to 13 measured air stream temperatures at 1.6 cm from the absorber plate, midway between the absorber plate and backplate, and 1.6 cm from the backplate. The inner backplate surface temperatures were measured by thermocouples 14, 15 and 16. Thermocouple 1 measured the ambient air temperature.

Engine waste heat utilization

A 170.9-cm^3 Briggs and Stratton internal combustion engine with a rating of 3.73 kW at 3600 r/min was used in the tests.

Fan-engine performance Prior to tests on availability of waste heat from the engine, tests on performance characteristics of fan-engine combination were conducted to determine operating points of the system

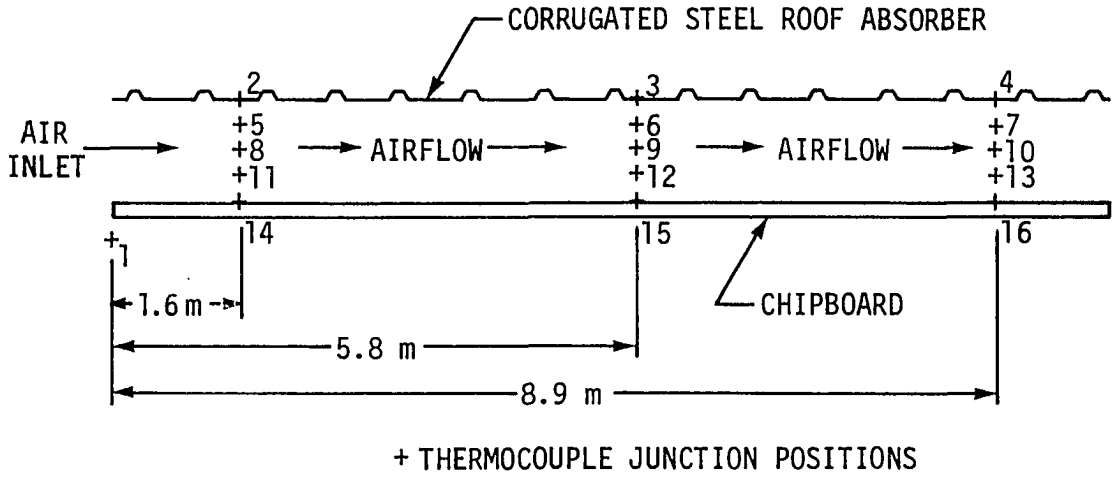

Figure 25. Schematic diagram of collector channel showing thermocouple junction positions

at different engine governor settings and fan static loads. The procedure included varying the airflow rate through the system by adjusting a cover on top of the drying bin until a desired static pressure at the plenum was obtained. Airflow rates were determined from air pressure drop readings on the collector and the calibration chart of Figure 23.

The engine governor was adjusted to 25, 50, 75 and 100 percent of full standard engine governor control setting. Air temperature rise due to the engine as a function of airflow and engine governor setting was also recorded.

Engine speed-torque performance A dynamometer shown in Figure 26 was used in determining engine speed and torque characteristics. Test on the engine was conducted by subjecting it to a series of loads. This test was useful in defining the power output of the engine at various test conditions. Engine speed, torque and power output were recorded and plotted on graphs.

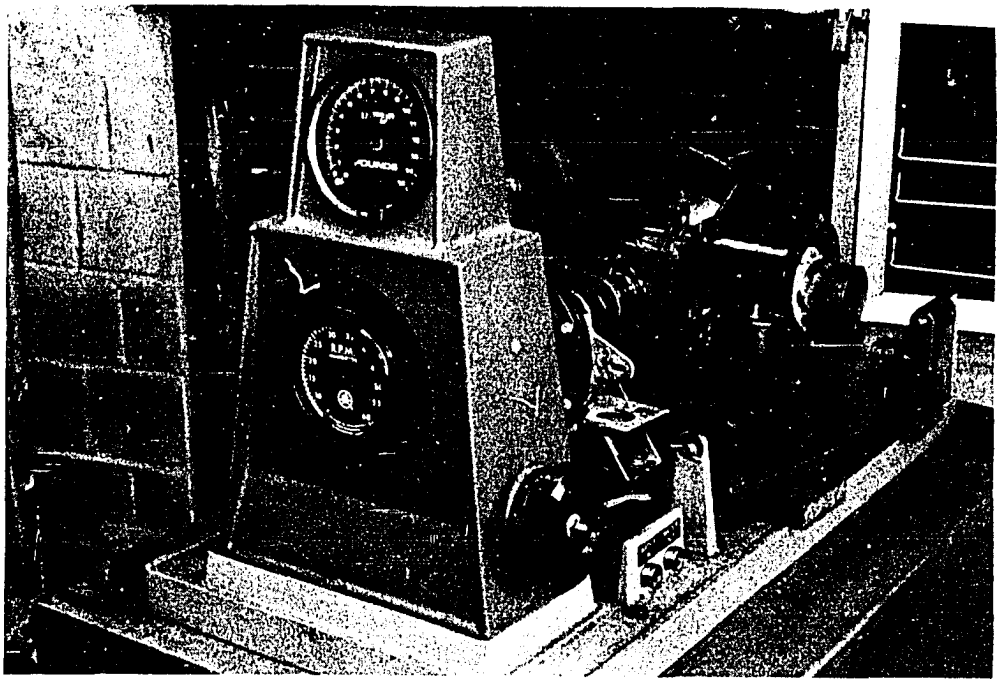

Figure 26. Dynamometer

Available engine waste heat Tests on available waste heat from the fan engine were conducted simultaneously with collector performance tests. Tests were run continuously for 8 hours.

The amount of waste heat from the engine, q_{en}, was determined from the heat equation

$$q_{en} = m_a \, c_p \, \Delta T_2 \quad kJ/h$$

where

m_a = air mass flow rate, kg/h

c_p = air specific heat, kJ/kg·°C

ΔT_2 = air temperature rise due to the engine, °C

Air mass flow rate, m_a, was obtained using the method discussed under collector performance. Specific heat for air is constant at 1.012 kJ/kg·°C. Air temperature rise, ΔT_2, was obtained from the difference between the average 8-hour air temperature readings at the plenum chamber and collector outlet as recorded by the Brown recording potentiometer:

$$\Delta T_2 = T_{pl} - T_{fo}$$

where

T_{pl} = plenum chamber air temperature, °C

T_{fo} = collector outlet air temperature, °C

Air temperature rise due to the engine includes the engine waste heat and heat loss due to fan inefficiency. Engine exhaust was not put in the air stream.

Grain drying tests

Two drying tests were conducted in the fall when wet corn was available. Wet shelled corn of known moisture content was brought in by pick-up truck and unloaded into the drying bin with an auger.

During the drying operation, grain samples were taken every 2 hours for moisture content determination using a Dole 300 moisture tester (Figure 27). Moisture content obtained was the average of grain samples taken by a 1.54-m long Seedburo grain sampling probe from the bottom, middle and top layers on the drying bin.

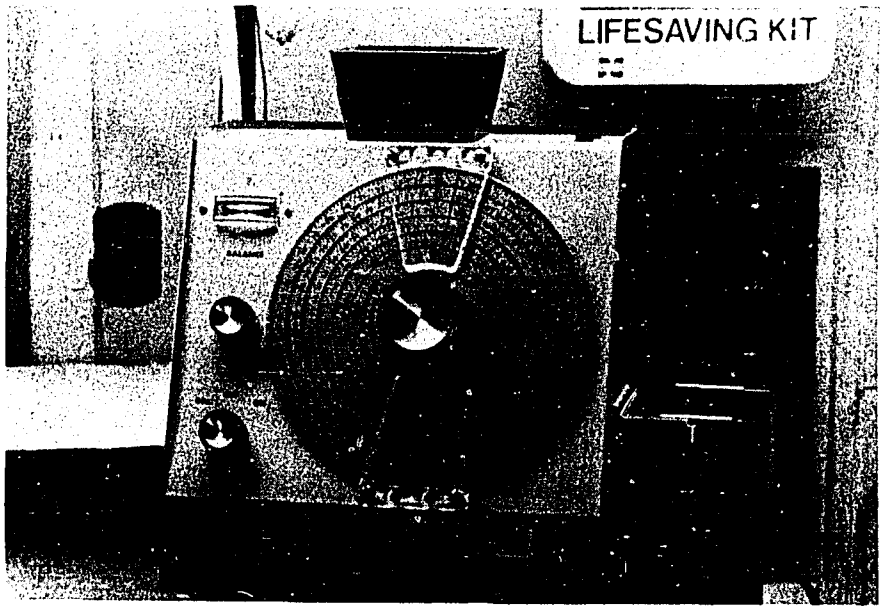

Figure 27. Dole 300 moisture tester

Airflow rates through the collector, engine and drying bin were derived from the air pressure drop readings in the collector and the airflow-pressure drop calibration chart of Figure 23. The drying system was operated for 8 hours from 8:30 a.m. to 4:30 p.m. solar time.

Test data recorded were the airflow rate, initial grain volume, average grain initial and final moisture contents, drying time, and fan engine fuel consumption rate. All temperatures and weather data including ambient air conditions and insolation rates were also recorded.

Evaluation of Test Results

Collector performance

Airflow and insolation rates were found to be the main factors that influenced collection efficiency, useful heat gain and air temperature rise in the collector. Results of 8-hour tests on the performance of the bare-plate solar heat collector are summarized in Table VI. Atmospheric conditions during each test are described in Table VII. Instantaneous data taken at 30-minute intervals for each test are tabulated with instantaneous collection efficiencies in Appendix D.

Effect of airflow rate The independent effect of airflow on collector performance was isolated by comparing results of tests having fairly constant insolation rates as shown in Table VIII. Tests 1 and 2, and tests 6, 8 and 10 received a fairly constant insolation rate during the 8-hour test period thus the effect of insolation may be eliminated.

In both comparisons, higher airflow rates resulted in higher collection efficiencies and useful heat gains. The average 8-hour air temperature rise in the collector, however, decreased at higher airflows.

The effect of airflow rate on collector performance is further illustrated in Figure 28 using data of tests 6, 8 and 10. The three tests were chosen because of similarity in insolation rates and atmospheric conditions. As shown in the figure, collection efficiency and useful heat gain in the collector increase with increasing airflows. On the other hand, air temperature rise in the collector decreases. It can also be observed that the rate of increase in collection efficiency and

Table VI. Summary of test results on collector performance and related data

Test number	Test date	Airflow rate[a] (m^3/s)	ΔT_l^b (°C)	I_{coll}^c (MJ/m^2)	q_u^d (MJ/m^2)	η_{coll}^e (%)
1	6/29/79	0.371	7.62	23.17	3.86	16.7
2	6/30/79	0.533	7.56	23.24	5.46	23.5
3	7/1/79	0.300	6.33	20.84	2.57	12.3
4	7/9/79	0.300	9.33	21.92	3.76	17.3
5	7/10/79	0.406	7.93	18.19	4.22	23.2
6	7/11/79	0.425	9.11	21.63	5.17	23.9
7	7/15/79	0.557	6.95	22.37	5.21	23.3
8	7/16/79	0.557	7.45	22.76	5.64	24.8
9	7/17/79	0.557	6.89	21.93	5.24	23.8
10	7/19/79	0.288	10.39	22.41	4.07	18.1

[a]Based on airflow-pressure drop calibration chart constructed from a previous test.

[b]Air temperature rise in the collector (difference between collector inlet and outlet temperatures).

[c]Total insolation rate incident on collector tilted at 20° from horizontal facing south. Values were derived from total horizontal insolation recorded by the pyranometer, using a method proposed by Liu and Jordan (1960).

[d]Useful heat gain in the collector.

[e]8-hour collector efficiency.

Table VII. Description of atmospheric conditions during collector performance tests

Test number	Ambient Air[a] temp. (°C)	Ambient Air[a] RH (%)	Wind speed[b] (m/s)	Wind direction	Sky conditions[c]
1	24.6	50.1	4.5	NW	C-PC
2	28.6	32.7	9.0	NW	C-PC
3	28.0	42.5	4.5	SE	C-PC
4	27.0	53.5	2.2	SW	C
5	27.7	60.5	2.2	SW	C-PC
6	27.5	69.2	2.2	NE	C-PC
7	27.5	58.0	2.2	NW	C-PC
8	26.1	51.1	2.2	NE	C-PC
9	25.5	51.3	4.5	NE	C-PC
10	25.6	45.2	2.2	NE	C

[a]Average for 8-hour test period.

[b]Maximum speed observed during each test.

[c]Clear skies (C) or clear to partly cloudy (C-PC).

useful heat gain decrease at higher airflow rates. Further increase in airflow is hence undesirable as collection efficiency and useful heat gain would only level off at the expense of higher fan power input.

Table VIII. Effect of airflow rate on useful heat gain and collection efficiency

Test number	Insolation (MJ/m^2)	Airflow (m^3/s)	Air temp. rise (°C)	Useful heat gain (MJ/m^2)	Collector efficiency (percent)
1	23.17	0.371	7.62	3.86	16.7
2	23.24	0.533	7.56	5.46	23.5
10	22.41	0.288	10.39	4.07	18.1
6	21.68	0.425	9.11	5.17	23.9
8	22.76	0.557	7.45	5.64	24.8

Similar findings on the effect of airflow on collection efficiencies and air temperature rise in the collector have been reported earlier by Sobel and Buelow (1963), Kline (1977) and Chau et al. (1978).

Effect of insolation rate The effect of insolation rate on collector performance independent of airflow is shown in Table IX. Comparison of tests 3 and 4 in Table IX shows that for a constant airflow rate of 0.30 m^3/s, a 5 percent increase in insolation rate resulted in a 47 percent increase in useful heat gain in the collector and a 47 percent increase in air temperature rise in the collector. The large difference in the collection efficiencies of tests 3 and 4 may have been influenced by higher wind speed of 4.5 m/s observed in test 3 compared with only 2.2 m/s in test 4.

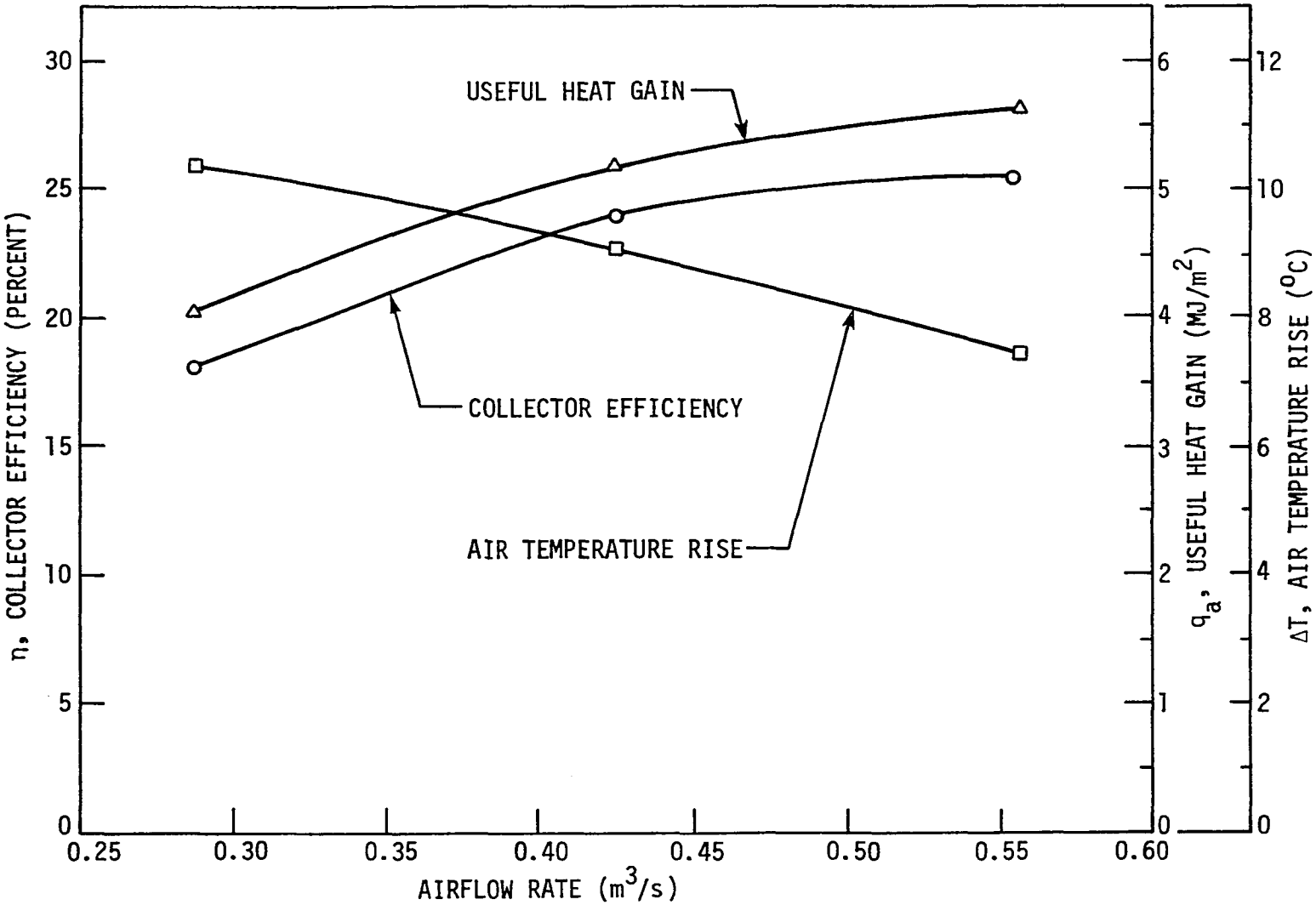

Figure 28. Effects of airflow rate on collector efficiency, useful heat gain and air temperature rise in the collector

Table IX. Effect of insolation rate on useful heat gain and collection efficiency

Test number	Airflow (m^3/s)	Insolation (MJ/m^2)	Air temp. rise (°C)	Useful heat gain (MJ/m^2)	Collector efficiency (percent)
3	0.300	20.84	6.33	2.57	12.3
4	0.300	21.92	9.33	3.76	17.2
7	0.557	22.37	6.95	5.21	23.3
8	0.557	22.76	7.45	5.64	24.8

Comparison of tests 7 and 8 in Table IX showed an 8 percent increase in useful heat gain and 7.2 percent increase in air temperature rise in the collector with a 1.7 percent increase in insolation rate. Airflow rates in tests 7 and 8 were higher at 0.557 m^3/s. Similar wind speeds were observed in both tests 7 and 8.

Variations in insolation rates during the 8-hour test period also affected the instantaneous collection efficiency, useful heat gain and air temperature rise in the collector. A typical effect of hourly variation in insolation rate on useful heat gain and collection efficiency is illustrated in Figure 29. Hourly variation in insolation rate was also plotted with collector inlet and outlet air temperatures as shown in Figure 30. Air temperature rise in the collector is the difference between the collector outlet and inlet air temperatures at a given time.

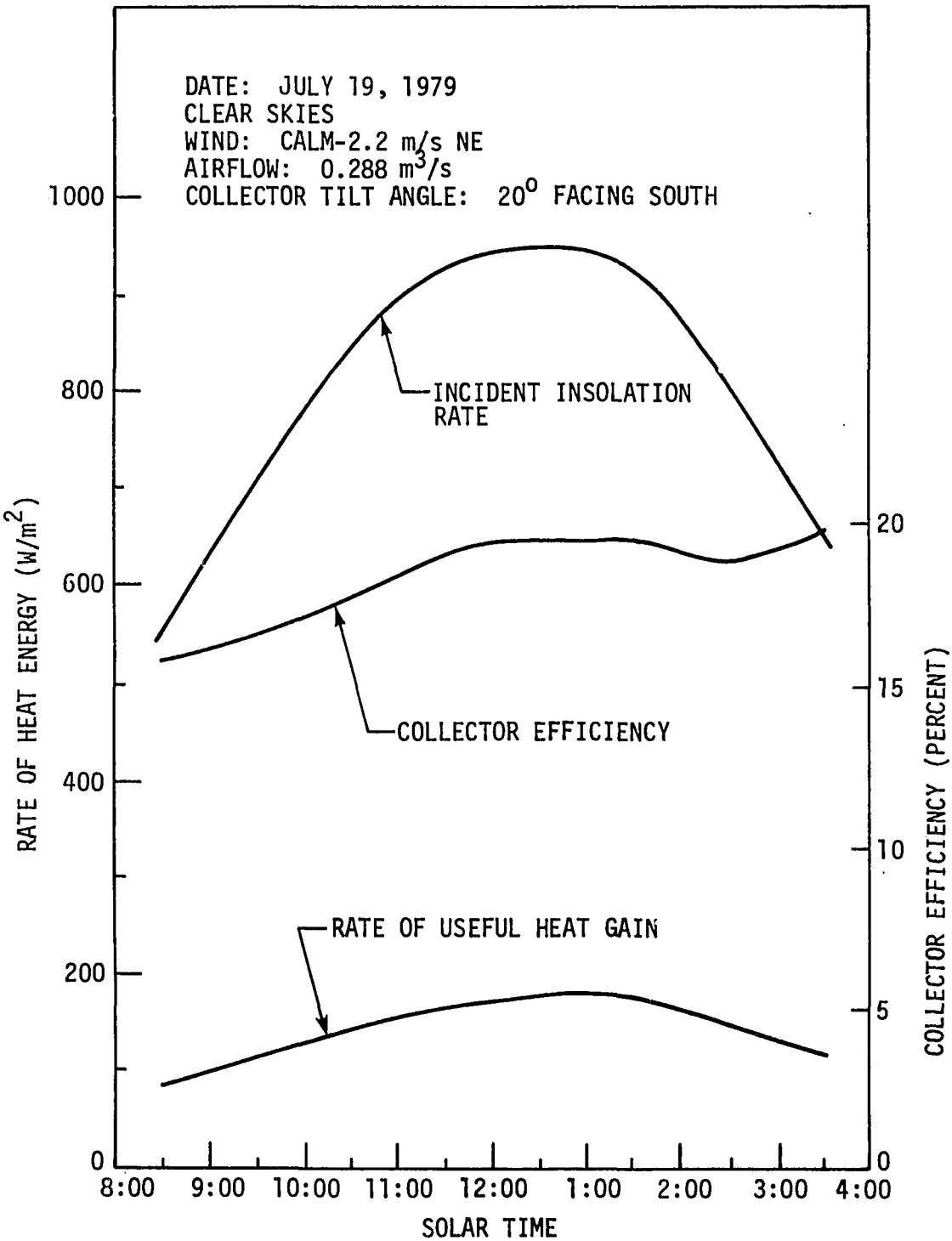

Figure 29. Hourly variation in insolation rate, collector efficiency and useful heat gain in the collector

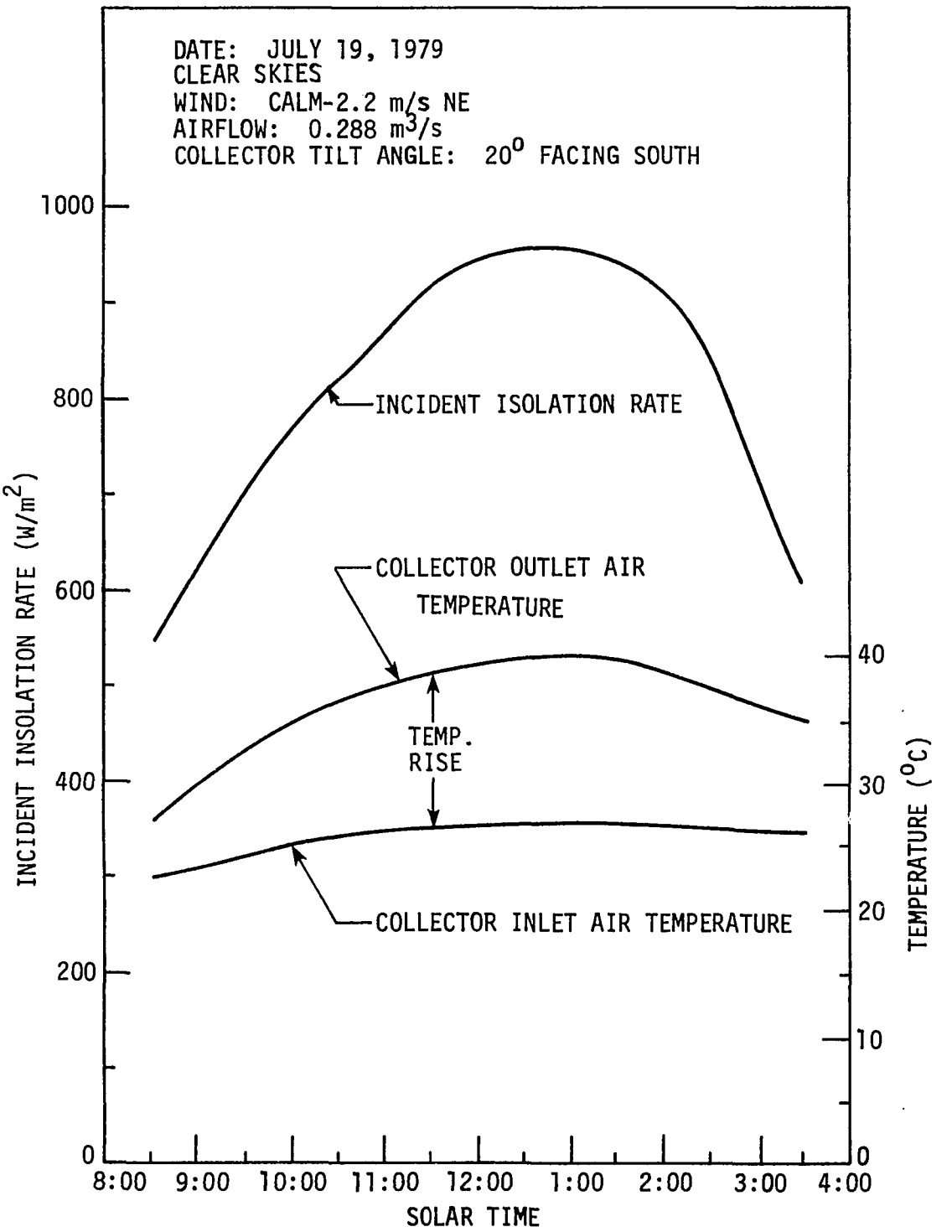

Figure 30. Hourly variation in insolation rate and air temperatures at inlet and outlet of the collector

Data used in both Figures 29 and 30 were taken from results of test 10 tabulated in Appendix D. Airflow rate was 0.288 m^3/s. Clear skies were observed during the test with winds calm to 2.2 m/s in the northeasterly direction. From both Figures 29 and 30, it can be observed that useful heat gain and air temperature rise in the collector increase with increasing insolation and decrease correspondingly. The instantaneous collection efficiency is observed to vary with both the insolation and useful heat gain. Collector efficiency is equal to useful heat gain divided by the incident insolation.

Although inconclusive, ambient air temperature, wind speed and direction account for some variations in the test results as bare-plate collectors with no covers are exposed and hence sensitive to changes in atmospheric conditions.

Temperature distribution along the collector Another point of interest investigated was the variation in temperatures along the collector channel. Figures 31 to 33 illustrate the temperature distribution along the collector channel at 11:00 a.m., 12:00 solar noon, and 1:00 p.m., respectively.

As observed from the three figures, absorber plate temperatures, fluid air stream temperatures and backplate temperatures increase along the length of the collector. Profile temperatures of the air fluid stream indicated that air stream temperatures were highest near the absorber plate and decreased with increasing distance from the absorber plate. Temperatures were also observed to increase from 11:00 a.m. to

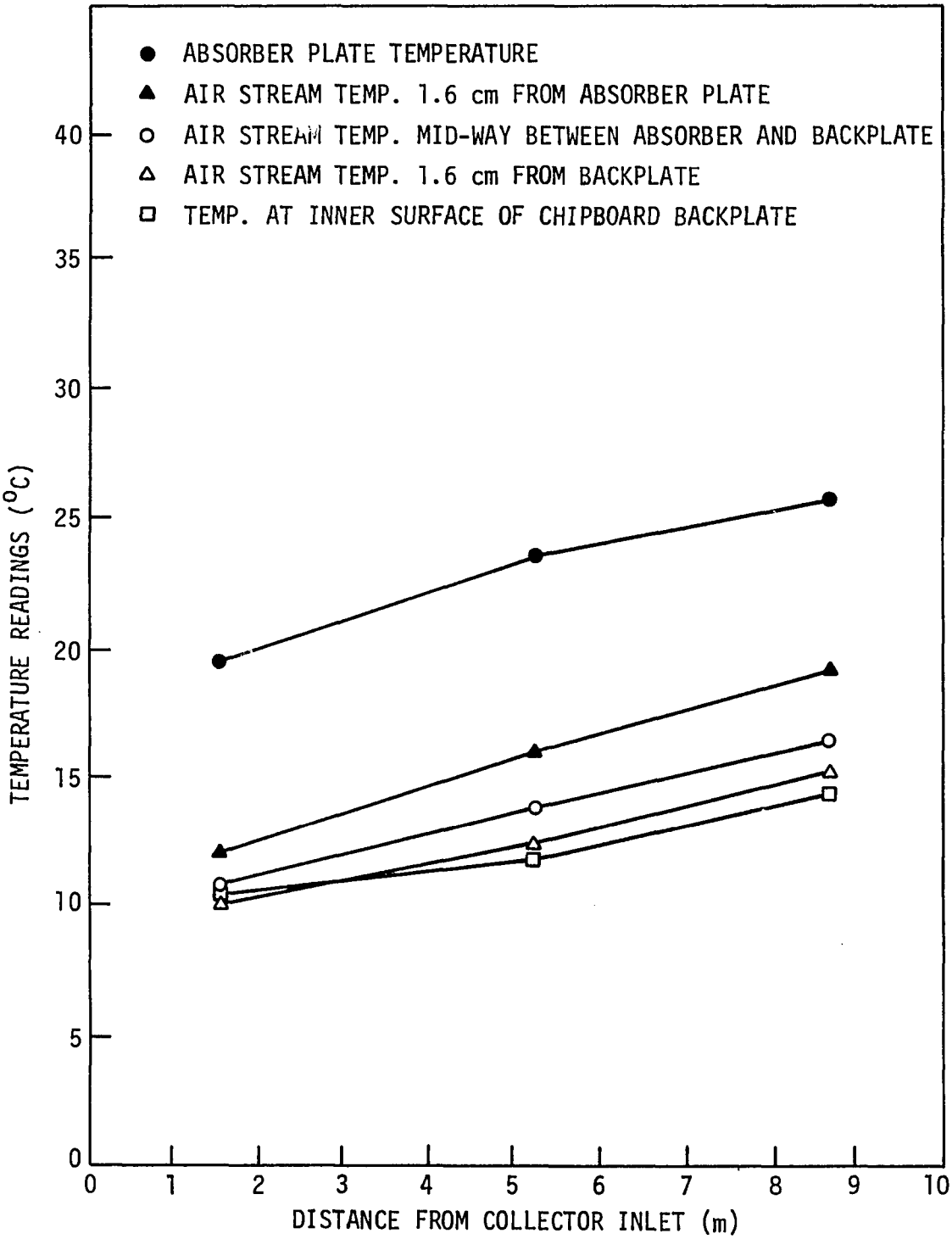

Figure 31. Temperature distribution along collector channel at 11:00 a.m., October 28, 1978

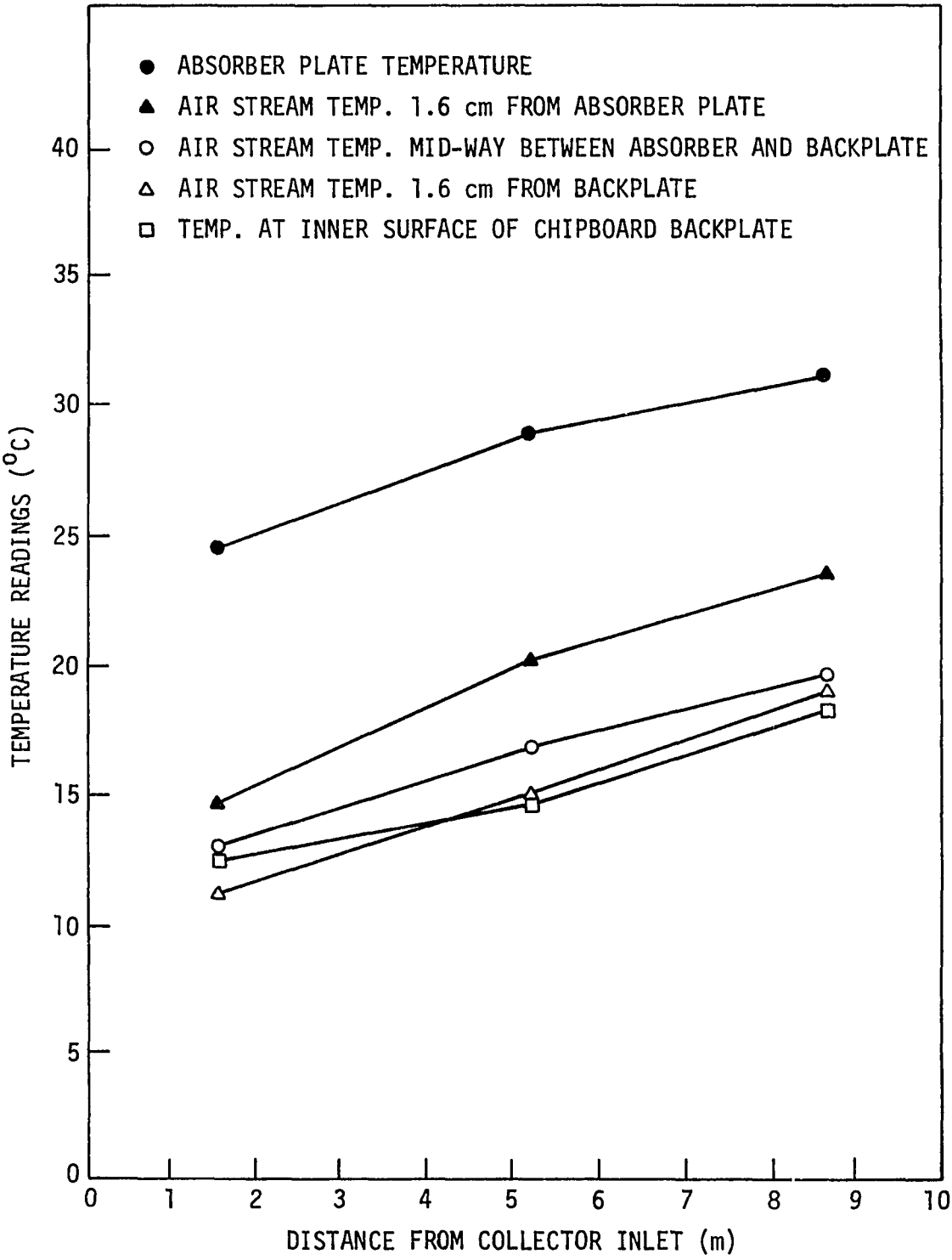

Figure 32. Temperature distribution along collector channel at solar noon, October 28, 1978

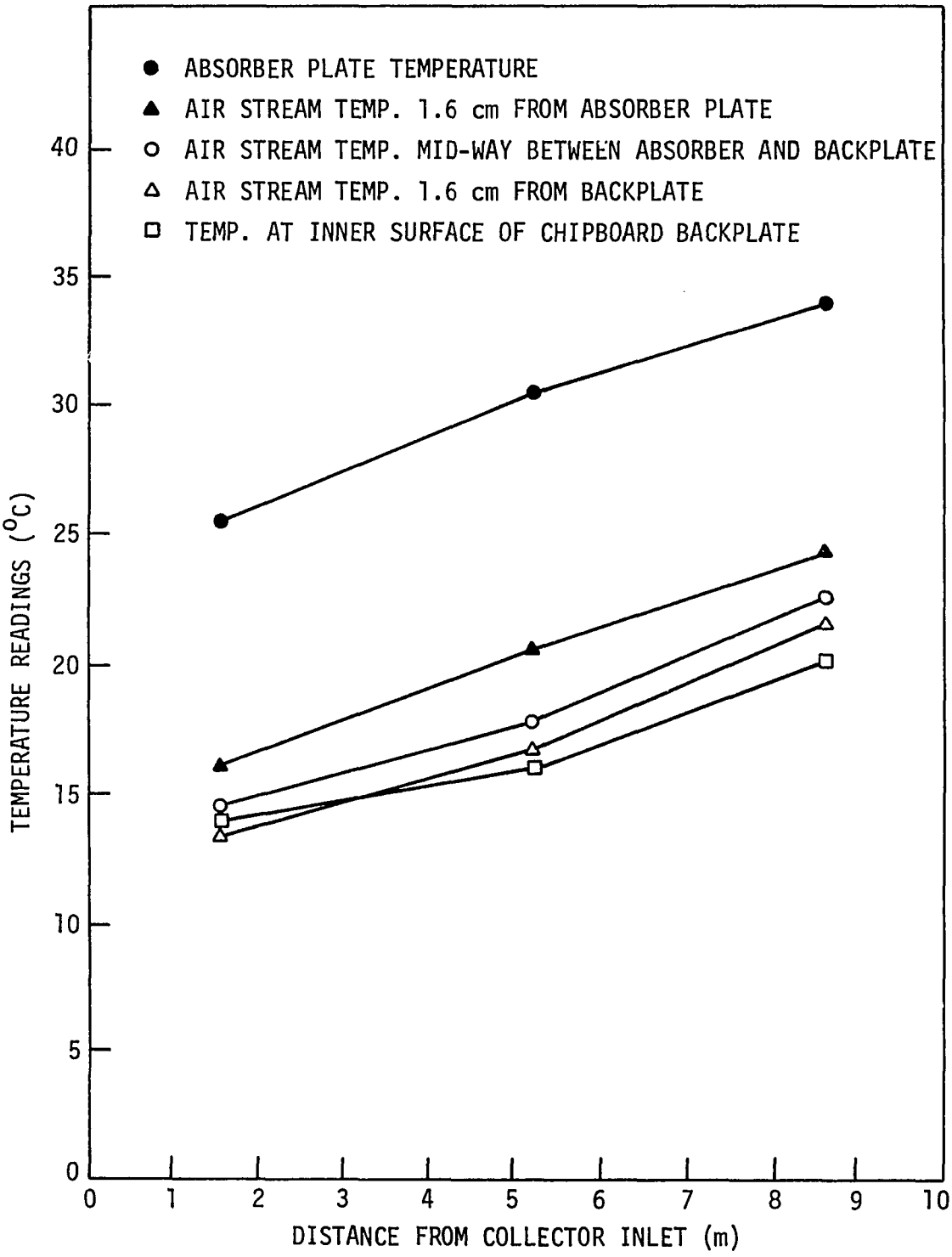

Figure 33. Temperature distribution along collector channel at 1:00 p.m., October 28, 1978

1:00 p.m. solar time. This lag in temperature increase may be attributed to heat storage in the absorber plate.

Results of the test point to the fact that collector length has a significant effect on air temperature rise through the collector.

Available waste heat from the engine

A measure of the effective removal of waste heat from the fan engine is the engine waste heat recovery, defined as the ratio of waste heat energy transferred to the air from the engine block and portion of the exhaust pipe, to the fuel energy input of the engine.

Results of the tests and related data on the availability of waste heat energy from the fan engine are presented in Table X. Comparison of test data revealed that waste heat recovery of the fan engine depends primarily on the fan-engine operating conditions defined by the engine speed, fan static load and airflow rate.

High airflows (tests 7, 8 and 9) resulted in higher waste heat recovery although air temperature rise through the engine was low. Waste heat energy added to the air was highest at higher engine speeds (tests 1 and 2), however, waste heat recovery was low which meant that more fuel energy was used up. Note that test 2 had a higher waste heat recovery than test 1 even though test 1 has a higher engine speed. This can be explained by the higher airflow in test 2 which resulted in higher heat added to the air.

Both high engine speeds and low airflow rates (tests 1 and 10) as well as low engine speeds and low airflow rates (tests 3 and 4) resulted in higher air temperature rise through the engine.

Table X. Test results on available waste heat energy from fan engine[a]

Test number	1	2	3	4	5	6	7	8	9	10
Static press., Pa	199.0	99.5	143.0	143.0	94.6	93.3	47.3	47.3	47.3	187.0
Engine speed, r/min	3630	3495	3265	3265	3275	3275	3285	3285	3285	3465
Airflow rate, m^3/s	0.371	0.533	0.300	0.300	0.406	0.425	0.557	0.557	0.557	0.288
Air temp. rise °C	7.6	5.6	6.8	7.0	5.6	5.0	4.3	4.5	4.7	7.0
Heat energy added to air, MJ/h	11.56	12.13	8.24	8.50	9.14	8.53	9.65	10.22	10.69	8.24
Fuel consumption, l/h	1.57	1.48	0.965	1.02	0.979	0.985	0.987	0.907	0.970	1.06
Fuel energy[b], MJ/h	51.84	48.96	31.86	33.77	32.33	32.51	29.95	29.95	32.04	34.92
Waste heat recovery, %	22.3	24.8	25.9	25.2	28.3	26.2	32.2	34.1	33.4	23.6

[a]Based on gasoline engine with 170.9-cm^3 displacement.

[b]Based on 33.02 MJ/l, the lower heating value for gasoline.

Results of tests on air temperature rise through the engine as a function of airflow rate and engine speed are described in Figure 34. Engine speeds during the tests were regulated by adjusting the standard engine governor control knob to 25, 50, 75 and 100 percent of the full setting. As shown in Figure 34, higher temperature rises through the engine were obtained at higher engine speeds, however, at higher airflow rates, air temperature rise decreased.

The performance characteristics of the fan-engine combination during the tests are described in Figure 35. Engine torque and power output are plotted in Figures 36 and 37, respectively, as functions of standard engine governor control setting and engine speed.

Combined solar collector-engine waste heat system

A summary of the combined results of tests on solar collector performance and engine waste heat utilization is presented in Table XI. Highest total heat energy added to the system was obtained from tests 2, 6, 7, 8 and 9. Airflow rates in these tests were also the highest. Highest percentage of solar contribution was observed in test 6 at 64.3 percent solar and 35.7 percent engine waste heat.

Taking the entire heating system into consideration, the tests shown in Table XII resulted in higher total heat energy added to the system, higher solar collection efficiency and higher engine waste heat recovery. Test conditions in tests 2 and 6 would be more desirable than tests 7, 8 and 9 because of the higher static loads which meant more grain load in the drying bin.

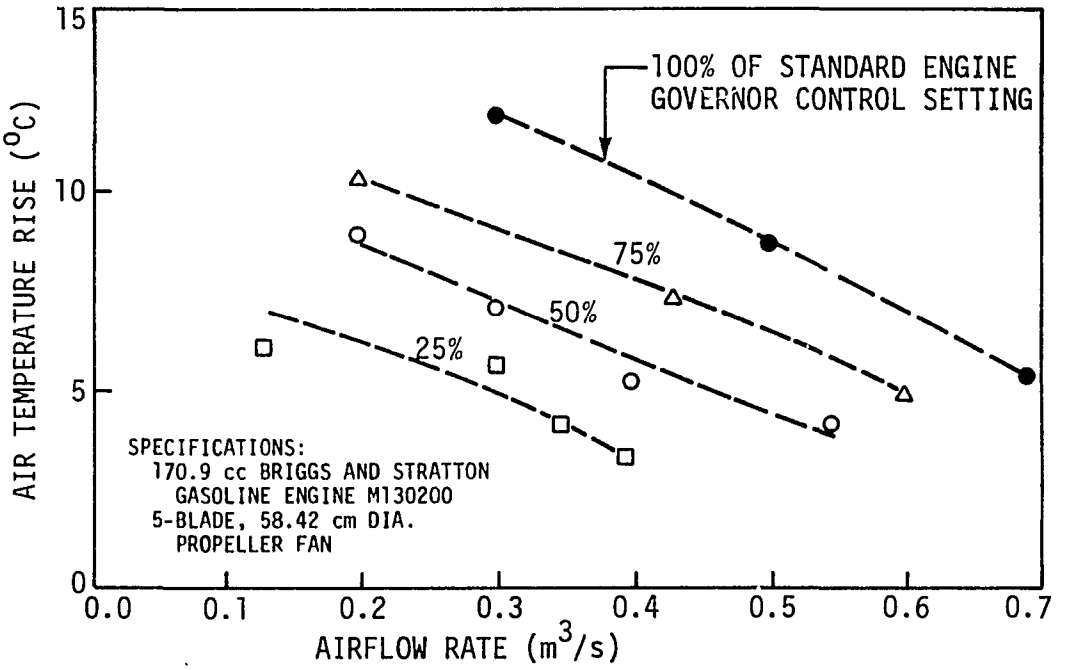

Figure 34. Air temperature rise through the engine as a function of engine governor setting and airflow rate

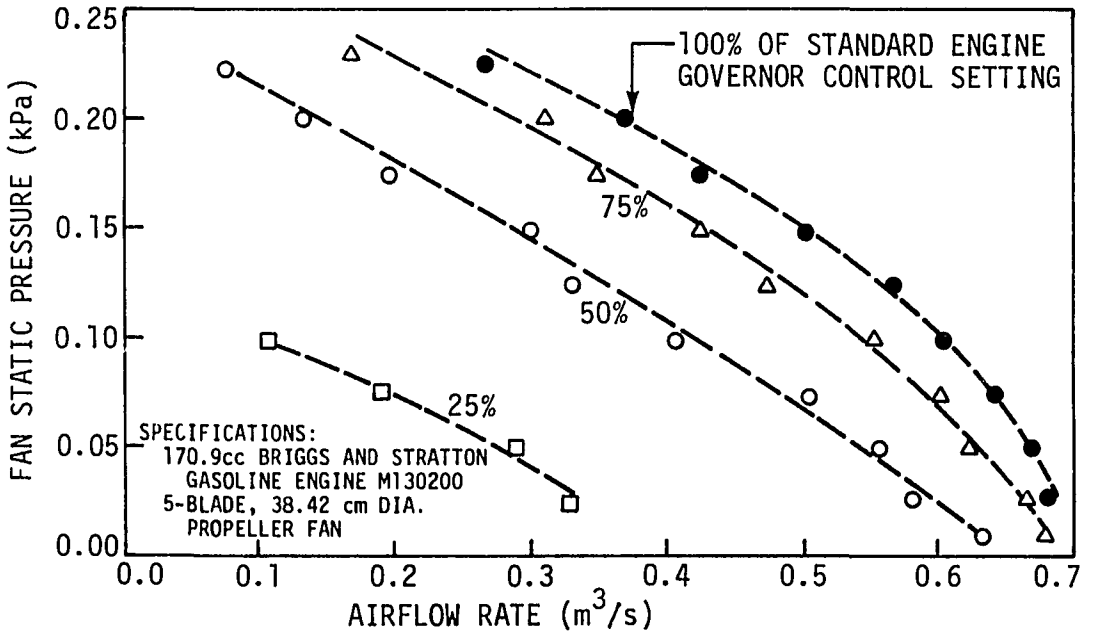

Figure 35. Fan-engine performance characteristics

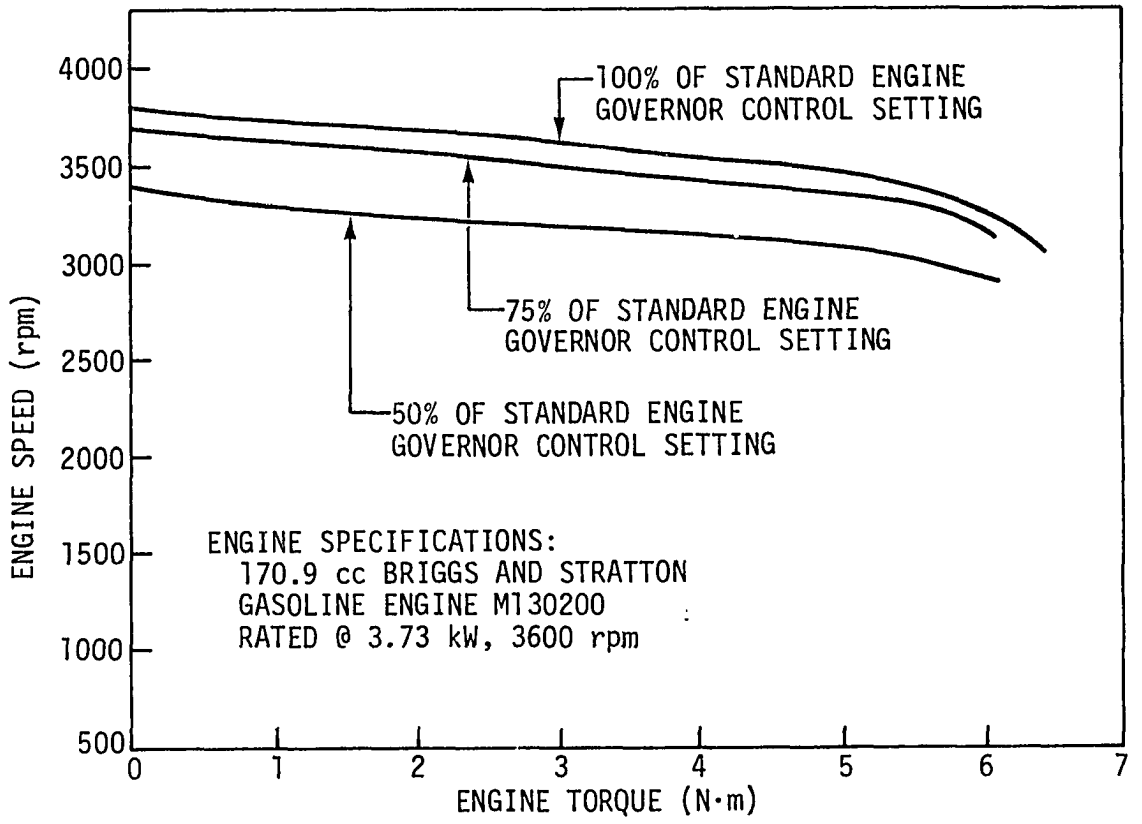

Figure 36. Engine speed-torque curves

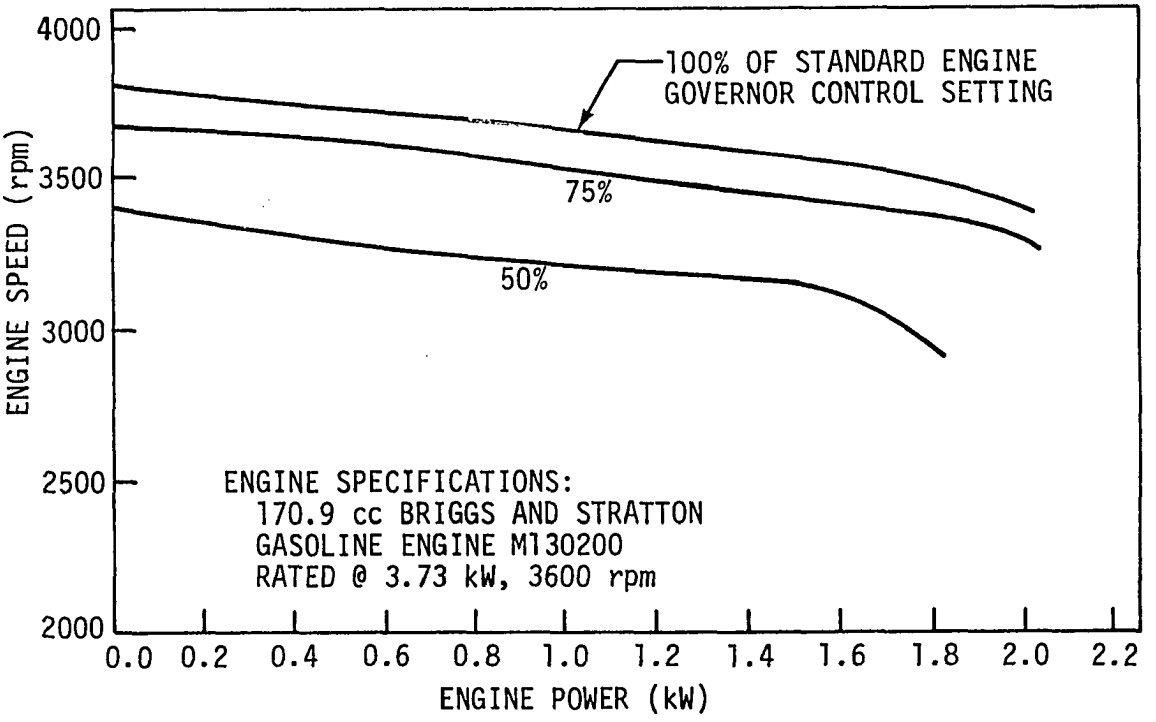

Figure 37. Engine speed and power output at different engine governor settings

Table XI. Combined test results[a] of solar collector performance and engine waste heat utilization

Test number	1	2	3	4	5	6	7	8	9	10
Airflow, m^3/s	0.3705	0.5333	0.2997	0.2997	0.4059	0.4247	0.5569	0.5569	0.5569	0.2879
Static press., Pa	199.0	99.5	143.0	143.0	94.6	93.3	47.3	47.3	47.3	187.0
ΔT_{tot}, °C	15.2	13.2	13.1	16.3	13.5	14.1	11.2	12.0	11.6	17.4
T_{pl}, °C	39.8	41.8	41.1	43.4	41.3	41.8	38.9	38.1	37.1	43.6
q^b_{coll}, MJ	91.96	129.80	61.12	89.52	102.80	123.10	124.10	134.20	124.60	96.79
q_{en}, MJ	92.45	97.06	65.95	67.97	73.15	68.26	77.18	81.79	85.54	65.95
q_{tot}, MJ	184.41	226.86	127.07	157.49	175.95	191.36	201.28	215.99	210.14	162.74
% solar	49.9	57.2	48.1	56.8	58.4	64.3	61.6	62.1	59.3	59.5
% engine	50.1	42.8	51.9	43.2	41.6	35.7	38.4	37.9	40.7	40.5

[a]Based on 8-hour test period.

[b]Based on 23.8 m^2 of solar collector area.

Table XII. Summary of test conditions which resulted in highest heat added to the system, highest solar collector efficiency, and highest engine waste heat recovery

Test number	2	6	7, 8, 9[a]
Airflow, m^3/s	0.533	0.425	0.557
Engine speed, r/min	3495	3275	3285
Static pressure, Pa	99.5	93.3	47.3
Collector efficiency, %	23.5	23.9	24.0
Engine waste heat recovery, %	24.8	26.2	33.2
Total heat added[b], MJ	226.86	191.36	209.14
% solar	57.2	64.3	61.0
% engine	42.8	35.7	39.0

[a]Average for three tests.

[b]Based on 8-hour test period.

Grain drying test

Results of the first corn drying test indicated that the solar-heated drying system supplemented by engine waste heat is capable of drying a load of 1.32 m^3 of grain from 26.3 to 13.9 percent moisture content, wet basis, in 12 hours of drying time over 1.5 days.

During the first 8 hours of drying on October 11, 1979, grain moisture content dropped from 26.3 percent down to 16.8 percent, wet basis. Total heat added to the system during the 8-hour period was 178.05 MJ with solar heat energy contributing 42.6 percent and engine waste heat 57.4 percent. Engine fuel consumption was 11.2 l of gasoline.

Data recorded in the test included an initial grain depth of 0.4 m, airflow rate of 0.425 m^3/s, air pressure drop through the collector of 21.2 Pa, fan static pressure of 141.8 Pa and engine speed of 3476 r/min.

Hourly variations in insolation rate, collection efficiency and useful heat gain in the collector during the first 8-hour drying period are shown in Figure 38. Fluctuation in the curves during the first half of the day was largely due to variable cloudiness. The average 8-hour collection efficiency was 17.1 percent. Maximum instantaneous collection efficiency was 19.7 percent.

The average 8-hour temperature rise in the collector was 5.3° C with a maximum of 8.9° C. The average air temperature rise due to the engine was 7.1° C.

The first drying test was continued the following day for another 4 hours from 10:00 a.m. to 2:00 p.m. solar time, until the average grain moisture content reached 13.9 percent, wet basis. The 4-hour collection efficiency on October 12, 1979, was 17.5 percent. Total heat added during the 4-hour period was 107.88 MJ with solar heat representing 46.6 percent. Engine fuel consumption was 5.6 l of gasoline.

Results of the 12-hour corn drying test from October 11 to October 12, 1979 are summarized in Table XIII. A total of 285.93 MJ was added to the system by both solar and waste engine heat. Solar heat energy represented 41.8 percent of the total. Sensible heat utilization, defined as the ratio of heat energy added to the system to the weight of water removed from the grains, was 3.3 MJ/kg of water removed.

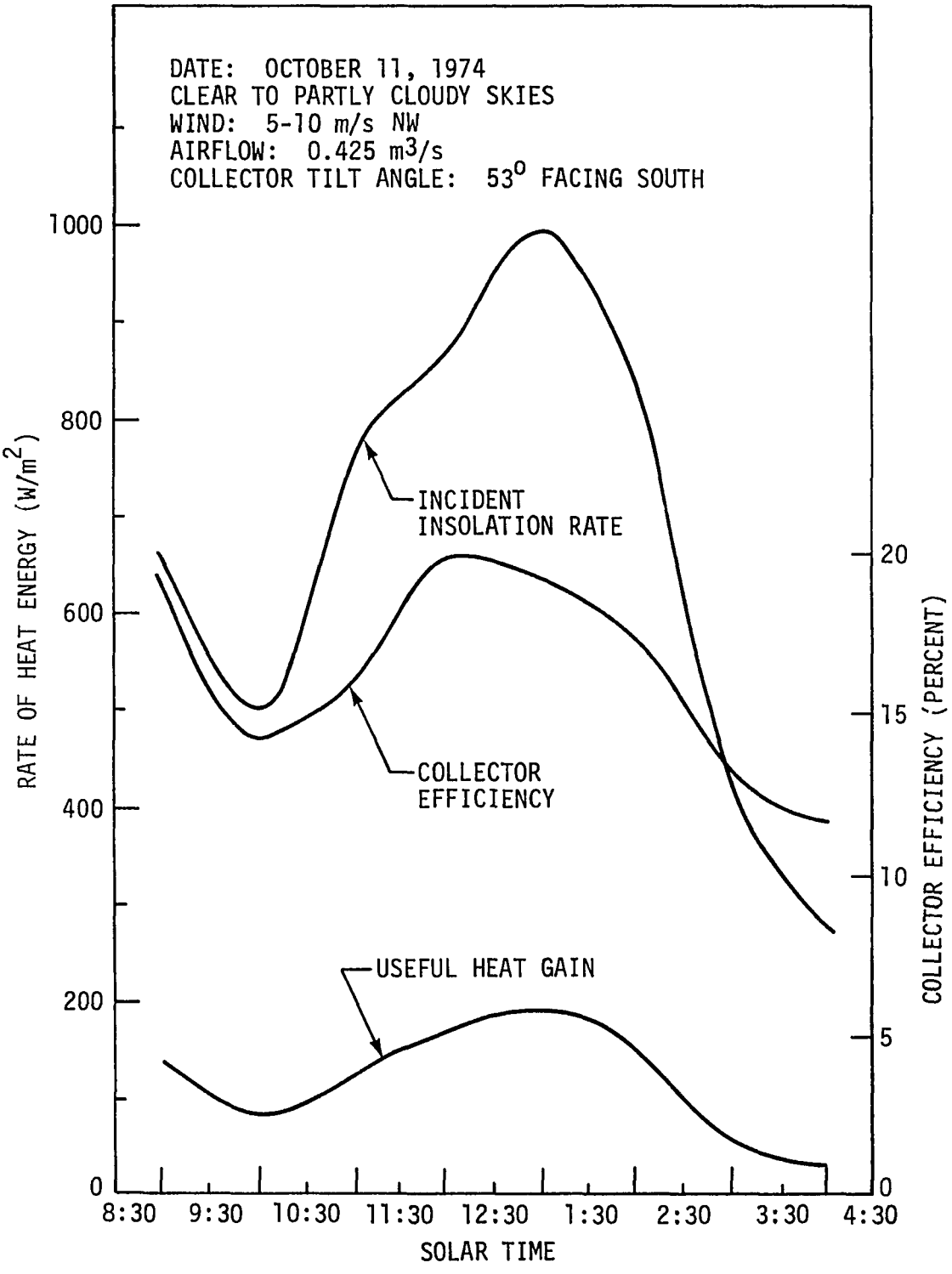

Figure 38. Hourly variation in insolation rate, collector efficiency and useful heat gain in the collector

Table XIII. Summary of corn drying test results on October 11 to October 12, 1979

Grain volume m^3	1.32
Ave. initial moisture content, % w.b.	26.3
Ave. final moisture content, % w.b.	13.9
Drying time, hr.	12.0
Airflow rate, m^3/s	0.425
Total heat added, MJ	285.93
% solar	41.8
% engine waste heat	58.2
Engine fuel consumption, l	16.8
Sensible heat utilization, MJ/kg water removed	3.3

In the second corn drying test conducted on October 17, 1979, the drying bin was filled with 24.5 percent moisture corn to a depth of 0.46 m. Airflow rate measured was 0.406 m^3/s at a fan static pressure of 169.2 Pa. Engine speed was maintained at 3476 r/min.

After 8 hours of drying, the average grain moisture content was down to 16.3 percent, wet basis. Results of the second drying test are summarized in Table XIV. The average 8-hour collector efficiency was 22.9 percent at an average 8-hour air temperature rise of 8.0° C. The higher collector efficiency and air temperature rise in the collector during the second test was largely due to higher insolation rates as compared with the first drying test. The average air temperature rise due to the engine was 8.4° C.

Table XIV. Results of 8-hour corn drying test on October 17, 1979

Grain volume, m^3	1.53
Ave. initial moisture content, % w.b.	24.5
Ave. final moisture content, % w.b.	16.3
Airflow rate, m^3/s	0.406
Total heat added to system, MJ	225.77
% solar	48.9
% engine waste heat	51.1
Engine fuel consumption, l	12.0
Sensible heat utilization, MJ/kg water removed	2.5

Hourly variations in insolation rate, collection efficiency and useful heat gain in the collector are shown in Figure 39. It should be noted from the figure that the instantaneous collector efficiency is dependent on the relative values of both the insolation rate and useful heat gain.

Drying operations were not continued on the following days due to inclement weather. Both drying tests, however, demonstrated the capability of the system to dry a load of grain in a short time without the need of fossil fuels for direct air heating.

From actual rice drying data reported by the Institute of Agricultural Engineering and Technology of the University of the Philippines (Anonymous, 1976), the estimated sensible heat utilization was 2.3 MJ/kg

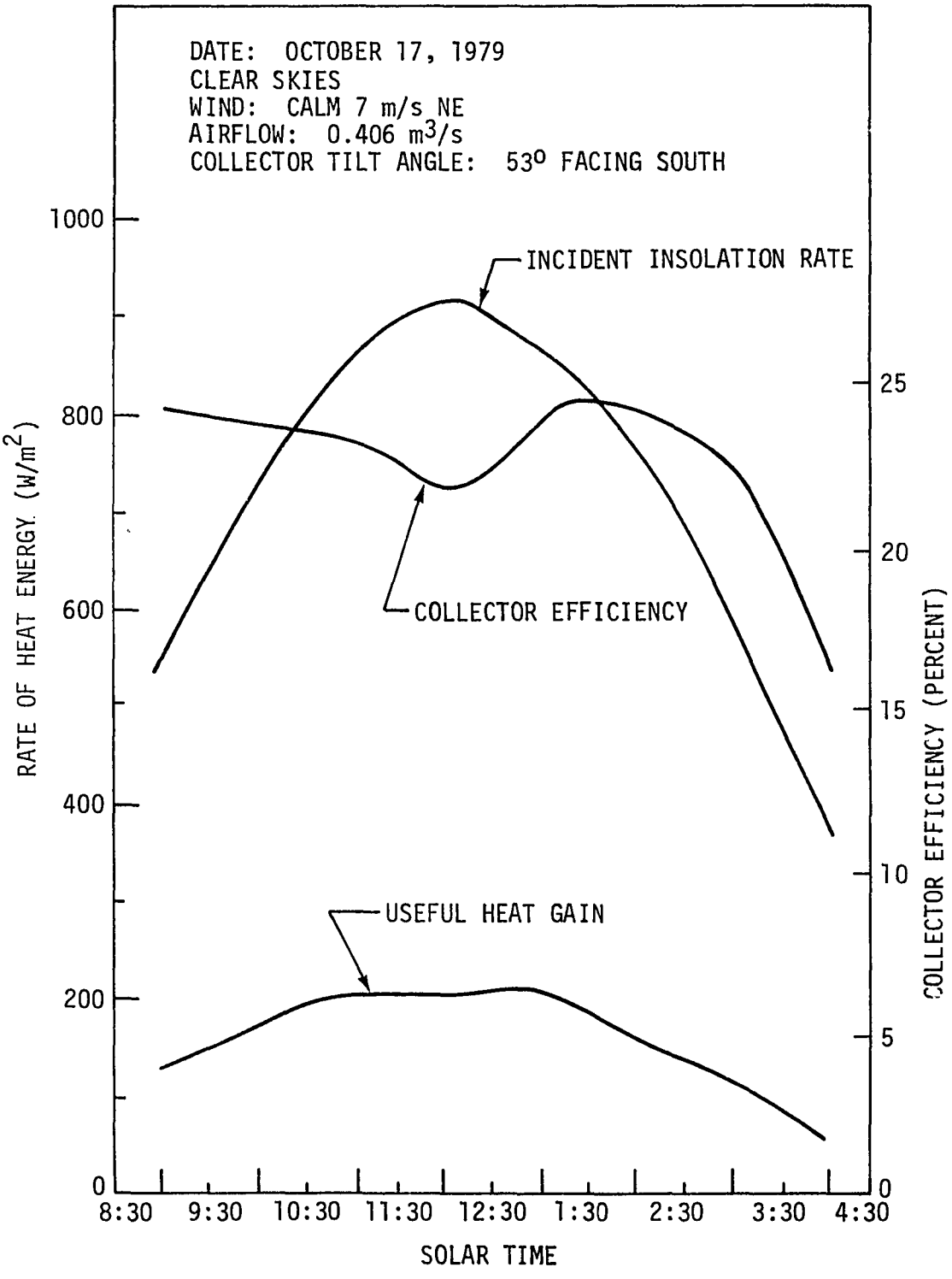

Figure 39. Hourly variation in insolation rate, collector efficiency and useful heat gain in the collector

of water removed. It therefore shows that more heat is required to remove moisture from shelled corn compared to rice.

ECONOMIC ANALYSIS

Based on information gathered from the experimental study, an economic analysis was made on a solar-heated grain drying system supplemented by engine waste heat. In the analysis, the bare-plate solar collector was considered to be part of a building roof structure. Hence, the actual cost of the solar collector is less than the cost of the experimental solar collector. Included in the analysis are the total installed cost of the system, total drying cost per unit volume of grain, estimated fuel savings and cost-effectiveness of the solar collector and the entire drying system.

Total Installed Cost

The total cost incurred in constructing the experimental solar grain drying system was $1422.00 including labor. Of this, the experimental solar collector cost $540.00 (excluding labor) representing 38 percent of the total construction cost. The high percentage of solar collector cost was largely due to the cost of corrugated steel roofing materials and collector frame supports which amounted to $303.00 or 56 percent of the collector cost.

For an integrated building solar roof collector, cost of the roof and frame structure are charged to the building costs rather than to the solar collector. Hence, the actual collector cost is only 46 percent of $540.00 or $248.40, excluding labor.

A breakdown of costs of a solar heated grain drying system with an integrated solar roof collector is presented in Table XV. Cost of the

grain drying bin, fan-engine assembly and labor were all derived from the actual costs incurred in the construction of the experimental set-up. From the table, labor cost represented approximately one-third of the estimated total installed cost of $1130.40 for the entire system. Based on the experimental solar collector area of 23.8 m^2, the unit cost of solar roof collector is estimated at $10.44/$m^2$, excluding labor.

Table XV. Breakdown of total installed cost of solar grain drying system with an integrated building roof solar collector

Item	Cost[a], $	Percent of total cost
Materials		
Solar collector	248.40	22
Grain drying bin	224.00	20
Fan-engine assembly	308.00	27
Labor	350.00	31
Total	1130.40	100

[a]Based on 1978 prices in Ames, Iowa.

Total Drying Cost

System capacity

In order to arrive at an estimate of the total drying cost of the system per unit volume of grain handled, data from the first corn drying test were used. It was further assumed that the system will be operated

for five months in the tropics, consisting of two months during the dry season harvest and three months during the wet season harvest.

Using the data shown in Table XVI, the estimated annual capacity of the system is 66 m^3 of shelled corn.

Table XVI. Data used in determining annual capacity of solar grain drying system

Factor	Specification
Drying period, months/year	5
Percent probable sunshine, %	50
Batch dryer capacity, m^3 of shelled corn	1.32
Drying time per batch, days	1.5

Cost analysis

Data shown in Table XVII were used in the calculation of the total drying costs of the system. Depreciation cost was calculated using the straight line method.

Calculations on operating costs were based on the assumption that the farmer operates the system. The cost of gasoline is $0.26/l. Engine fuel consumption of 16.8 l per batch of 1.32 m^3 of grain was based on actual experimental data.

Table XVII. Data used in the cost analysis of the solar grain drying system

Factor	Specification
Expected system lifetime, yrs	15
Installed cost (cost new), $	1130.40
Salvage value, % of cost new	5
Annual interest rate, % of 1/2 (cost new)	8
Maintenance cost, % of cost new	3
Taxes and insurance, % of 1/2 (cost new)	1.5

Fixed cost

$$\text{Depreciation} = \frac{1130.40 - 5\% \text{ of } 1130.40}{15} = \$\ 71.59 \text{ per yr}$$

Interest = 8% of 1/2 (1130.40) = 45.22 per yr

Housing (nil)

Taxes and insurance = 1.5% of 1/2 (1130.40) = 8.48 per yr

Total annual fixed cost $125.29

Fixed cost per m^3 1.90

Operating cost

$$\text{Fuel cost} = \frac{16.8\ l}{1.32\ m^3} \times \frac{\$0.26}{1} \times 66\ m^3 = \$218.40 \text{ per yr}$$

Maintenance cost = 3% of 1130.40 = 33.91 per yr

Total annual operating cost $252.31

Operating cost per m^3 3.82

Total drying cost per m^3 5.72

Estimated Fuel Savings

The estimated savings in heating costs were based on the substitution of solar energy and waste engine heat for kerosene fuel. Kerosene-fired burners are prevalently used in portable mechanical grain dryers introduced in the developing countries of the tropics. With a heating value of 35.17 MJ/l, a direct-fired kerosene burner can provide heat energy at a unit cost of $4.26/GJ (based on kerosene fuel cost of $0.15/l).

From data on the first corn drying test, total heat energy supplied to the system was 285.93 MJ per batch of 1.32 m^3 of shelled corn dried from 26.3 to 13.9 percent moisture content, wet basis. Hence, for an annual system capacity of 66 m^3 of grain,

$$\text{Annual system fuel savings} = \frac{285.92\ \text{MJ}}{1.32\ m^3} \times 66\ m^3 \times \frac{\$4.26}{\text{GJ}}$$

$$= \$60.92/\text{yr}$$

Based on the first corn drying test, total heat supplied by the solar collector alone was 119.52 MJ per batch of 1.32 m^3 of grain. At an annual system capacity of 66 m^3 of grain, the estimated annual fuel savings due to the solar collector alone is

$$\text{Annual collector fuel savings} = \frac{119.52\ \text{MJ}}{1.32\ m^3} \times 66\ m^3 \times \frac{\$4.16}{\text{GJ}}$$

$$= \$25.46/\text{yr}$$

Difference between the system and collector fuel savings is due to engine waste heat.

It should be noted that the average collector efficiency during the first corn drying test was 15.7 percent which is considered low for tropical conditions. Annual fuel savings is therefore expected to be much higher in the tropics. Further savings in fuel costs is expected in the tropics due to the relatively higher fuel costs.

Cost-Effectiveness of Solar Collector and Solar Grain Drying System

High fuel costs and expected annual fuel cost increases as well as annual interest rates and expected lifetimes have a significant influence on the economic feasibility of solar collectors and solar grain drying systems.

To determine the economically justifiable investment in a solar-heating system based on expected savings in heating costs over the life of the system, compound-interest calculations were used.

Kreider and Kreith (1977) used the following expression in determining the economically justifiable investment in a system given the annual savings in heating costs:

$$P = P_o \frac{(1 + i_{eff})^t - 1}{i_{eff} (1 + i_{eff})^t}$$

where

P = present worth of the system (capital investment), $

P_o = annual savings in fuel cost, $/yr

i_{eff} = effective interest rate, percent

t = payback or recovery, years

The effective interest rate, i_{eff}, is related to the annual interest rate, i_{ann}, and the expected increase in fuel cost, j, by the expression

$$i_{eff} = \frac{1 + i_{ann}}{1 + j} - 1 \simeq i_{ann} - j$$

Kreider and Kreith (1974) and Heid (1978) cited long-term fuel cost increases of 5 to 10 percent per year. The influence of steadily increasing fuel costs and high fuel cost on the bare-plate solar collector and the entire solar drying system are shown in Tables XVIII and XIX, respectively, for a number of different lifetimes of the system and interest rates. Figures below the lines in both Tables XVIII and XIX indicate economically justifiable investments at the given conditions for a solar collector cost of $248.40 and an entire drying system cost of $1130.40, respectively.

The justifiable investments on both the solar collector and the entire drying system increase with expected annual increases in fuel costs but decrease with increasing interest rates. It should be pointed out that the estimated fuel cost savings were derived from experimental data wherein the performance of the solar collector was considered low under tropical conditions and hence are conservative estimates.

Data in Table XVIII show that for the solar collector alone, economically justifiable investments can be attained even when the expected collector lifetime is only 10 years, given a projected fuel cost increase of 10 percent per year and the annual interest rate of up to 10 percent. Given the same projected fuel cost increase of 10

percent per year, the entire solar drying system has to have an expected system lifetime of 15 years at an annual interest rate of only 7 percent to be economically justifiable.

Table XVIII. Economically justifiable investment[a] (dollars) in the solar collector at present fuel savings of $25.46/yr

Expected system lifetime (yr)	Projected fuel cost increase (% per yr)	Interest rate (% per yr) 7	10	12
10	0	178.82	156.44	143.85
	5	228.70	196.60	178.82
	10	302.18	254.60	228.70
	15	414.39	341.26	302.18
	20	592.51	476.42	414.39
15	0	231.88	193.65	173.41
	5	327.14	264.27	231.88
	10	491.51	381.90	327.14
	15	793.36	589.89	491.59
	20	1385.86	981.97	793.36
20	0	269.72	216.76	190.17
	5	416.25	317.29	269.72
	10	711.97	509.20	416.25
	15	1368.35	911.22	711.97
	20	2977.59	1839.55	1368.35

[a]Based on: $P = P_o \frac{(1 + i_{eff})^t - 1}{i_{eff}(1 + i_{eff})^t}$, where

P = present worth (capital investment); P_o = annual savings in fuel cost; t = expected collector lifetime; $i_{eff} = i_{ann} - j$; i_{ann} = annual interest rate; j = projected fuel cost increase.

Hence, use of an integrated building solar roof collector can be more easily justified economically than the entire solar grain drying system. Effects of taxes, insurance, maintenance and inflation were not considered in this particular analysis.

Table XIX. Economically justifiable investment[a] (dollars) in the solar grain drying system at present fuel savings of $60.92/yr

Expected system lifetime (yr)	Projected fuel cost increase (% per yr)	Interest rate (% per yr) 7	10	12
10	0	427.88	374.33	344.21
	5	547.22	470.41	427.88
	10	723.06	609.20	547.22
	15	991.54	816.55	723.06
	20	1417.74	1139.97	991.54
15	0	554.85	463.36	414.92
	5	782.78	632.33	554.85
	10	1176.06	913.80	782.78
	15	1898.32	1411.48	1176.06
	20	3316.05	2347.64	1898.32
20	0	645.39	518.65	455.04
	5	996.00	759.20	645.39
	10	1703.59	1218.40	996.00
	15	3274.15	2180.34	1703.59
	20	7124.70	4401.63	3274.15

[a]Based on: $P = P_o \dfrac{(1 + i_{eff})^t - 1}{i_{eff}\,(1 + i_{eff})^t}$, where

P = present worth (capital investment); P_o = annual savings in fuel cost; t = expected system lifetime; $i_{eff} = i_{ann} - j$; i_{ann} = annual interest rate; j = projected fuel cost increase.

SUMMARY AND CONCLUSIONS

The potential use of solar energy as an alternative energy source for grain drying has been a subject of numerous research studies. Most of the studies, however, were confined to low-temperature solar and solar-assisted grain drying systems involving temperature rises of a few degrees and drying over extended periods of several weeks or months while the grain is in storage.

In the tropics, ambient air temperature and humidity are so much higher that grains, especially rice, are readily susceptible to germination and spoilage unless steps are taken to quickly reduce the grain moisture content to a safe level of 14 percent, wet basis.

A review of previously developed solar collector designs provided a basis for the selection, design and construction of a simple, low-cost solar heat collector for use in developing tropical countries. Analysis of solar collector performance and a theoretical design calculation also helped in the understanding of factors that influenced solar collector efficiency and useful heat gain in the collector.

An experimental solar grain drying system utilizing a bare-plate solar heat collector with a collection area of 23.8 m^2 was constructed and tested. The solar collector was originally conceived as an integrated building roof solar collector wherein minor modification can be made with a minimum of construction costs. Available waste heat from the dryer fan engine was also utilized to provide supplemental heating.

Basic information on the performance of the solar-heated grain drying system was derived from results of tests and calculations.

The bare-plate solar heat collector was found to be capable of contributing as much as 60 percent of the heat added to the system. Higher airflow and insolation rates resulted in higher collection efficiencies and useful heat gain in the collector. Eight-hour collection efficiencies obtained from the tests ranged from 12.3 to 24.8 percent. With greater insolation rates expected in the tropics, it is expected that useful heat gain in the collector would be higher than those obtained from the tests.

Performance of the solar collector was also found to vary during the day. Air temperature rise and useful heat gain in the collector increase with increasing insolation and decrease correspondingly. A lag in temperature rise in the collector was observed after the insolation peaked. This was attributed to heat storage in the collector absorber plate. Collector length was also found to have a significant effect on the air temperature rise in the collector.

Available waste heat from the dryer fan engine constituted a significant source of heat energy for the grain drying system. Higher engine waste heat recovery was observed when engine speed and airflow rates were increased. However, high engine speed and low airflow rates resulted in lower waste heat recovery. Engine waste heat recovery obtained from a 170.9-cm^3 gasoline engine at different fan-engine operating characteristics ranged from 22.3 to 34.1 percent. Air temperature rise

through the engine was also found to increase at higher engine speeds but decrease at higher airflow rates.

Results of corn drying test indicated that the solar grain drying system supplemented by engine waste heat is capable of drying a load of wet corn grains from 26.3 to 13.9 percent moisture content, wet basis, in 12 hours covering 1.5 days. It is also expected that drying time under tropical conditions would be less on account of higher insolation rates. Higher ambient air temperatures and low wind speeds in the tropics would further reduce heat losses from the collector and hence higher useful heat gain is expected. Higher ambient air temperature reduces the temperature difference between the solar collector and the surroundings thus minimizing outward heat loss.

Cost analysis of the solar grain drying system assuming an integrated solar roof collector showed an estimated total installed cost of $1130.40. The unit collector cost excluding labor was estimated at $10.44/m^2 of collector area. The estimated total drying cost of the system based on an expected system lifetime of 15 years and an annual system capacity of 66 m^3 of grain is $5.72/m^3 of grain.

The estimated fuel savings of the system resulting from substitution of solar energy and engine waste heat for kerosene fuel amounted to $60.92/yr. The estimated fuel savings due to the solar collector was $25.46/yr.

With fuel prices likely to increase, the economic advantage of the solar collector and solar grain drying system become more attractive. Lower labor costs in developing tropical countries would further reduce

the cost of the solar grain drying system to less than the estimated cost of $1130.40. Higher fuel costs and expected fuel cost increases in developing countries could significantly increase the justifiable investments for solar collectors and solar grain drying systems.

Based on the results of the research study and calculations, the following conclusions were drawn:

1. High airflow and insolation rates resulted in higher collection efficiencies and useful heat gain in the bare plate solar collector.
2. Collector length was found to have a significant effect on the air temperature rise in the collector.
3. Available waste heat from the dryer fan engine represents a significant source of heat energy for the grain drying system.
4. Under the conditions of the tests, the solar-heated grain drying system supplemented by engine waste heat was found to be capable of drying a load of wet corn grains in a short period of time without the need of fossil fuels for direct air heating.
5. With higher fuel costs and expected fuel cost increases in developing tropical countries, the economic advantage of the solar collector and the entire solar grain drying system becomes more attractive.

RECOMMENDATIONS FOR FUTURE STUDY

In connection with the research study undertaken, the following suggestions are made for future study:

1. Construct, test and evaluate the solar-heated grain drying system under actual tropical conditions.
2. Develop a computer simulation technique to predict the performance of solar heat collectors and solar grain drying systems under tropical conditions.
3. Incorporate the exhaust heat of the dryer fan engine into the drying air stream and test for quality of the dried product.
4. Vary the collector length and width, air channel depth and air flow rate in the bare-plate solar collector and evaluate their effects on collector performance and cost per unit of heat delivered.
5. Modify the design of existing solar heat collector by incorporating a coverplate such as fiberglass or polyethylene plastic or by using fiberglass roofing materials instead of corrugated steel roofing sheets and utilizing the chipboard backplate as the primary absorber by painting it flat-black. These schemes can then be compared with the original design as to performance and economic feasibility.
6. Following a similar approach used in the research study, design, construct and test a solar-heated drying system for other tropical crops.

REFERENCES

Aldrich, R. A., M. F. Brugger, R. A. Keppeler, and V. Jonsson. 1972. Radiosities of metal building sheets exposed to solar energy. ASAE Paper No. 72-421.

Anonymous. 1976. Build a rice dryer for your farm. UPLB-NFAC Grain Processing Program, Institute of Agricultural Engineering and Technology, University of the Philippines, Los Baños, Laguna, Philippines.

ASHRAE. 1977. Handbook of fundamentals. American Society of Heating, Refrigerating and Air-conditioning Engineers, Inc., New York, N.Y.

Association of Japanese Agricultural Scientific Societies. 1975. Rice in Asia. University of Tokyo Press, Tokyo, Japan.

Bailey, P. H. and W. F. Williamson. 1965. Some experiments on drying grain by solar radiation. J. Agr. Engr. Res. 10(3):191-196.

Baryeh, E. A. 1972. Design of a corn dryer for tropical conditions. Unpublished M.S. thesis. Library, Iowa State University, Ames, Iowa.

Bauman, B. S. and M. F. Finner. 1979. Reducing energy costs in a solar corn drying system. ASAE-CSAE Paper No. 79-3025.

Bauman, B. S., M. F. Finner, and G. C. Shove. 1975. Low temperature grain drying with supplemental solar heat from an adjacent metal building. ASAE Paper No. 75-3514.

Becker, C. F. and J. S. Boyd. 1957. Solar radiation availability on surfaces in the U.S. as affected by season, orientation, latitude and cloudiness. Solar Energy 1(1):13-21.

Bliss, R. W. 1959. The derivation of several "plate-efficiency factors" useful in the design of flat-plate solar heat collectors. Solar Energy 3(4):55-64.

Boyd, J. 1976. Tools for agriculture. Second edition. Intermediate Technology Publications Ltd., London, England.

Brooker, D. B., F. W. Bakker-Arkema, and C. W. Hall. 1974. Drying cereal grains. The AVI Publishing Company, Inc., Westport, Conn.

Buelow, F. H. 1956. The effect of various parameters on the design of solar energy air heaters. Unpublished Ph.D. thesis. Library, Michigan State University, East Lansing, Mich.

Buelow, F. H. 1958. Drying grain with solar heated air. Mich. Agr. Exp. Sta. Quarterly Bull. 41(2):421-429.

Buelow, F. H. 1967. Solar energy received by inclined surfaces. Mich. Agr. Exp. Sta. Quarterly Bull. 49(3):294-300.

Buelow, F. H. and J. S. Boyd. 1957. Heating air by solar energy. Agricultural Engineering 38(1):28-30.

Carnes, A. 1932. Heating water by solar energy. Agricultural Engineering 13(6):156-159.

Chau, K. V., C. D. Baird, and L. O. Bagnall. 1978. Drying of corn and soybeans with solar energy in the Southeast. ASAE Paper No. 78-3014.

Cooper, P. I. 1969. The absorption of solar radiation in solar stills. Solar Energy 12(3):333-346.

Duffie, J. A. and W. A. Beckman. 1974. Solar energy thermal processes. John Wiley and Sons, New York, N.Y.

Exell, R. H. B. and S. Kornsakoo. 1978. Solar rice dryer. AIT Review (Thailand) 17(14):1.

Farber, E. A. and C. A. Morrison. 1977. Clear-day design values. Applications of Solar Energy for Heating and Cooling of Buildings. American Society of Heating, Refrigerating and Air-conditioning Engineers, Inc., New York, N.Y.

Foster, G. H. and R. M. Peart. 1976. Solar grain drying progress and potential. Agric. Info. Bull. No. 401. USDA, Washington, D.C.

Fritz, S. 1955. Transmission of solar energy through the earth's clear and cloudy atmosphere. Conference on the Use of Solar Energy 1:17-36.

Hall, M. D. 1978. Machine storage building with solar roof for grain drying. ASAE Paper No. 78-3068.

Heid, W. G., Jr. 1978. The performance and economic feasibility of solar grain drying systems. USDA Agr. Economic Report No. 396.

Henderson, S. M. and R. L. Perry. 1976. Agricultural process engineering. Third edition. The AVI Publishing Company, Inc., Westport, Conn.

Hottel, H. C. and A. Whillier. 1955. Evaluation of flat-plate solar collector performance. Conference on the Use of Solar Energy 2:74-104.

Hottel, H. C. and B. B. Woertz. 1942. The performance of flat-plate solar-heat collectors. Trans. of ASME 64:91-104.

Howe, E. D. 1955. Solar distillation. Conference on the Use of Solar Energy 3:159-169.

Johnson, F. S. 1954. The solar constant. J. Meteorol. 11(6):431-439.

Kimball, H. H. 1927. Measurements of solar radiation intensity and determination of its depletion by the atmosphere. U.S. Monthly Weather Review 55:155-159.

Klein, W. H. 1948. Calculation of solar radiation and the solar heat load on man. J. Meteorol. 5(4):119-129.

Klein, S. A., J. A. Duffie, and W. A. Beckman. 1974. Transient considerations of flat-plate solar collectors. Trans. of ASME Ser A 96(2):109-113.

Kline, G. L. 1977. Solar collectors for low temperature grain drying. ASAE Paper No. 77-3007.

Kranzler, G. A., C. J. Bern, and G. L. Kline. 1975. Grain drying with supplemental solar heat. ASAE Paper No. 75-3001.

Kreider, J. F. and F. Kreith. 1977. Solar heating and cooling. Revised first edition. McGraw-Hill Book Company, New York, N.Y.

Kreith, F. 1973. Principles of heat transfer. Third edition. Intext Educational Publishers, New York, N.Y.

Lambert, A. J. and D. H. Vaughan. 1978. Batch peanut and grain drying using an integrated shed solar collector. ASAE Paper No. 78-3069.

Lipper, R. I. and C. P. Davis. 1960. Drying crops with solar energy. Agricultural Research 8(11):14.

Liu, B. Y. H. and R. C. Jordan. 1960. The interrelationship and characteristic distribution of direct, diffuse and total solar radiation. Solar Energy 4:1-19.

Löf, G. O. G. and R. A. Tybout. 1972. A model for optimizing solar heating design. ASME Paper 72-WA/Sol-8.

Longhouse, H. A. 1961. Design, construction and testing of a stationary solar collector. Unpublished M.S. thesis. Library, West Virginia University, Morgantown, West Virginia.

McLendon, B. D. and J. M. Allison. 1978. Solar energy utilization in alternate grain drying systems in the southeast. ASAE Paper No. 78-3013.

Meyer, G. E., H. M. Keener, and W. L. Roller. 1975. Solar heated air drying of soybean seed and shelled corn. ASAE Paper No. 75-3002.

Midwest Plan Service. 1977. Structures and environment handbook. Ninth edition. Iowa State University, Ames, Iowa.

Moon, P. 1940. Proposed standard radiation curves for engineering use. J. Franklin Inst. 230:538-617.

Morey, R. V., H. M. Keener, T. L. Thompson, G. M. White, and F. W. Bakker-Arkema. 1978. The present status of grain drying simulation. ASAE Paper No. 78-3009.

Morrison, D. W. and G. C. Shove. 1975. Bare plate solar collector grain drying bin. ASAE Paper No. 75-3513.

Pelletier, R. J. 1959. Solar energy: present and forseeable uses. Agricultural Engineering 40(3):143-144.

Peterson, W. H. 1973. Solar heat for drying shelled corn. ASAE Paper No. NC73-302.

Peterson, W. H. and M. A. Hellickson. 1976. Solar-electric drying of corn in South Dakota. Trans. of ASAE 19(2):349-353.

Pierce, R. O. and T. L. Thompson. 1976. Solar grain drying in the north central region - simulation results. ASAE Paper No. 76-3517.

Remmers, H. E. 1962. Plate collector of solar energy for heating air. Unpublished M.S. thesis. Library, University of California, Davis, California.

Roa, G. M. and I. C. Macedo. 1976. Drying of 'carioca' dry beans with solar energy in a stationary bin. ASAE Paper No. 76-3021.

Smith, G. W. 1973. Engineering economy. Second edition. The Iowa State University Press, Ames, Iowa.

Sobel, A. T. and F. H. Buelow. 1963. Galvanized steel roof construction for solar heating. Agricultural Engineering 44(6):312.

Soemangat, M., M. L. Esmay, and W. J. Chancellor. 1973. Rice drying with waste engine heat. ASAE Paper No. 73-322.

Stone, R. P. and J. C. Currelly. 1979. Experiences with a solar-assisted low temperature grain dryer. ASAE-CSAE Paper No. 79-3020.

Tabor, H. 1955. Solar energy collector design. Conference of the Use of Solar Energy 2:1-23.

Tan, H. M. and W. W. S. Charters. 1970. An experimental investigation of forced-convective heat transfer for fully-developed turbulent flow in a rectangular duct with asymmetric heating. Solar Energy 13:121-125.

Tani, T. 1975. General status of rice storage in southeast Asia. Rice in Asia. Edited by the Association of Japanese Agricultural Scientific Societies. University of Tokyo Press, Tokyo, Japan.

Thekaekara, M. P. and A. J. Drummond. 1971. Standard values for the solar constant and its spectral components. Nat. Phys. Sci. 296:6.

Thompson, T. L. 1972. Temporary storage of high moisture shelled corn using continuous aeration. Trans. of ASAE 15(2):333-337.

Threlkeld, J. L. and R. C. Jordan. 1958. Direct solar radiation available on clear days. Trans. of ASHRAE 64:45.

Troeger, J. M. and J. L. Butler. 1977. Simulation of solar peanut drying. ASAE Paper No. 77-3537.

UPLB Weather Station Summary Report. 1977. University of the Philippines, Los Baños, Laguna, Philippines.

Whillier, A. 1953. Solar energy collection and its utilization for house heating. Unpublished Sc. D. thesis. Dept. of Mechanical Engineering, MIT, Boston, Mass.

Whillier, A. 1977. Prediction of performance of solar collectors. Applications of Solar Energy for Heating and Cooling of Buildings. American Society of Heating, Refrigerating and Air-conditioning Engineers, Inc., New York, N.Y.

Williams, E. E., M. R. Okos, R. M. Peart, and A. F. Badenhop. 1976. Solar grain drying and collector evaluation. ASAE Paper No. 76-3512.

Wrubleski, E. M., H. R. Davidson, and H. C. Korven. 1979. Three solar collectors assessed for applications. ASAE-CSAE Paper No. 79-3021.

Yellott, J. I. 1977. Solar radiation measurement. Applications of Solar Energy for Heating and Cooling of Buildings. American Society of Heating, Refrigerating and Air-conditioning Engineers, Inc., New York, N.Y.

ACKNOWLEDGEMENTS

The author wishes to express his sincerest gratitude to Dr. C. W. Bockhop and Dr. C. J. Bern, head and associate professor of Agricultural Engineering, for their invaluable support and guidance in all phases of the author's graduate study.

Special thanks is due to the other members of the guidance committee: Dr. S. J. Marley and Dr. R. J. Smith, professors of Agricultural Engineering; Dr. G. H. Junkhan, professor of Mechanical Engineering; Dr. T. H. Kuehn, assistant professor of Mechanical Engineering; and Mr. G. L. Kline, Agricultural Engineer, USDA-SEA-AR; for their guidance and help.

Appreciation is extended to the World Food Institute for making this research study possible. Appreciation is also expressed for the indispensable assistance of Lib, Barb, Lois and Phyllis of the Department of Agricultural Engineering secretarial pool.

A very special thanks is due to the author's wife, Yoly, for preparing the draft of the thesis and for her patience and endurance throughout the course of the author's study.

APPENDIX A: EXTRATERRESTIAL SOLAR RADIATION INTENSITY AND RELATED DATA FOR THE TWENTY-FIRST DAY OF EACH MONTH, BASE YEAR 1964[1]

Month	I_{oN} (W/m^2)	δ (deg)	A (W/m^2)	B (Dimensionless)	C (Dimensionless)
JAN	1395.6	-20.0	1295.5	0.142	0.058
FEB	1384.3	-10.8	1213.7	0.144	0.060
MAR	1363.4	0.0	1185.3	0.156	0.071
APR	1340.7	+11.6	1134.9	0.180	0.097
MAY	1320.6	+20.0	1103.4	0.196	0.121
JUNE	1309.8	+23.45	1087.6	0.205	0.134
JULY	1311.1	+20.6	1084.5	0.207	0.136
AUG	1324.1	+12.3	1106.5	0.201	0.122
SEPT	1344.5	0.0	1150.7	0.177	0.092
OCT	1366.9	-10.5	1191.6	0.160	0.073
NOV	1387.7	-19.8	1220.0	0.149	0.063
DEC	1398.4	-23.45	1232.6	0.142	0.057

[1]Source: ASHRAE Handbook of Fundamentals (1977).

APPENDIX B: SAMPLE CALCULATIONS FOR INCIDENT SOLAR RADIATION ON THE TILTED COLLECTOR ($\Sigma = 14°$) AT 8:00 A.M. SOLAR TIME ON SEPTEMBER 21, LATITUDE 14° NORTH

At 8:00 a.m., number of hours from solar noon is 4 hours, hence, hour angle ω, from equation (5) is

$$\omega = (15)\ (4) = 60°$$

From equation (4), solar declination angle for September 21 ($n = 264$ days) is

$$\delta = 23.45 \sin \left(360 \frac{284 + 264}{365}\right) = 0°$$

The solar altitude angle, β, from equation (3) is hence

$$\beta = \sin^{-1} (\cos 14 \cos 0 \cos 60 + \sin 14 \sin 0) = 29.02°$$

For a south-facing surface, solar-surface azimuth, γ, is equal to solar azimuth, ϕ, and from equation (8)

$$\sin \phi = \frac{\cos \delta \sin \omega}{\cos \beta}$$

hence

$$\gamma = \phi = \sin^{-1} \left(\frac{\cos 0 \sin 60}{\cos 29.02}\right) = 82.04°$$

and from equation (7), solar incidence angle, θ, is

$$\theta = \cos^{-1} (\cos 29.02 \cos 82.04 \sin 14 + \sin 29.02 \cos 14)$$
$$= 60°$$

The direct solar radiation incident on collector surface, I_{Dcoll}, from equation (6), is

$$I_{Dcoll} = I_{DN} \cos \theta$$

where I_{DN} is the direct normal solar radiation given in equation (2).

From information in Appendix A, on September 21, apparent solar radiation A, is 1150.6 W/m^2 and atmosphere extinction coefficient B, is 0.177, hence,

$$I_{DN} = \frac{A}{\exp\ (B/\sin\ \beta)} = \frac{1150.6}{\exp\ (0.177/\sin\ 29.02)} = 798.8\ W/m^2$$

and

$$I_{Dcoll} = 798.85 \cos 60 = 399.43\ W/m^2$$

The diffuse sky radiation falling on collector surface is calculated from equation (9), wherein the diffuse sky radiation factor, C, from Appendix A is 0.092 and the angle factor, F_{ss}, is

$$F_{ss} = \frac{1 + \cos\ \Sigma}{2} = \frac{1 + \cos\ 14}{2} = 0.985$$

The diffuse sky radiation is hence

$$I_{dcoll} = CI_{DN}\ F_{ss} = (0.092)(798.85)(0.985) = 72.4\ W/m^2$$

The total insolation on the tilted collector is the sum of the direct and diffuse components:

$$I_{coll} = I_{Dcoll} + I_{dcoll} = 399.43 + 72.4 = 471.8\ W/m^2$$

APPENDIX C: VALUES OF r and I_{oN} USED IN THE CALCULATIONS OF DIFFUSE HORIZONTAL SOLAR RADIATION DURING THE TEST PERIOD

Test date	δ (degrees)	r[1] (dimensionless)	I_{oN} (W/m^2)
June 29	23.24	0.96658	1346.83
June 30	23.18	0.96660	1346.86
July 1	23.12	0.96660	1346.86
July 9	22.36	0.96723	1347.74
July 10	22.24	0.96735	1347.91
July 11	22.11	0.96750	1348.12
July 15	21.52	0.96812	1349.98
July 16	21.35	0.96830	1349.23
July 17	21.18	0.96845	1349.44
July 19	20.83	0.96882	1349.96

[1]Source: Liu and Jordan (1960).

APPENDIX D: INSTANTANEOUS DATA ON SOLAR COLLECTOR PERFORMANCE TESTS FROM JUNE 29 TO JULY 19, 1979

Table D.1. Instantaneous data on solar collector performance test[a] on June 29, 1979

Solar time	T_{fi}^{b} (°C)	T_{fo}^{b} (°C)	RH^{b} (%)	H^{c} (W/m^2)	I_{coll}^{d} (W/m^2)	η_{coll}^{e} (%)
8:30	21.3	25.2	66.0	546.2	527.6	13.1
9:00	22.0	27.1	64.7	625.5	617.3	14.7
9:30	22.6	28.3	60.7	697.2	699.2	14.5
10:00	23.2	29.8	57.0	768.0	799.9	14.8
10:30	23.9	30.9	54.3	825.2	845.9	14.6
11:00	24.3	32.0	52.5	856.8	883.5	15.4
11:30	24.7	32.7	50.0	908.8	942.2	15.0
12:00	25.3	33.6	50.3	885.0	917.3	15.8
12:30	25.5	34.3	49.0	884.1	916.3	17.5
1:00	25.5	35.8	48.3	931.9	967.7	18.7
1:30	25.9	35.6	46.3	901.2	931.8	18.3
2:00	25.8	34.8	45.0	856.8	879.8	17.8
2:30	25.9	34.8	42.3	808.1	822.4	18.8
3:00	25.8	34.7	39.5	764.6	769.1	20.2
3:30	26.0	33.2	38.3	739.9	732.3	17.2
4:00	25.7	32.4	38.0	663.1	640.2	18.3

[a] Based on airflow rate of 0.371 m^3/s.

[b] Average values at 30-minute intervals ending at solar time.

[c] 30-minute integrated total horizontal insolation measured by an Eppley pyranometer.

[d] Converted total incident insolation rate from total horizontal insolation.

[e] Instantaneous collector efficiency.

Table D.2. Instantaneous data on solar collector performance test[a] on June 30, 1979

Solar time	T_{fi}^{b} (°C)	T_{fo}^{b} (°C)	RH^{b} (%)	H^{c} (W/m^2)	I_{coll}^{d} (W/m^2)	η_{coll}^{e} (%)
8:30	24.3	28.0	45.3	460.8	445.7	20.9
9:00	25.6	31.3	42.0	613.6	605.4	23.4
9:30	26.6	32.2	39.7	673.3	674.6	20.8
10:00	27.5	34.3	37.5	758.6	770.2	22.3
10:30	28.2	35.5	35.3	818.4	838.9	21.9
11:00	29.2	37.0	33.3	868.7	896.8	22.0
11:30	29.3	37.7	32.0	901.2	934.2	22.4
12:00	29.8	38.9	32.0	923.3	959.7	23.7
12:30	29.7	39.2	30.0	960.1	1000.0	23.7
1:00	29.7	39.2	29.0	927.6	963.4	24.6
1:30	29.9	39.2	28.0	915.7	948.8	24.5
2:00	29.8	38.4	28.0	867.0	891.3	24.0
2:30	29.8	38.3	28.0	844.0	860.7	24.7
3:00	29.4	37.2	28.0	757.8	762.3	25.4
3:30	29.6	36.7	27.0	733.0	725.6	24.5
4:00	29.4	35.8	27.5	658.0	635.8	25.4

[a]Based on airflow rate of 0.533 m^3/s.

[b]Average values at 30-minute intervals ending at solar time.

[c]30-minute integrated total horizontal insolation measured by an Eppley pyranometer.

[d]Converted total incident insolation rate from total horizontal insolation.

[e]Instantaneous collector efficiency.

Table D.3. Instantaneous data on solar collector performance test[a] on July 1, 1979

Solar time	T_{fi}^{b} (°C)	T_{fo}^{b} (°C)	RH^{b} (%)	H^{c} (W/m^2)	I_{coll}^{d} (W/m^2)	η_{coll}^{e} (%)
8:30	25.0	30.0	58.0	529.1	512.0	13.7
9:00	26.1	31.7	56.0	551.3	543.2	14.6
9:30	26.7	32.8	51.8	621.3	621.0	13.9
10:00	27.2	33.4	48.5	639.2	644.8	13.7
10:30	27.8	34.5	45.2	756.9	772.9	12.2
11:00	27.8	34.5	42.5	866.2	894.2	10.5
11:30	28.4	36.7	40.8	838.0	865.4	13.4
12:00	28.9	37.1	37.5	893.5	927.4	12.4
12:30	29.0	37.4	36.5	846.5	875.8	13.4
1:00	29.1	35.9	37.8	606.8	616.3	15.4
1:30	28.8	35.0	37.5	698.9	712.8	12.4
2:00	28.8	34.7	39.0	768.0	785.3	10.5
2:30	29.4	37.0	36.8	814.9	831.7	12.8
3:00	28.4	33.3	36.0	725.4	728.9	9.3
3:30	28.5	33.9	38.0	669.9	662.2	11.6
4:00	27.9	31.2	38.5	604.2	584.4	8.0

[a]Based on airflow rate of 0.30 m^3/s.

[b]Average values at 30-minute intervals ending at solar time.

[c]30-minute integrated total horizontal insolation measured by an Eppley pyranometer.

[d]Converted total incident insolation rate from total horizontal insolation.

[e]Instantaneous collector efficiency.

Table D.4. Instantaneous data on solar collector performance test[a] on July 9, 1979

Solar time	T_{fi}^{b} (°C)	T_{fo}^{b} (°C)	RH^{b} (%)	H^{c} (W/m^2)	I_{coll}^{d} (W/m^2)	η_{coll}^{e} (%)
8:30	24.5	29.3	68.8	488.1	474.1	14.3
9:00	25.4	31.8	64.8	549.6	543.4	16.7
9:30	26.6	33.5	60.8	629.8	632.3	15.3
10:00	26.7	34.9	58.2	699.8	711.0	16.2
10:30	27.4	36.7	56.0	776.6	797.4	16.3
11:00	27.3	37.1	53.5	832.9	861.4	16.0
11:30	27.5	37.9	52.0	879.8	915.1	16.0
12:00	27.5	38.0	52.0	889.2	926.2	15.9
12:30	27.4	38.6	52.0	863.6	898.0	17.5
1:00	27.0	38.3	50.0	837.2	867.8	18.3
1:30	27.5	38.6	50.0	818.4	846.7	18.4
2:00	27.7	38.6	49.0	790.2	812.3	18.4
2:30	27.7	38.5	46.0	800.5	818.6	18.6
3:00	27.4	37.8	45.2	791.1	800.8	18.3
3:30	27.7	36.9	47.5	693.8	689.8	18.8
4:00	27.2	35.4	50.5	599.9	583.1	19.8

[a] Based on airflow rate of 0.30 m^3/s.

[b] Average values at 30-minute intervals ending at solar time.

[c] 30-minute integrated total horizontal insolation measured by an Eppley pyranometer.

[d] Converted total incident insolation rate from total horizontal insolation.

[e] Instantaneous collector efficiency.

Table D.5. Instantaneous data on solar collector performance test[a] on July 10, 1979

Solar time	T_{fi}^{b} (°C)	T_{fo}^{b} (°C)	RH^{b} (%)	H^{c} (W/m^2)	I_{coll}^{d} (W/m^2)	η_{coll}^{e} (%)
8:30	25.2	28.5	73.3	479.6	466.0	13.4
9:00	25.2	30.8	72.0	484.7	478.2	22.4
9:30	26.0	31.3	71.5	568.4	571.8	17.6
10:00	26.0	35.4	68.7	704.9	717.1	24.9
10:30	27.9	37.4	66.5	760.4	780.3	22.8
11:00	28.4	38.9	62.5	756.1	778.2	25.6
11:30	28.8	40.3	58.5	813.3	842.6	25.7
12:00	28.4	37.9	57.3	630.7	641.7	28.2
12:30	28.5	38.4	55.7	717.7	737.3	25.5
1:00	29.4	40.0	54.3	863.6	898.1	22.4
1:30	28.1	33.3	54.5	389.9	386.5	25.3
2:00	28.7	35.8	54.3	576.0	581.4	23.3
2:30	28.7	36.0	65.7	611.9	617.7	22.3
3:00	28.7	36.9	54.7	684.4	690.0	22.5
3:30	28.4	35.6	54.5	640.9	636.7	21.3
4:00	27.6	31.3	55.3	294.4	285.6	24.8

[a] Based on airflow rate of 0.406 m^3/s.

[b] Average values at 30-minute intervals ending at solar time.

[c] 30-minute integrated total horizontal insolation measured by an Eppley pyranometer.

[d] Converted total incident insolation rate from total horizontal insolation.

[e] Instantaneous collector efficiency.

Table D.6. Instantaneous data on solar collector performance test[a] on July 11, 1979

Solar time	T_{fi}^{b} (°C)	T_{fo}^{b} (°C)	RH^{b} (%)	H^{c} (W/m^2)	I_{coll}^{d} (W/m^2)	η_{coll}^{e} (%)
8:30	24.0	29.1	80.0	463.4	441.1	23.0
9:00	25.2	31.3	76.0	570.1	541.2	22.7
9:30	25.8	33.1	75.0	646.9	613.5	23.6
10:00	26.8	34.8	75.0	716.8	679.4	23.3
10:30	26.9	36.9	74.5	775.7	740.8	26.7
11:00	27.9	36.7	70.3	804.7	831.9	20.8
11:30	28.5	39.2	68.0	859.3	893.5	23.6
12:00	28.7	39.4	68.0	889.2	927.8	22.6
12:30	28.7	40.3	66.5	920.8	962.4	23.7
1:00	29.0	40.9	64.5	914.8	955.3	24.6
1:30	28.6	39.9	65.0	838.0	868.9	25.6
2:00	29.0	39.9	64.7	877.3	908.2	23.6
2:30	28.8	39.4	64.0	866.2	817.5	25.6
3:00	28.3	36.6	66.3	685.2	649.0	25.3
3:30	28.3	35.8	64.7	667.3	631.2	23.4
4:00	28.1	34.7	64.3	584.6	553.2	23.4

[a]Based on airflow rate of 0.425 m^3/s.

[b]Average values at 30-minute intervals ending at solar time.

[c]30-minute integrated total horizontal insolation measured by an Eppley pyranometer.

[d]Converted total incident insolation rate from total horizontal insolation.

[e]Instantaneous collector efficiency.

Table D.7. Instantaneous data on solar collector performance test[a] on July 15, 1979

Solar time	T_{fi}^{b} (°C)	T_{fo}^{b} (°C)	RH^{b} (%)	H^{c} (W/m^2)	I_{coll}^{d} (W/m^2)	η_{coll}^{e} (%)
8:30	23.0	25.6	82.3	305.5	297.0	22.7
9:00	24.2	28.9	75.5	535.9	515.9	24.4
9:30	25.4	30.8	69.7	660.5	667.6	21.4
10:00	26.2	32.3	66.3	715.1	730.8	21.6
10:30	27.0	34.1	61.0	799.6	828.0	19.6
11:00	27.4	35.2	55.3	847.4	881.8	20.9
11:30	27.7	36.3	58.3	884.1	928.0	24.2
12:00	28.1	36.8	58.3	903.7	946.7	23.9
12:30	28.6	37.7	57.7	923.3	969.0	24.2
1:00	28.6	37.6	54.7	921.6	970.2	23.9
1:30	29.0	37.6	53.0	895.2	934.3	23.7
2:00	29.1	37.6	52.3	850.8	884.3	24.9
2:30	29.2	36.6	49.7	808.9	832.3	23.0
3:00	28.8	35.9	46.5	733.0	744.3	24.8
3:30	28.9	35.2	45.0	683.6	656.6	24.9
4:00	28.8	34.7	42.5	656.2	641.7	24.1

[a]Based on airflow rate of 0.557 m^3/s.

[b]Average values at 30-minute intervals ending at solar time.

[c]30-minute integrated total horizontal insolation measured by an Eppley pyranometer.

[d]Converted total incident insolation rate from total horizontal insolation.

[e]Instantaneous collector efficiency.

Table D.8. Instantaneous data on solar collector performance test[a] on July 16, 1979

Solar time	T_{fi}[b] (°C)	T_{fo}[b] (°C)	RH[b] (%)	H[c] (W/m^2)	I_{coll}[d] (W/m^2)	η_{coll}[e] (%)
8:30	23.2	26.6	67.3	509.5	497.8	18.3
9:00	24.2	28.8	63.3	591.4	589.4	20.9
9:30	24.9	30.9	61.0	669.9	678.1	23.1
10:00	25.2	32.0	58.5	738.2	756.3	23.8
10:30	26.1	33.3	54.5	795.3	822.3	23.1
11:00	26.9	34.9	51.5	847.4	882.5	23.6
11:30	27.2	35.9	50.0	894.3	936.4	24.6
12:00	26.9	36.3	49.5	884.9	926.5	26.4
12:30	27.8	37.6	47.5	954.9	1005.0	25.4
1:00	27.8	37.6	45.5	966.0	1007.3	25.5
1:30	27.0	35.9	44.0	908.8	950.6	24.5
2:00	27.2	36.4	44.0	883.2	920.0	26.4
2:30	26.6	34.1	44.0	734.8	752.8	26.2
3:00	25.8	34.0	45.3	732.2	744.2	28.9
3:30	25.4	31.6	46.0	583.7	581.6	27.7
4:00	25.6	31.0	46.0	607.6	594.6	24.4

[a] Based on airflow rate of 0.557 m^3/s.

[b] Average values at 30-minute intervals ending at solar time.

[c] 30-minute integrated total horizontal insolation measured by an Eppley pyranometer.

[d] Converted total incident insolation rate from total horizontal insolation.

[e] Instantaneous collector efficiency.

Table D.9. Instantaneous data on solar collector performance test[a] on July 17, 1979

Solar time	T_{fi}^{b} (°C)	T_{fo}^{b} (°C)	RH^{b} (%)	H^{c} (W/m^2)	I_{coll}^{d} (W/m^2)	η_{coll}^{e} (%)
8:30	23.0	26.9	68.7	507.8	496.6	20.8
9:00	23.8	28.6	68.3	588.0	586.4	21.8
9:30	24.4	30.6	64.3	669.9	678.9	24.0
10:00	25.2	31.6	61.7	720.2	738.1	22.8
10:30	25.5	32.3	57.0	791.1	818.6	21.8
11:00	25.9	33.7	52.3	770.6	798.1	25.6
11:30	26.6	34.8	49.3	960.9	1011.8	21.2
12:00	25.4	33.3	47.7	751.8	780.4	26.7
12:30	26.9	35.2	46.5	960.9	1012.6	21.4
1:00	27.1	37.1	42.5	997.6	1052.4	24.9
1:30	26.7	35.3	42.0	894.3	935.2	24.4
2:00	25.9	33.0	42.0	666.2	677.3	27.5
2:30	26.0	34.2	41.7	891.8	932.2	23.3
3:00	25.8	32.0	42.0	624.7	631.0	28.8
3:30	25.0	30.4	41.7	499.2	495.4	28.8
4:00	25.1	29.8	42.7	559.8	548.1	22.5

[a] Based on airflow rate of 0.557 m^3/s.

[b] Average values at 30-minute intervals ending at solar time.

[c] 30-minute integrated total horizontal insolation measured by an Eppley pyranometer.

[d] Converted total incident insolation rate from total horizontal insolation.

[e] Instantaneous collector efficiency.

Table D.10. Instantaneous data on solar collector performance test[a] on July 19, 1979

Solar time	T_{fi}^{b} (°C)	T_{fo}^{b} (°C)	RH^{b} (%)	H^{c} (W/m^2)	I_{coll}^{d} (W/m^2)	η_{coll}^{e} (%)
8:30	22.0	27.7	60.5	494.9	485.0	16.1
9:00	22.9	29.4	59.0	576.9	576.2	15.6
9:30	23.6	31.7	55.7	651.1	660.5	15.4
10:00	24.7	33.9	49.7	722.8	742.1	17.0
10:30	25.3	35.5	46.0	776.6	804.1	17.4
11:00	25.8	36.9	43.7	826.1	861.1	17.5
11:30	26.3	38.4	42.7	871.3	913.1	18.1
12:00	26.4	38.9	41.3	898.6	944.7	18.1
12:30	26.4	39.3	40.5	904.6	951.5	18.5
1:00	26.7	39.2	40.0	849.1	888.6	19.1
1:30	26.7	40.0	40.7	890.1	932.5	19.5
2:00	26.8	39.2	40.5	847.4	882.4	19.2
2:30	26.7	38.3	40.0	795.3	820.6	19.3
3:00	26.3	36.6	40.3	756.9	773.1	18.2
3:30	26.2	34.7	41.3	599.9	599.9	19.2
4:00	26.1	35.3	42.0	628.1	617.2	20.2

[a]Based on airflow rate of 0.288 m^3/s.

[b]Average values at 30-minute intervals ending at solar time.

[c]30-minute integrated total horizontal insolation measured by an Eppley pyranometer.

[d]Converted total incident insolation rate from horizontal insolation.

[e]Instantaneous collector efficiency.